Interazioni di partoni ad alta energia nella materia

Bibliografia

Testi:

Greiner, Neise, Stocker: Thermodynamics and statistical mechanics (Springer-Verlag)

Jackson: Classical Electrodynamics 3rd ed. (Wiley)

Aitchinson & Hey: Gauge Theories in particles Physics 2nd ed. (Adam Hilger)

Leader & Predazzi:An introduction to gauge theories and… (Cambridge monographs)

Lezioni & seminarii:

Maiani : Seminario a Milano 15/02/2007

Jacobs: QGP School, villa Gualino 11/05/2005

Armesto: QGP School, villa Gualino 11/05/2005

Muller: CERN Heavy Ion Forum 2/03/2007

Programma:

-Interazioni nucleo-nucleo ultrarelativistiche: motivazioni

-Stato del programma sperimentale

-Proprieta di un plasma di quark e gluoni

-Jets e jet quenching nelle collisioni nucleo-nucleo

-Perdita di energia dei partoni per collisione e per radiazione di gluoni

-Confronto con gli analoghi processi elettromagnetici:
dead cone effect
regime Bethe-Heitler e Landau-Pomeranchuk-Migdal

-Perdita di energia dei quark pesanti

-Problemi aperti per LHC

Lattice QCD

- In lattice QCD, non-perturbative problems are treated by discretization on a space-time lattice.

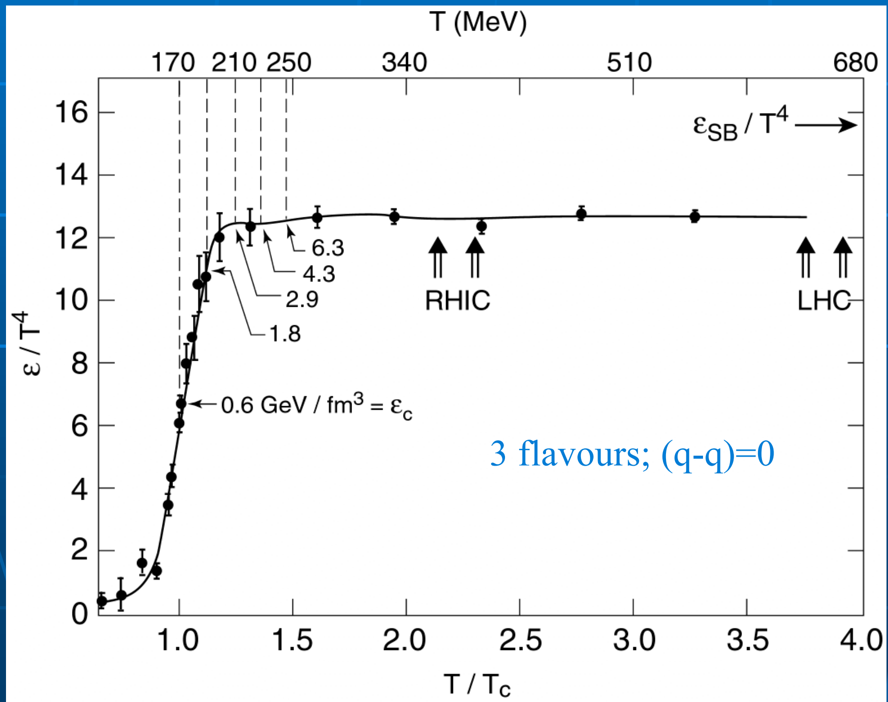

- zero baryon density, 3 flavours
- rapid change around T_c
- T_c = 170 MeV:
  $\rightarrow \varepsilon_c$ = 0.6 GeV/fm^3
- at T~1.2 T_c settling at about 80% of the Stefan-Boltzmann value for an ideal gas of q,q g (ε_{SB})

- How can we compress/heat matter to such cosmic energy densities?

- By colliding two heavy nuclei at ultrarelativistic energies we hope to be able to recreate, for a short time span (about 10^{-23}s, or a few fm/c) the appropriate conditions for deconfinement

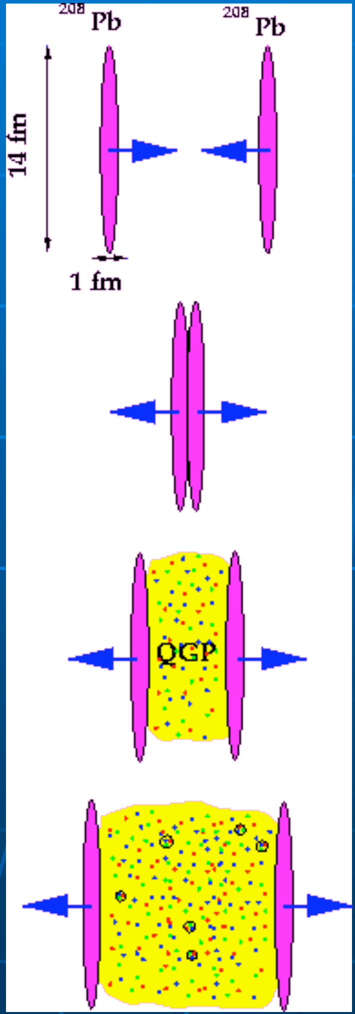

The mini Big Bang

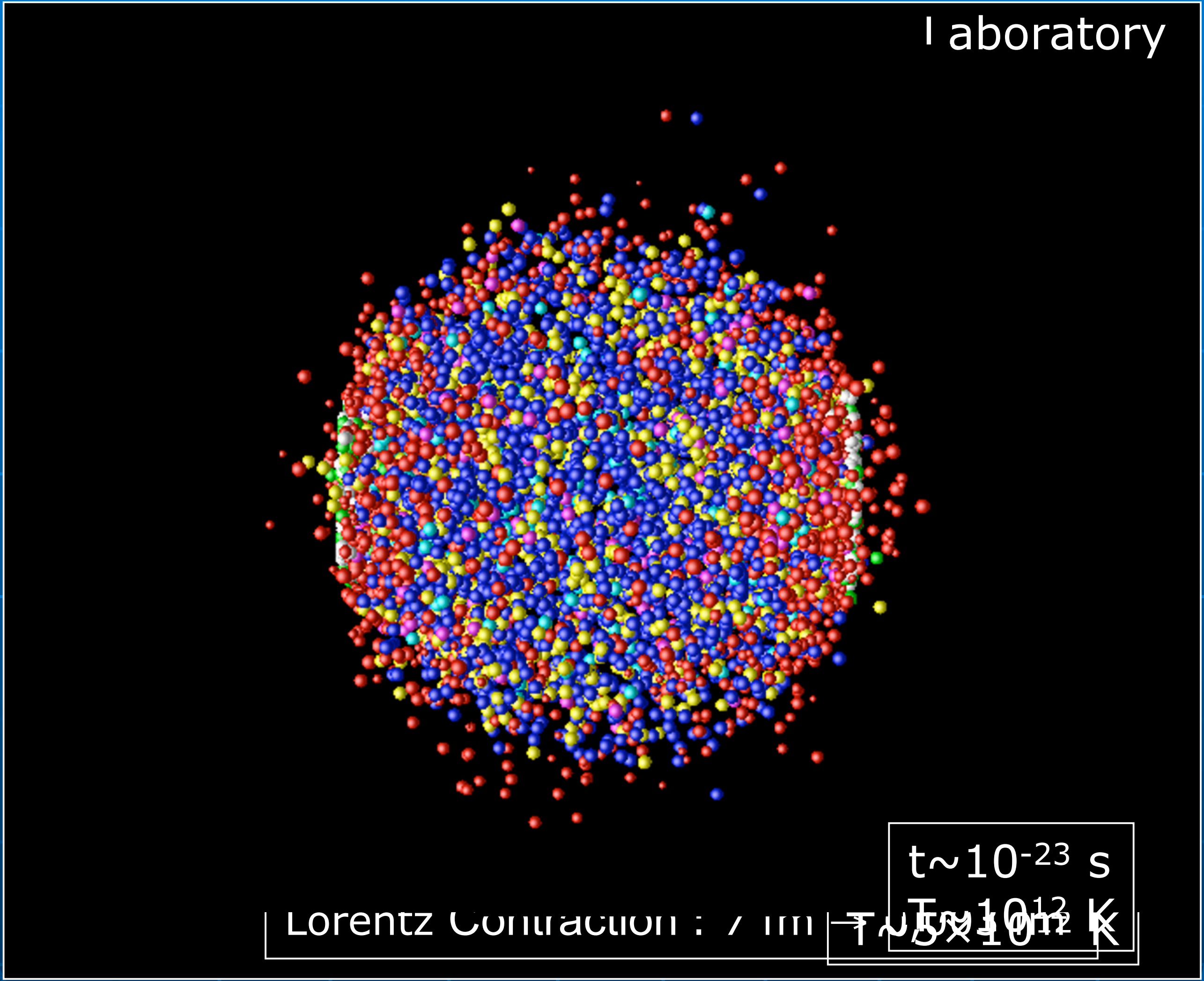

1. Accelerated ions will collide head on
2. The energy of collision is materialized into quarks and gluons
3. Quarks and gluons interact via the strong interaction: matter equilibrates
4. The system expands and cools down
5. Quarks and gluons condense into hadrons

QCD Thermodynamics

The Big Bang started here

Pb collisions at LHC will take us there

And we will study this trajectory

We are here

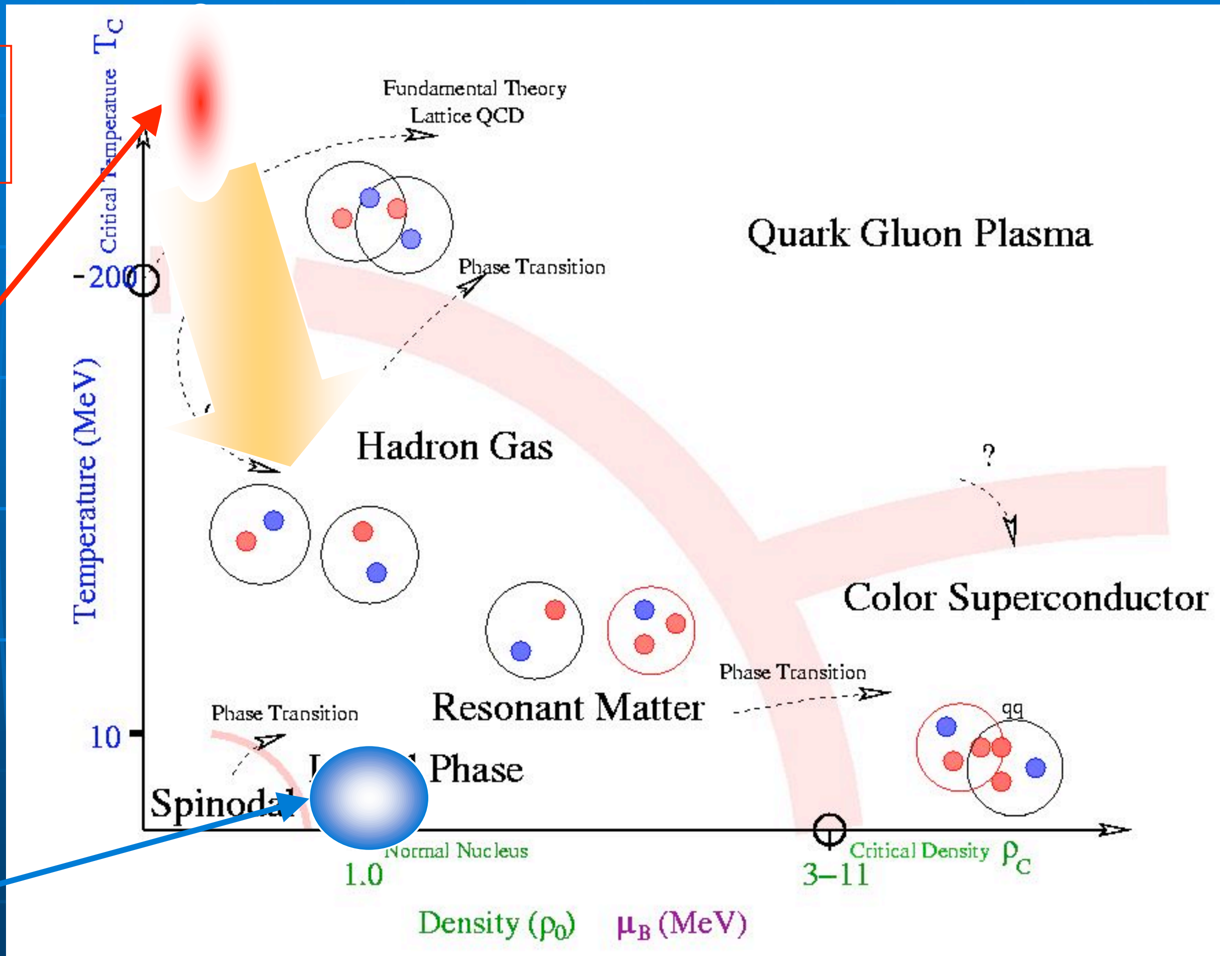

Where

- Alternating Gradient Synchrotron (AGS) at Brookhaven BNL
  - variety of beams, since 80's

  $\boxed{\sqrt{s_{NN}}\,\Big|^{AGS}_{Au+Au} \simeq 2-5\ GeV}$

- CERN SPS fixed target experiments
  - variety of beams, Pb-beams since 1994

  $\boxed{\sqrt{s_{NN}}\,\Big|^{SPS}_{Pb+Pb} < 17\ GeV}$

- <u>Relativistic Heavy Ion Collider</u> (RHIC) at Brookhaven BNL
  - start in 2000, so far p+p, Au+Au and d+Au

  $\boxed{\sqrt{s_{NN}}\,\Big|^{RHIC}_{Au+Au} \leq 200\ GeV}$

- <u>Large Hadron Collider</u> (LHC) at CERN
  - start in 2007 with p+p, in 2008 with Pb+Pb

  $\boxed{\sqrt{s_{NN}}\,\Big|^{LHC}_{Pb+Pb} = 5.5\ TeV}$

  - total cross section $\sigma^{Pb+Pb}_{total} = 8\ barn = 10^{-24}\ cm^2$
  - maximal luminosity $L^{Pb+Pb}_{max} \sim 10^{27}\ cm^{-2}\ s^{-1}$

  8000 collisions per second !

Machine	Start	Type	Beam	$\sqrt{s}$ [GeV/A]	ϵ_0^{AB} [GeV/fm^3]
BNL – AGS	1986	Fixed Target	^{28}Si	5	0.7
CERN – SPS	1986	Fixed Target	$^{16}O,^{32}S$	19	1.6
BNL – AGS	1992	Fixed Target	^{197}Au	5	1.5
CERN – SPS	1994	Fixed Target	^{208}Pb	17	3.7
BNL – RHIC	2000	Collider	^{197}Au	200	7.6
CERN – LHC	2007	Collider	^{208}Pb	5500	13

Table 1: Experimental facilities for high energy nuclear collisions; the light ion beam results are for heavy ($A = 200$) targets, the others for symmetric ($A - A$) collisions.

"...The challenge now passes to the Relativistic Heavy Ion Collider at Brookhaven and later to CERN's Large Hadron Collider."(Feb. 2000)

1. The Relativistic Heavy Ion Collider, Brookhaven, Summer 2000 to ...

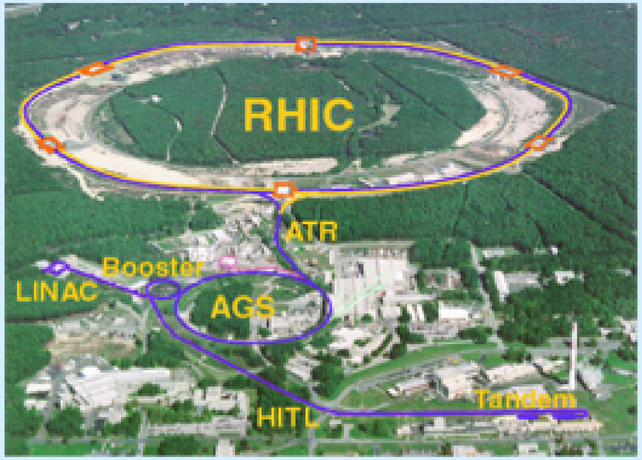

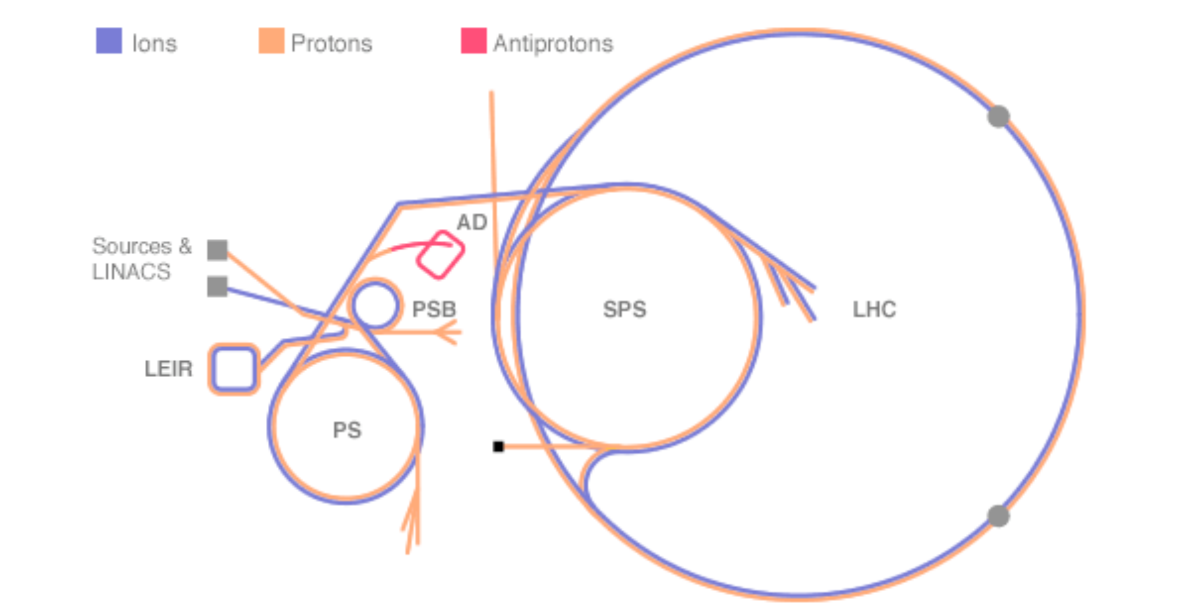

- 27 km circumference
- 40 m underground
- Cryogeny at 1.9 K

- Accelerates p @ 7×10^{12} eV & ions @ $2{,}76\times10^{12}$ eV (99.999993% c)
- ~10^8 ions cross 10^8 ions 10^6 times every second
- 8,000 collisions every second, out of which 1% produce "extraordinary" events

2. Early evidence of a new phase: CERN 2000

SPS: two "historic" QGP signatures

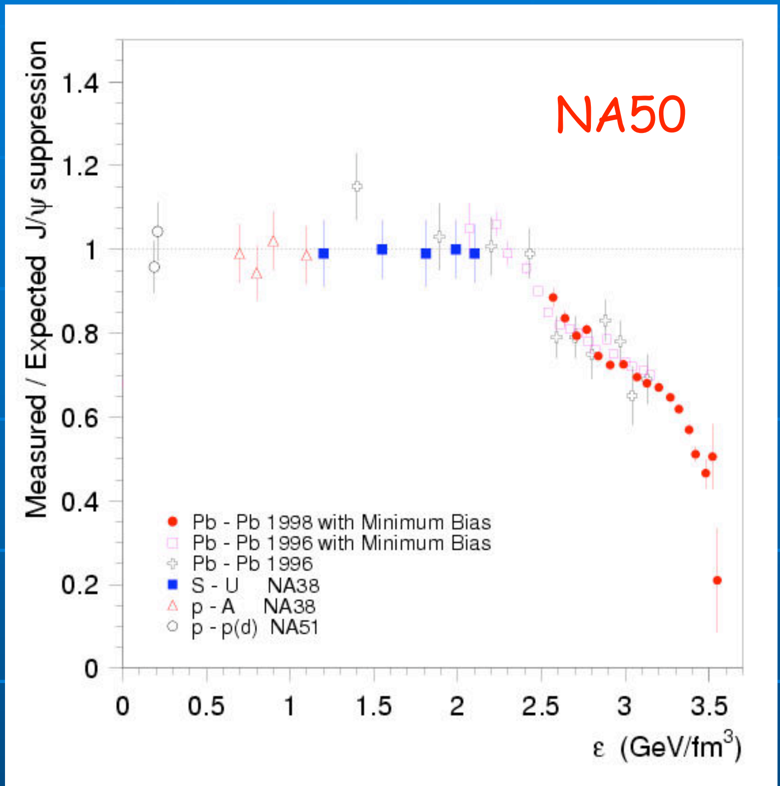

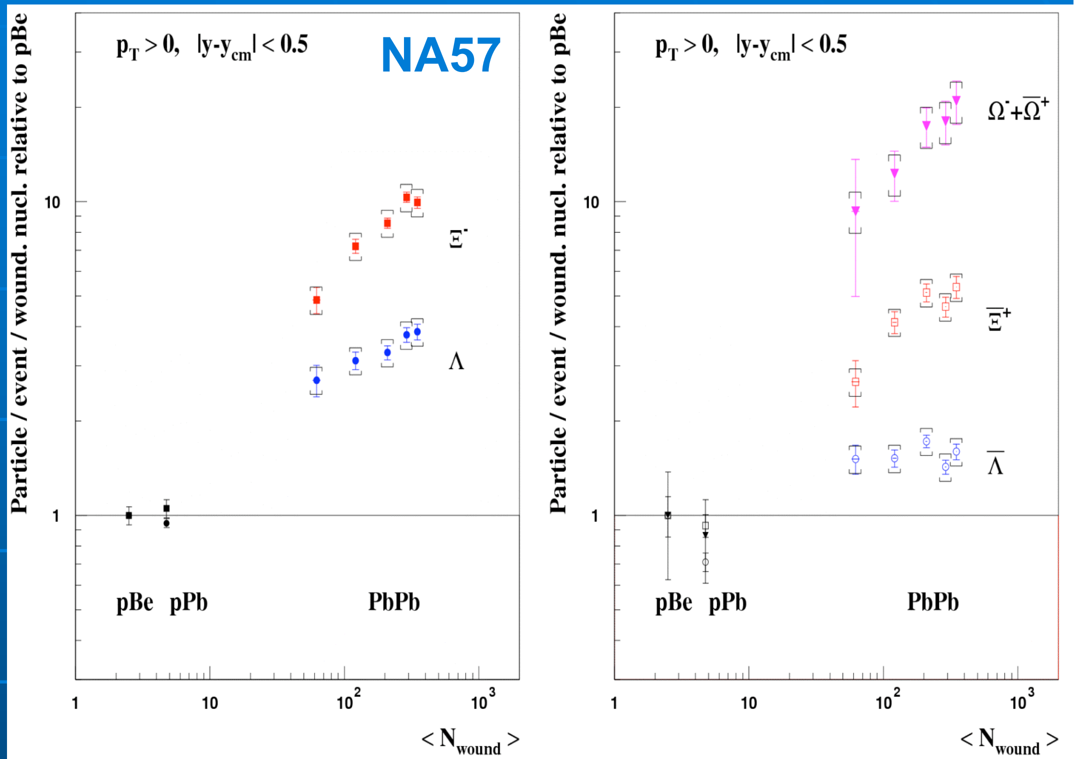

- J/ψ suppression
  NA50, NA60
- Hyperon enhancements
  WA97, NA49, NA57

@ SPS

- All indications are that deconfinement is seen @SPS
- strangeness enhancement and J/Ψ suppression are correlated (γ_S. vs centrality) !!
- SPS offers the unique possibility to study precisely the onset of deconfinement....
- to be considered in long term planning of the SPS!

Proprieta di un gas ideale di quark e gluoni

Potenziale chimico

Densita di quark e gluoni

Densita di energia

$\hbar = c = 1$ & K_B (Boltzmann) $= 1$

- ENERGIA, MOMENTO, MASSA — GeV (MeV, KeV, eV)
- LUNGHEZZA, TEMPO — GeV^{-1} "
- CARICA ELEMENTARE

$$\frac{e^2}{4\pi} \equiv \alpha_{em} \simeq \frac{1}{137} \qquad —$$

$$\frac{g^2}{4\pi} \equiv \alpha_{strong}(q^2) \qquad —$$

- TEMPERATURA — GeV "

RELAZIONI UTILI

$$1\ \text{fm} = 10^{-13}\ \text{cm} \simeq 5\ \text{GeV}^{-1}$$

$$1\ \text{GeV} = 5\ \text{fm}^{-1}$$

$$1\ \text{mb} = 10^{-27}\ \text{cm}^2 \simeq 2.56\ \text{GeV}^{-2}$$

$$1\ \text{GeV}^2 \simeq 0.389\ \text{mb}^{-1}$$

$$1\ \text{GeV} = \frac{1}{6.6 \times 10^{-25}}\ \text{sec}^{-1}$$

$$1\ \text{GeV} \simeq 1.16 \times 10^{13}\ {}^\circ\text{K}$$

ESEMPI:
- Densità $[M/L^3] \longrightarrow$ si misura in GeV^2
- Costante di Newton $[M^{-1} L^3 T^{-2}] \longrightarrow \text{GeV}^{-2}$

  $F = G \frac{M_1 M_2}{r^2}$
- $\frac{dE}{dx}$ $\left[\frac{E}{L}\right] \longrightarrow \text{GeV}^2$

DIGRESSIONE SU $\begin{cases} \text{POTENZIALE CHIMICO} \ \& \\ \text{EQUILIBRIO CHIMICO} \end{cases}$

Potenziale chimico $\quad \mu = \left(\dfrac{dF}{dN}\right)_{T,V}$ $\quad$ ($F \equiv$ energia libera)

Ex

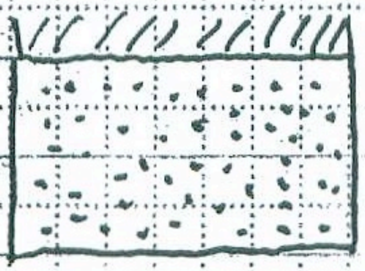

V & T costanti

N particelle

Lavoro necessario per aggiungere una particella al sistema

$$\delta W = \mu \, dN$$

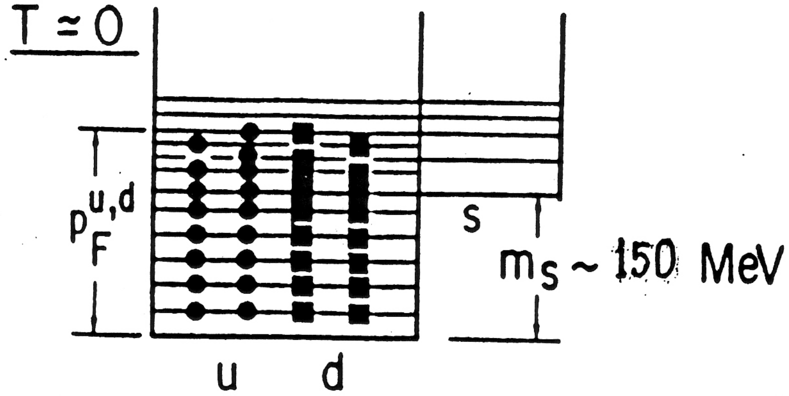

(se $\rho = \rho_0$ $\mu = 206$ MeV)

$$\mu_{u,d} \equiv E_F^{u,d} \simeq p_F^{u,d} = \left(\frac{\overset{\#\text{ of quarks in N}}{3}}{\underset{\text{flavor}}{2} \times \underset{\text{color}}{3}}\right)^{\frac{1}{3}} \left(\frac{\rho}{\rho_0}\right)^{\frac{1}{3}} \underbrace{p_F^N}_{260\text{ MeV/c}} \xrightarrow{\rho \simeq 10\rho_0} 450\text{ MeV} > m_s + m_{\bar{s}}$$

momento di Fermi dei quark u, d

momento di Fermi dei nucleoni nel nucleo

$\mu_{u,d}$ = potenziale bariochimico $\equiv \mu(\rho, T)$

$$\rho = 2\mu T^2/3 + 2\mu^3/3\pi^2$$

OCCUPATION NUMBERS

- Probabilità di occupazione di uno stato con energia E. ($T \equiv$ Temperatura)

- Bose-Einstein

$$\frac{e^{(\mu-E)/T}}{1-e^{(\mu-E)/T}} = \frac{1}{e^{(E-\mu)/T}-1}$$

- Fermi-Dirac

$$\frac{e^{(\mu-E)/T}}{1+e^{(\mu-E)/T}} = \frac{1}{1+e^{(E-\mu)/T}}$$

- Boltzmann limit (prob $\ll 1$)

$$e^{(\mu-E)/T}$$

$E = \sqrt{k^2+m^2} \longrightarrow k$ ultrarelativistic

$\mu =$ chemical potential (see next)

Attenzione: il simbolo μ è usato anche per il momento di Debye: $\mu = \dfrac{1}{r_{Debye}}$ (see next)

- Il volume nello spazio delle fasi occupato dai gluoni contenuti in un volume spaziale V, con momento K nell'intervallo dK è: $4\pi K^2 dK\, V$
- Ogni stato occupa un volume $(2\pi\hbar)^3$ nello spazio delle fasi $[\,(2\pi)^3$ se $\hbar = 1\,]$.
- Il numero degli stati caratterizzati da un momento K nell'intervallo dK è:

$$(4\pi K^2 \cdot dK \cdot V)/(2\pi)^3$$

- La probabilità di occupazione è

Bose Einstein $\quad 1/(e^{(K-\mu)/T}-1)$

- Il numero di gluoni per unità di volume è: $\quad \mu = 0 \quad (\beta = \frac{1}{T})$

$$n_g = \frac{c_g}{(2\pi)^3}\,\frac{V}{V}\,4\pi\int_0^\infty \frac{K^2}{(e^{\beta K}-1)}\,dK$$

$c_g = \underset{\text{colore}}{8} \times \underset{\text{spin}}{2}$

(gluon degeneracy)

$$n_g = \frac{c_g}{2\pi^2}\int_0^\infty \frac{K^2\,dK}{(e^{\beta K}-1)}$$

Integrali definiti utili | 1

$$\int_0^\infty \frac{x^{\nu-1}}{e^{\mu x}-1}\,dx = \frac{\Gamma(\nu)}{\mu^\nu}\,\zeta(\nu)$$

$$\int_0^\infty \frac{x^{\nu-1}}{e^{\mu x}+1}\,dx = \frac{1-2^{1-\nu}}{\mu^\nu}\,\Gamma(\nu)\,\zeta(\nu)$$

$(\mathrm{Re}\,\mu > 0,\ \mathrm{Re}\,\nu > 0)$

$\Gamma(\nu)$ funzione Gamma
$\zeta(\nu)$ funzione $\zeta(\nu)$ di Riemann

$$\Gamma(n+1) = n!$$

$\zeta(2) = \pi^2/6$ $\qquad \zeta(3) \simeq 1.202$

$$\zeta(4) = \pi^4/90$$

per altri valori:
Greiner, Neise, Stöcker Thermodynamics and Statistical Mechanics pag. 317

DENSITA DI GLUONI E QUARK nel QGP 2

$$n_g = \frac{16}{2\pi^2}\int_0^\infty K^2 dK \left(\frac{1}{e^{\beta K}-1}\right)$$

$$\boxed{\begin{array}{l}\beta \equiv \frac{1}{T} \\ \mu = 0\end{array}}\ !$$

$x = \beta K$

$$n_g = \frac{16}{2\pi^2} T^3 \int x^2 dx \left(\frac{1}{e^x - 1}\right)$$

$$= \frac{16}{2\pi^2} T^3\, \Gamma(3)\cdot\zeta(3) = \frac{16}{\pi^2}\, 1.202\, T^3$$

Ex $T = 250$ MeV $n_g \doteq 0.03\ \text{GeV}^3 = 3.8\ \frac{\text{gluoni}}{\text{fm}^3}$

Analogamente : $m_q = m_{\bar{q}} = 0$ $\mu = 0$

$$n_q = n_{\bar{q}} = \frac{g_q}{2\pi^2} T^3 \cdot \frac{3}{2}\zeta(3)$$

$$= \underset{N_c}{3}\cdot\underset{N_f}{3}\cdot\underset{N_{spin}}{2}\cdot T^3 \cdot \frac{1.8}{2\pi^2}$$

$$= 0.025\ \text{GeV}^3 = 3.2\ \frac{\text{quark}}{\text{fm}^3}$$

PROPRIETÀ QGP

Energia (momento) media dei gluoni $m=0$

$$\frac{\frac{16}{(2\pi)^3}\int_0^\infty k\,(e^{\beta k}-1)^{-1}\,d^3k}{\frac{16}{(2\pi)^3}\int_0^\infty (e^{\beta k}-1)^{-1}\,d^3k}$$

$d^3k = 4\pi k^2 dk$

$\beta = 1/T$

$k = x/\beta \qquad dk = dx/\beta$

$$= \frac{\int_0^\infty k^3(e^{\beta k}-1)^{-1}\,dk}{\int_0^\infty k^2(e^{\beta k}-1)^{-1}\,dk}$$

$$= \frac{\frac{1}{\beta^4}\int_0^\infty x^3(e^x-1)^{-1}\,dx}{\frac{1}{\beta^3}\int_0^\infty x^2(e^x-1)^{-1}\,dx} = T\cdot\frac{\Gamma(4)\,\zeta(4)}{\Gamma(3)\,\zeta(3)}$$

$$= T\,\frac{3!}{2!}\,\frac{\pi^4}{90\times 1.202} = 2.70\cdot T$$

$$\begin{cases} \langle E\rangle_{\substack{\text{bosoni}\\ m=0}} = 2.70\ T \\ \text{analogamente} \\ \langle E\rangle_{\substack{\text{fermioni}\\ m=0}} = 3.15\ T \\ \langle E\rangle_{\text{Boltzmann}} = 3\ T \end{cases}$$

Esercizio

Calcolo di $\langle p \rangle$

- gas relativistico

- Boltzmann appross.

$$\langle p \rangle = \frac{\left(\frac{1}{2\pi}\right)^3 \int p\, e^{-p/T}\, d^3p}{\left(\frac{1}{2\pi}\right)^3 \int e^{-p/T}\, d^3p} = \frac{6\, T^4}{2\, T^3} = 3T$$

$$a = \frac{1}{T}$$

$$\int x^m e^{ax} dx = \frac{e^{ax}}{a}\left\{ x^m - \frac{m}{a} x^{m-1} + \frac{m(m-1)}{a^2} x^{m-2} - \dots \right\}$$

Assumendo che QGP sia un free gas (?) di quarks e gluoni

Energy density of gluons $\quad \beta \equiv \frac{1}{T}$

$$\mathcal{E}_g = \frac{8\times 2}{(2\pi)^3}\int_0^\infty K\,(e^{\beta K}-1)^{-1}\,d^3K =$$

$$= \frac{16\times 4\pi}{(2\pi)^3}\,T^4\,\Gamma(4)\,\zeta(4) = \frac{8}{\pi^2}\,T^4 \times 6 \times \frac{\pi^4}{90}$$

$$= \frac{8\pi^2}{15}\,T^4$$

Energy density of quarks $\quad m=0 \quad q\ \&\ \bar{q}$

analogamente si trova

$$\mathcal{E}_{q\bar{q}} = 6\,N_f\left[\frac{7\pi^2}{120}\,T^4 + \frac{\mu^2}{4}\,T^2 + \frac{1}{8\pi^2}\,\mu^4\right]$$

μ = potenziale chimico

se $\mu = 0\ \&\ N_f = 3$

$$\mathcal{E} = \mathcal{E}_g + \mathcal{E}_{q\bar{q}} \simeq 16\,T^4$$

EX $\quad T = 250$ MeV $\qquad \mathcal{E} = 0.0625\ \text{GeV}^4$

$1\ \text{GeV} = 5\ \text{fm}^{-1} \qquad \mathcal{E} = 0.0625 \times 125\ \text{GeV/fm}^3$

$\simeq 7.8\ \text{GeV/fm}^3$

A word of warning!

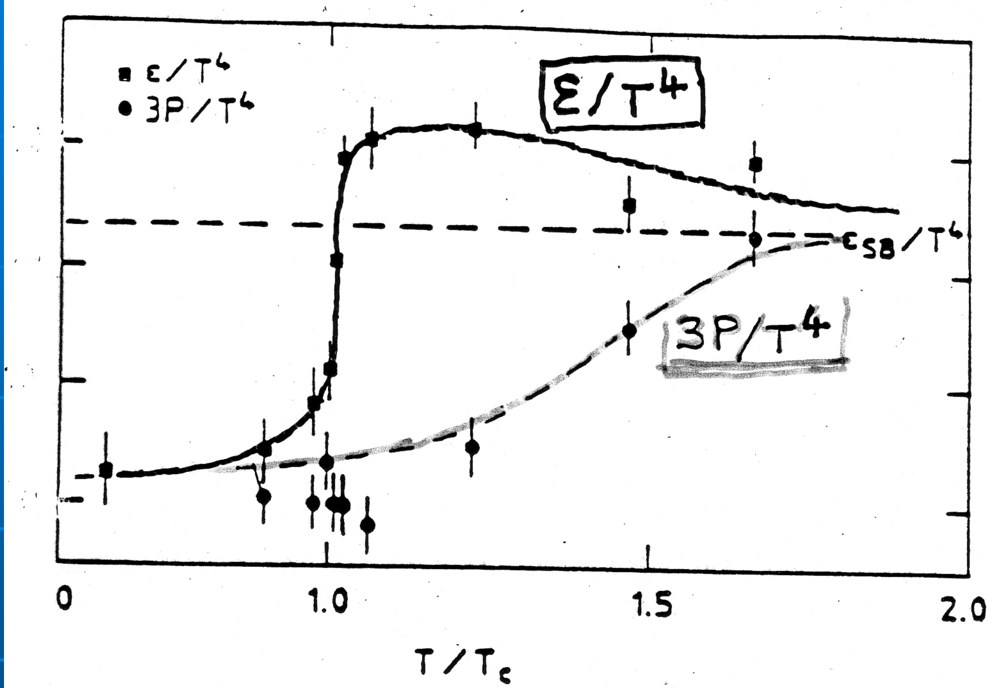

$\varepsilon \neq 3P$

gas relativistico ideale

$\varepsilon = 3$ Pressione

A glimpse at RHIC results

E. Shuryak @ Frascati

Main findings at RHIC

- Partciles are produced from matter which seems to be well equilibrated (by the time it is back in hadronic phase), N1/N2 =exp(-(M_1-M_2)/T)
- Very robust collective flows were found, indicating very strongly coupled Quark-Gluon Plasma (sQGP)
- Strong quenching of large pt jets: they do not fly away freely but are mostly (up to 90%)

absorbed by the matter. The deposited energy seem To go into hydrodynamical motion (conical flow)

Strangeness at RHIC

The strangeness "enhancement" is weaker than at SPS energy, as expected from chemical equilibrium paradigm!

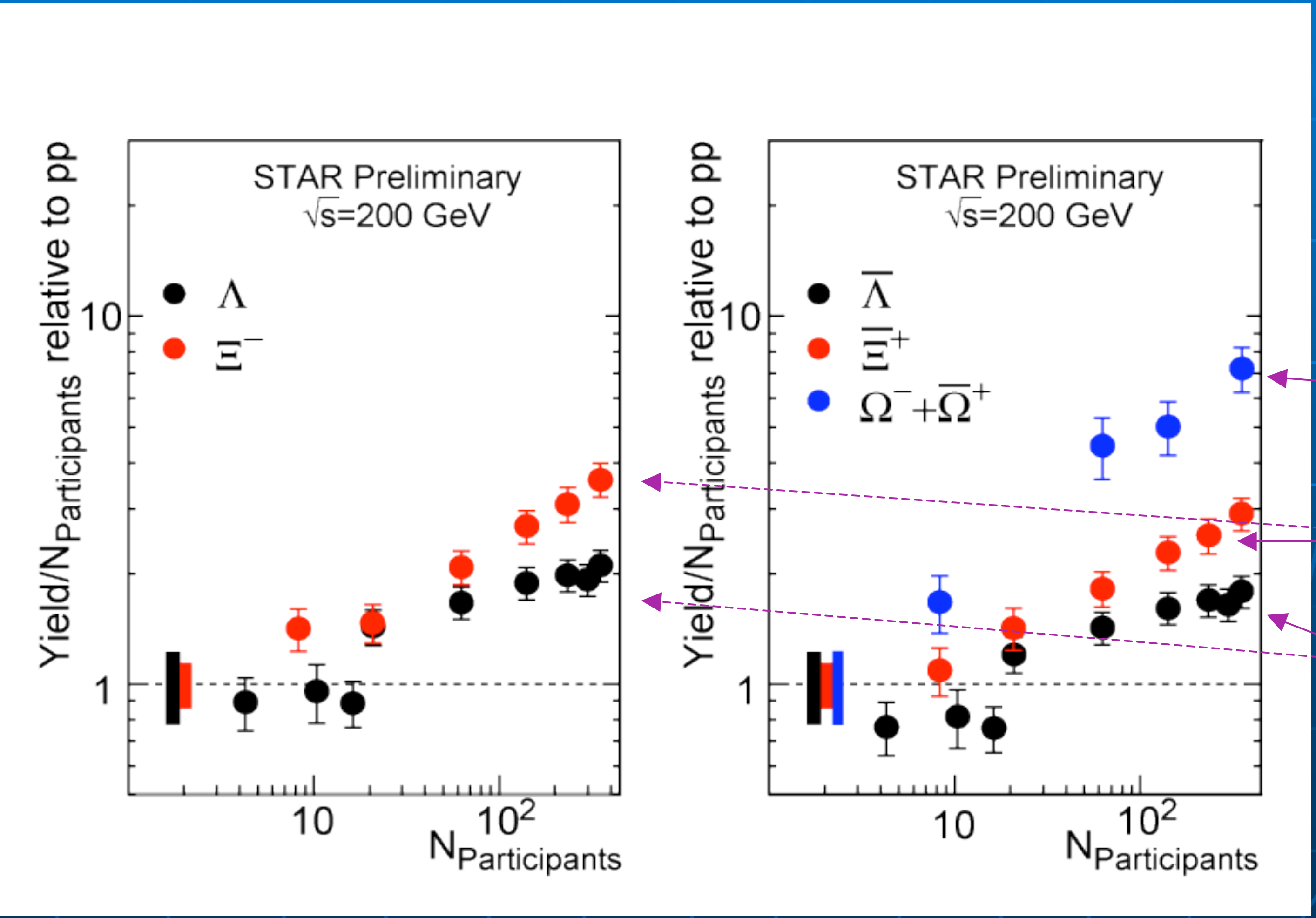

Not everything is better at RHIC !

Multi-strange baryon enhancement probes chiral symmetry restoration (disappearance of QCD quark mass) and quark deconfinement

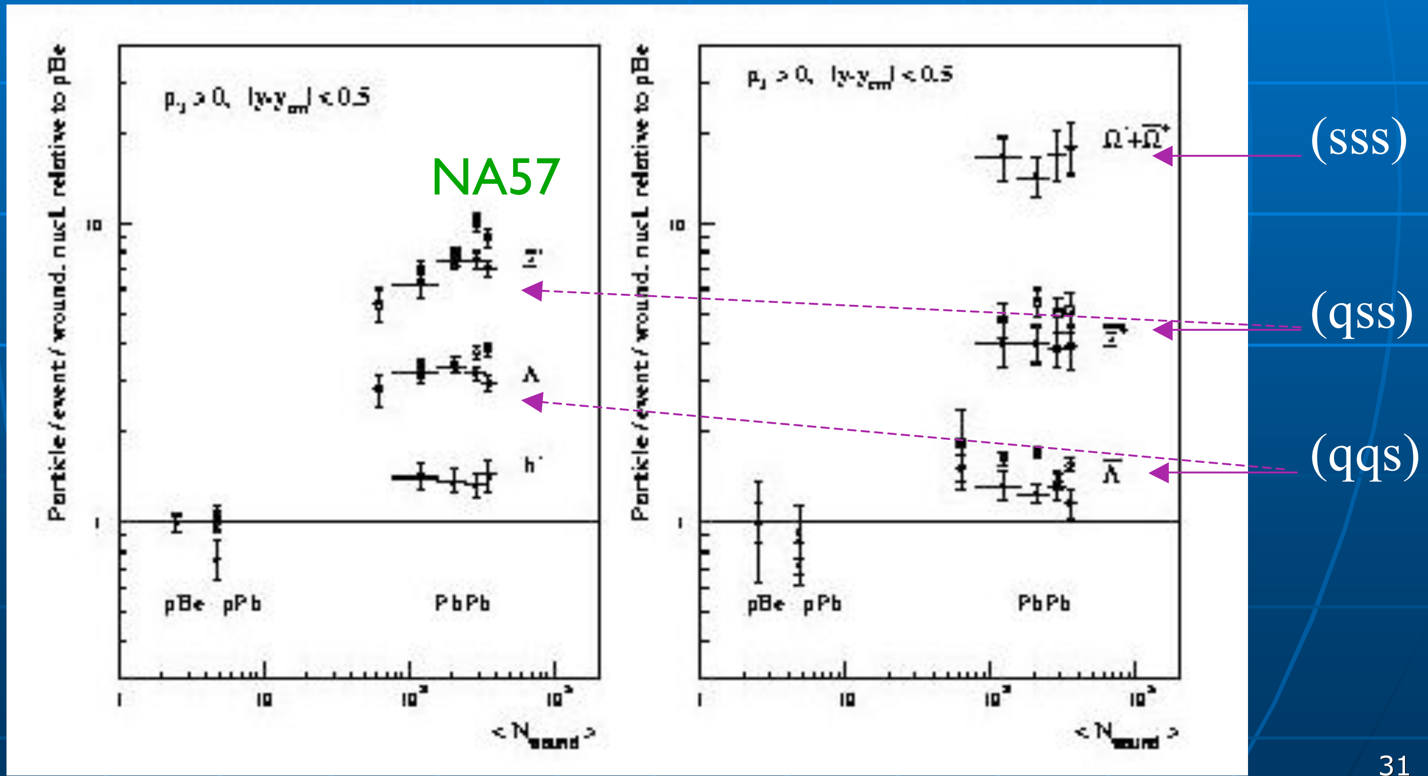

Jets & jet quenching

Running of α_s

$$\alpha_s(Q^2) = \frac{12\pi}{(33 - n_f)\ln(Q^2/\Lambda^2)}$$

The origin of jets: high energy quarks and gluons dress themselves in a spray of hadrons

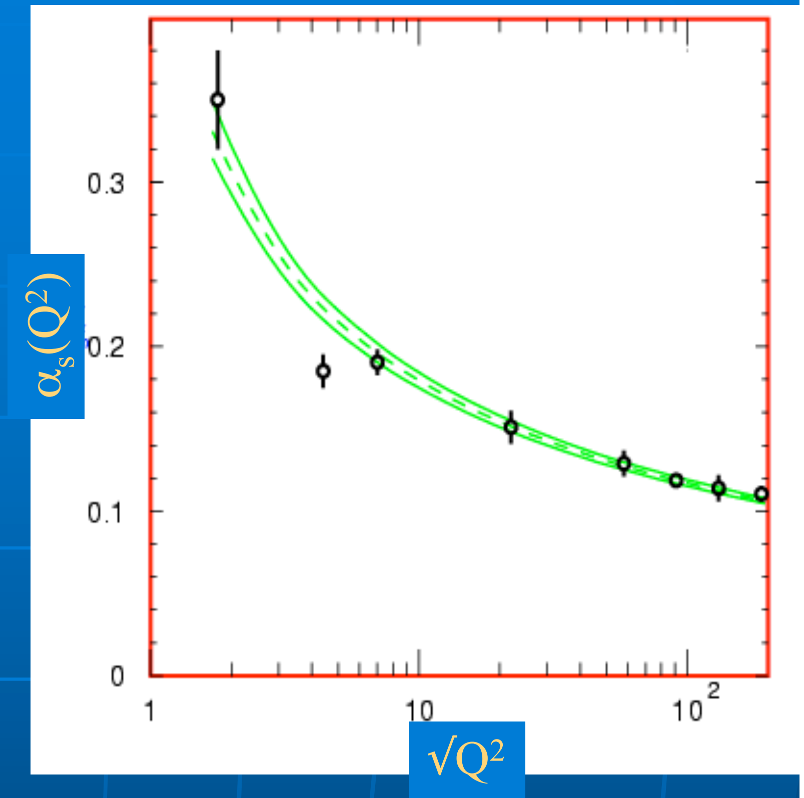

α_s diverges as $Q^2 \to$ small (long distance)

$\Rightarrow$ no free quarks or gluons

Confining potential

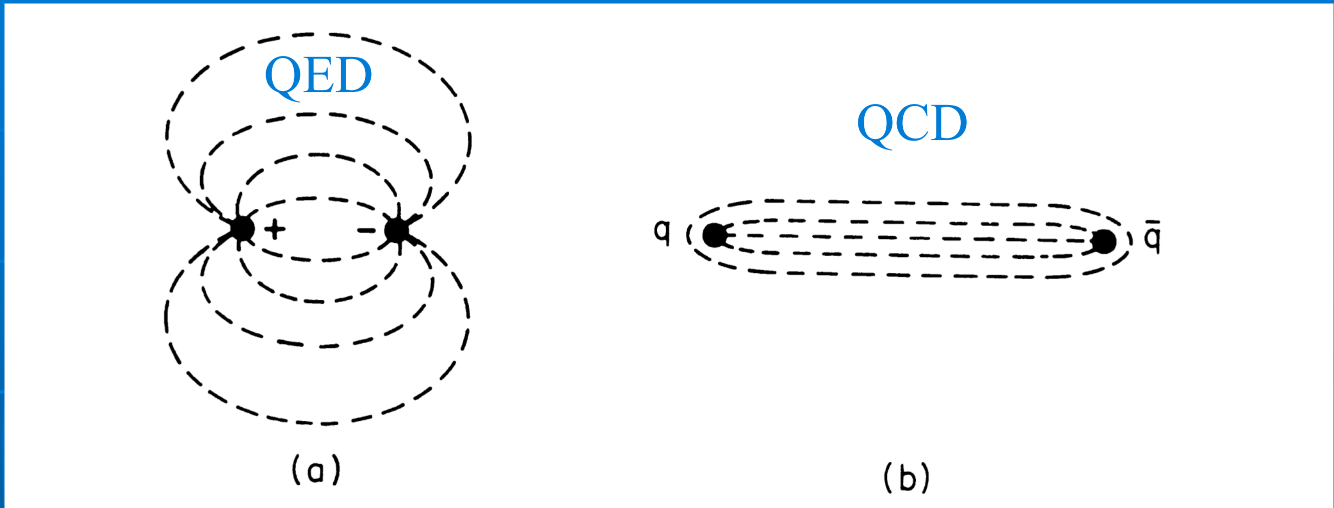

- In QCD, the field lines are compressed into a "flux tube" (or "string") of constant cross-section (~fm^2), leading to a long-distance potential which grows linearly with r:

$$V_{long} = kr$$

with k ~ 1 GeV/fm

String breaking

- If one tries to pull the string apart, when the energy stored in the string ($k\,r$) reaches the point where it is energetically favourable to create a qq pair, the string breaks…
- …and one ends up with two colour-neutral strings (and eventually hadrons)

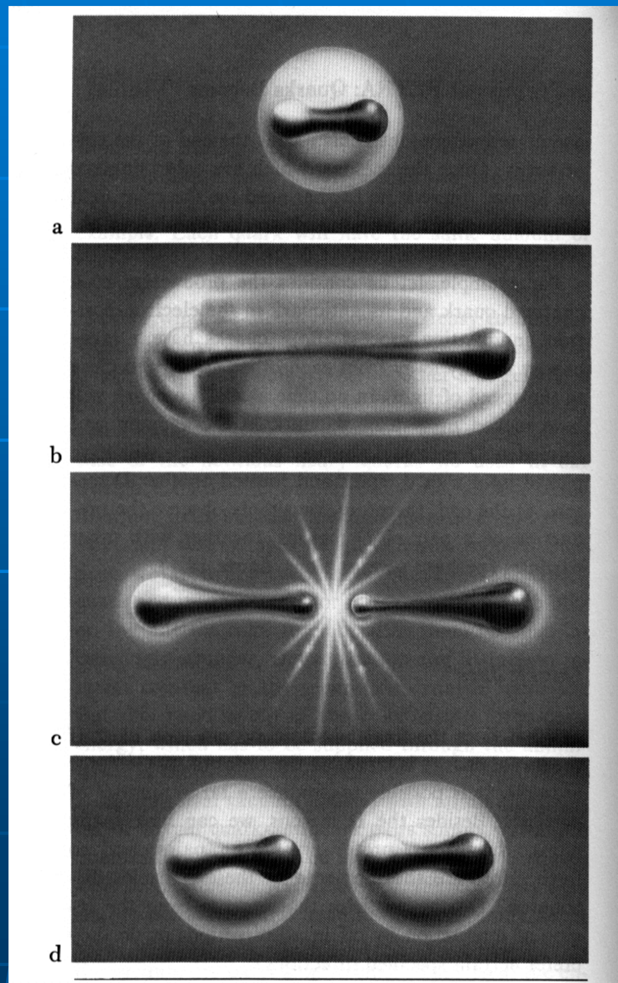

[illustration from Fritzsch]

Fig. 27.2. When a deep inelastic probe strikes a parton (*a*) and (*b*), it flies off with large momentum (*c*) until some confining mechanism pulls extra parton–antiparton pairs from the vacuum, creating new particles (*d*).

deep inelastic probe wavelength << interquark distance

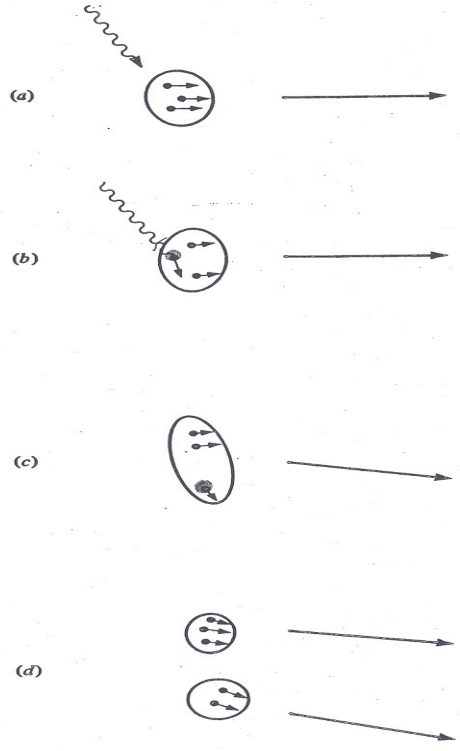

lines of force of the colour field form a flux tube or string

Pulling out this string, the stored energy reaches the point where it is energetically favourable to create a $Q\bar{Q}$ pair

Fig. 33.6. Head-on hadron–hadron collisions are described by simple quark and gluon processes, such as one-gluon exchange, which give rise to jets of hadrons emerging from the collisions.

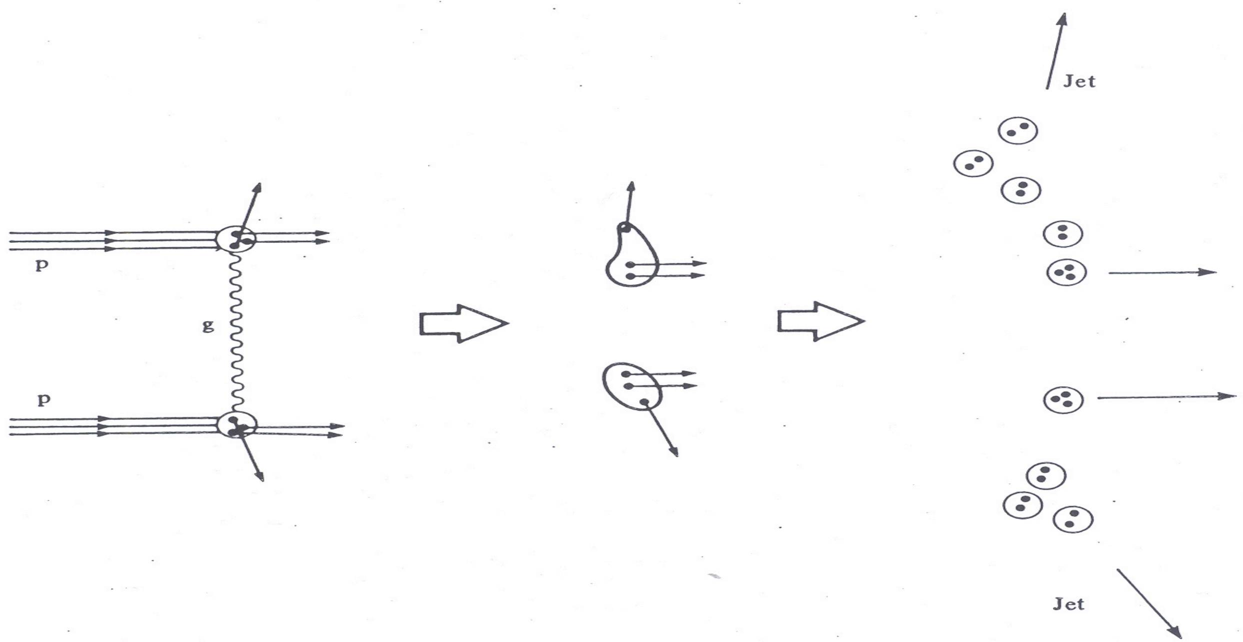

Jet and hadron production

Factorization:

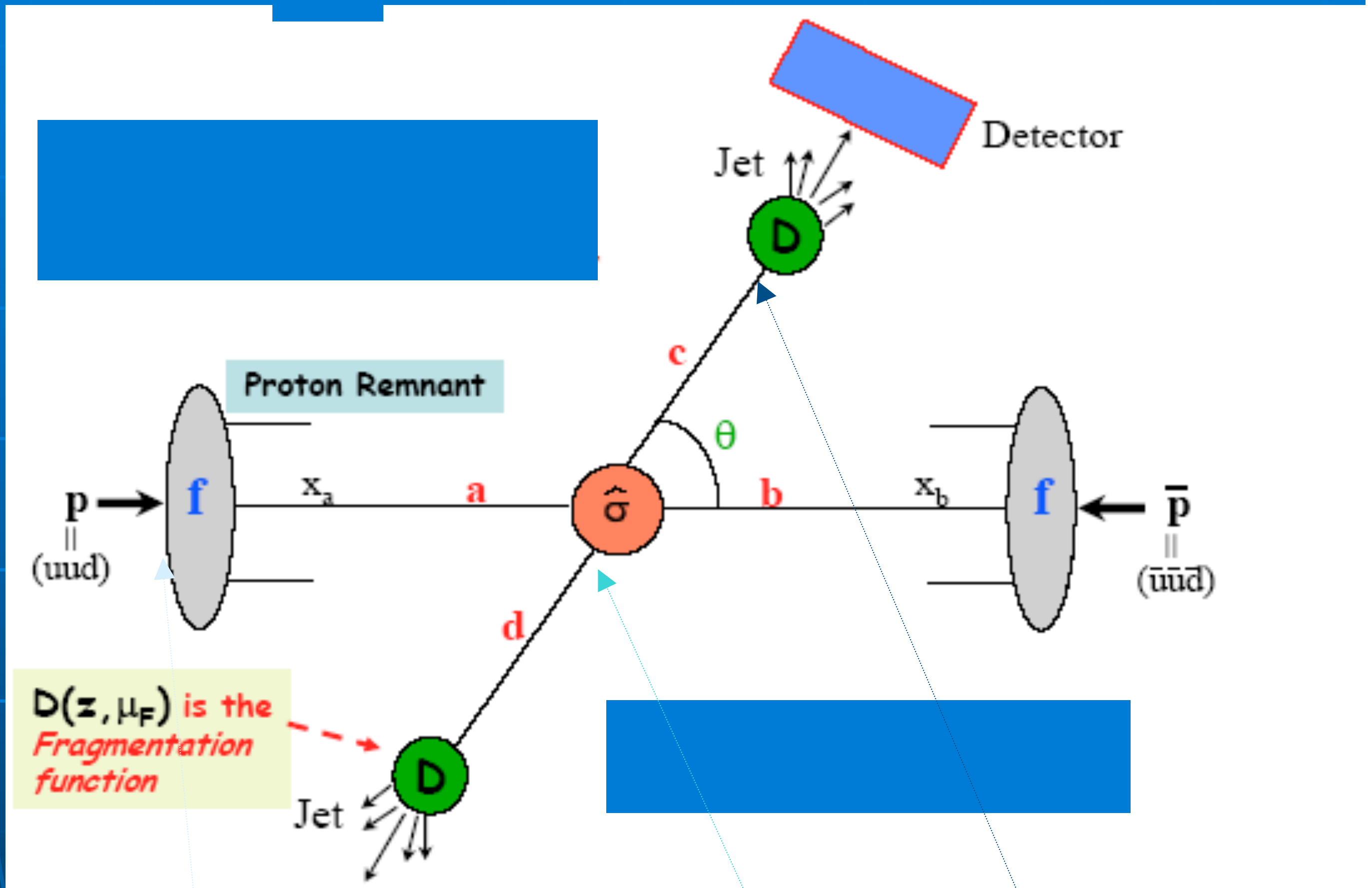

$$E\frac{d^3\sigma}{dp^3} \propto f_{a/A}\left(x_a, Q^2\right) \otimes f_{b/B}\left(x_b, Q^2\right) \otimes \frac{d\hat{\sigma}^{ab\to cd}}{dt} \otimes D_{h/c}\left(z_c, Q^2\right)$$

Hadrons to partons: jet reconstruction

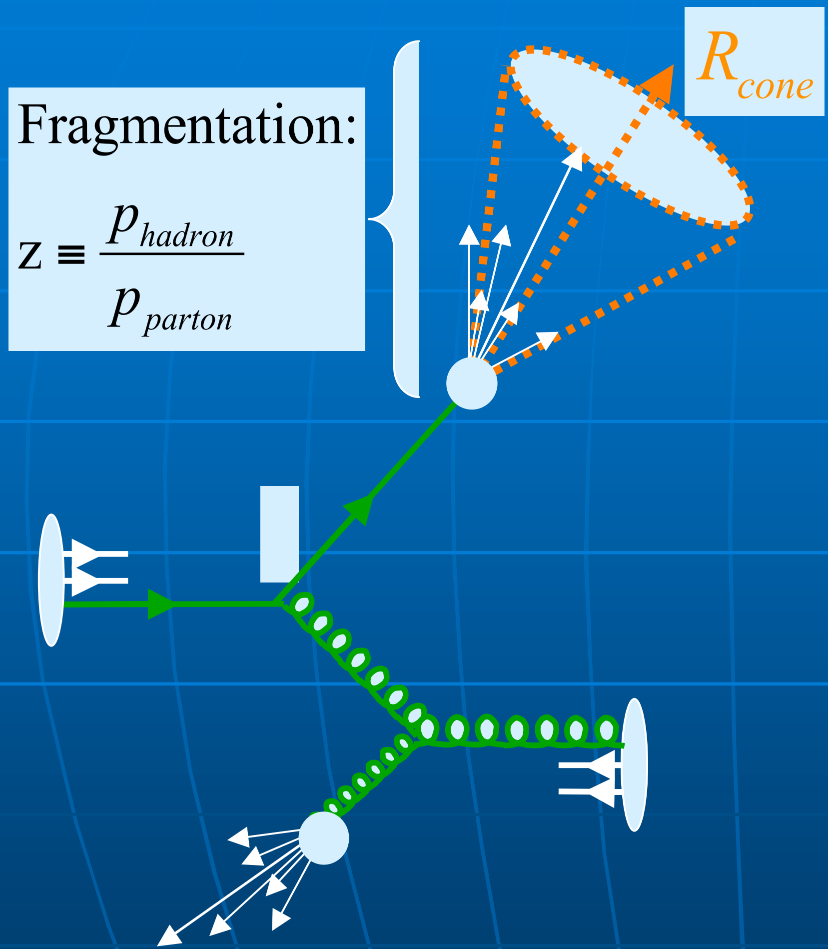

How to re-associate hadrons to reconstruct the partonic kinematics?

- experiment measures fragments of partons: hadrons and calorimeter towers (clusters of hadrons)
- pQCD theory calculates partons

Apply "same" jet clustering algorithm to data and theoretical calculations

- no unique prescription

p+pbar → dijet at Tevatron

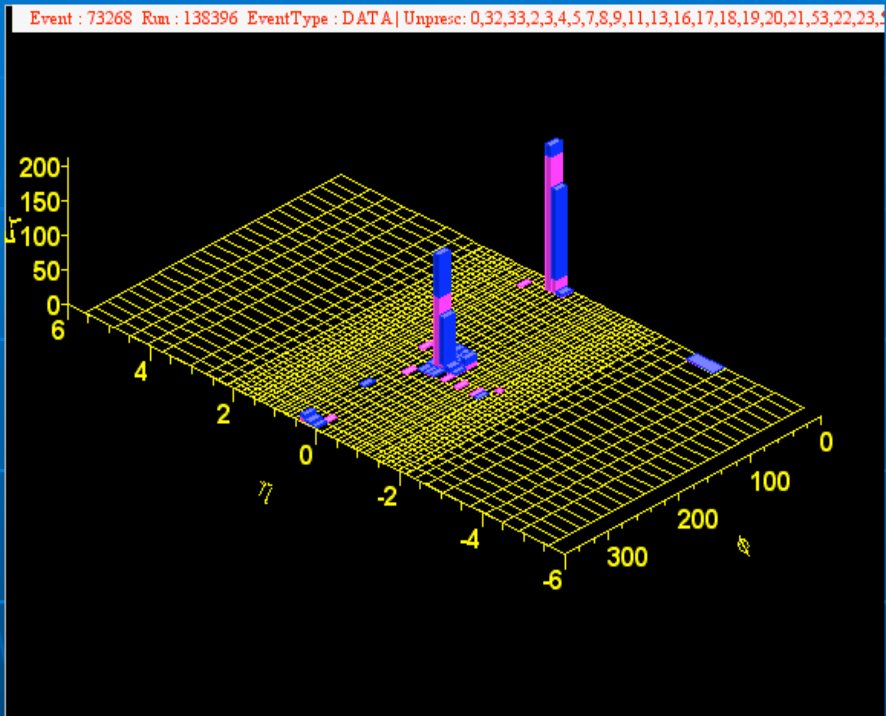

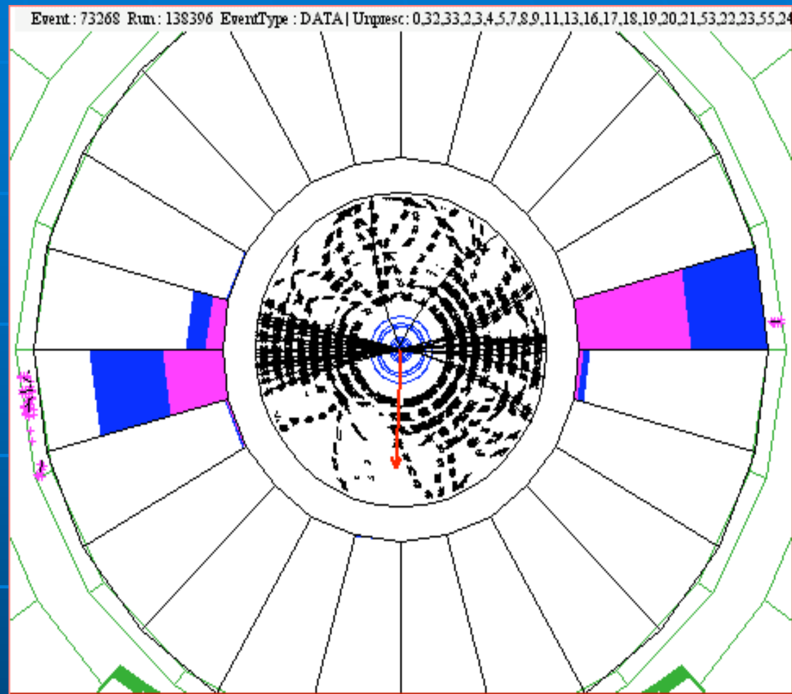

Aspetti sperimentali del JET Finding

LEP

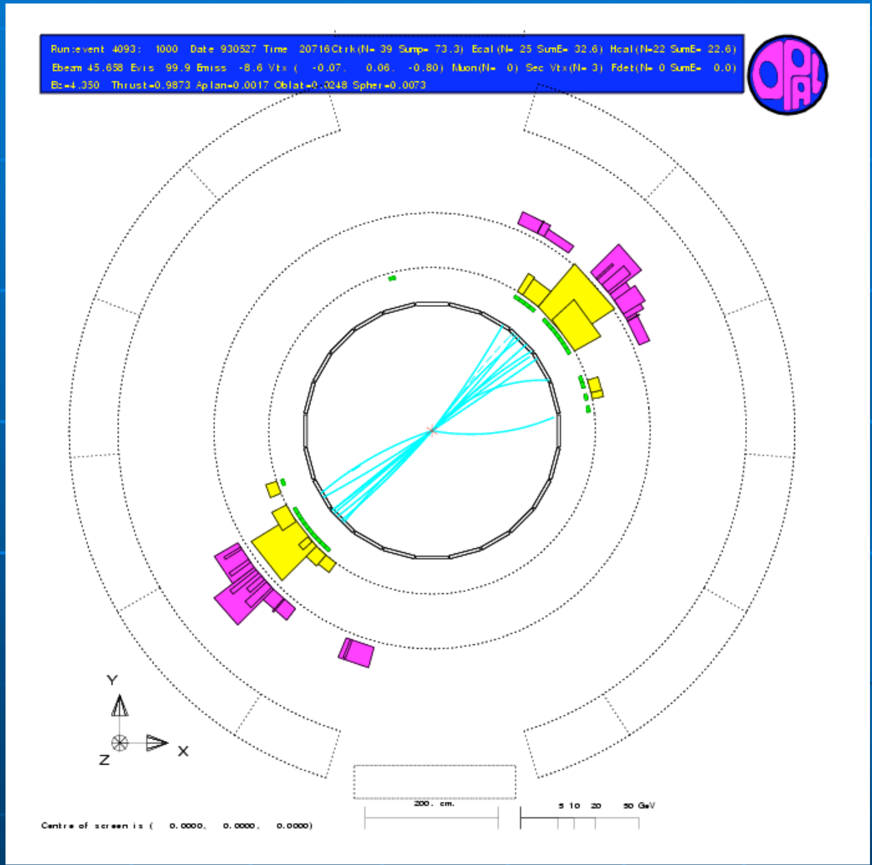

RHIC

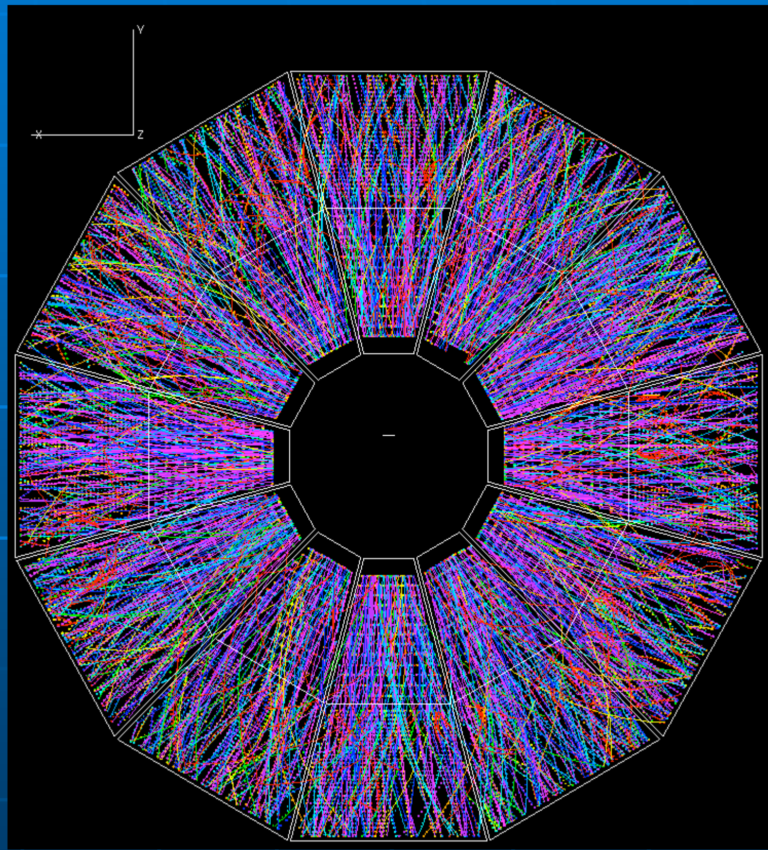

Inclusive jet production vs pQCD

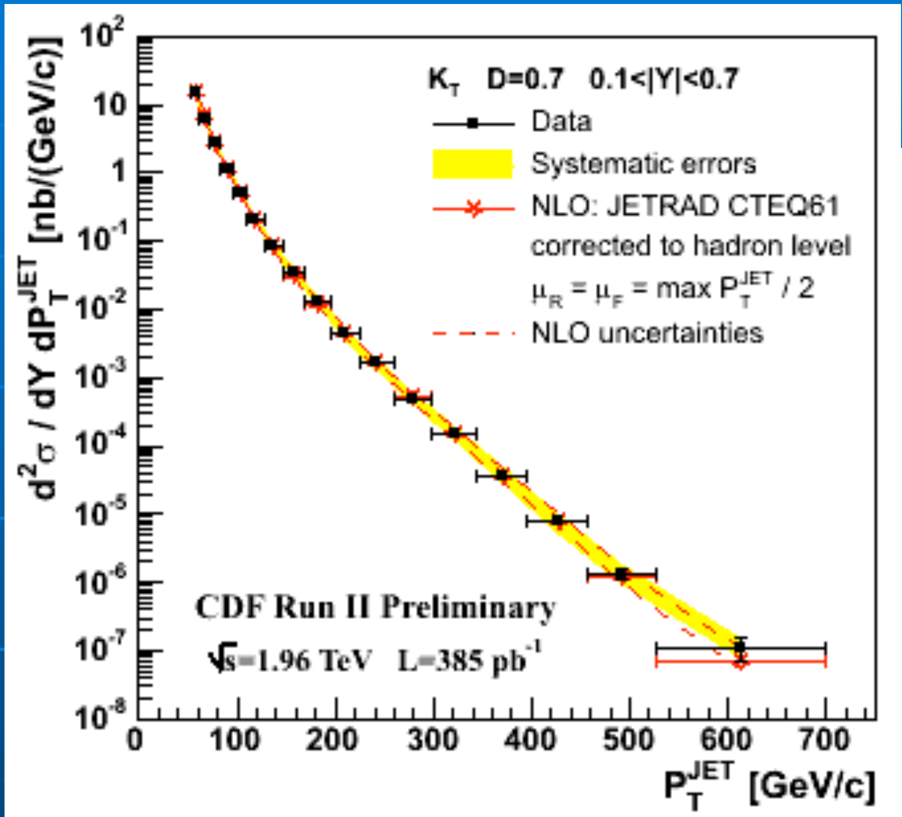

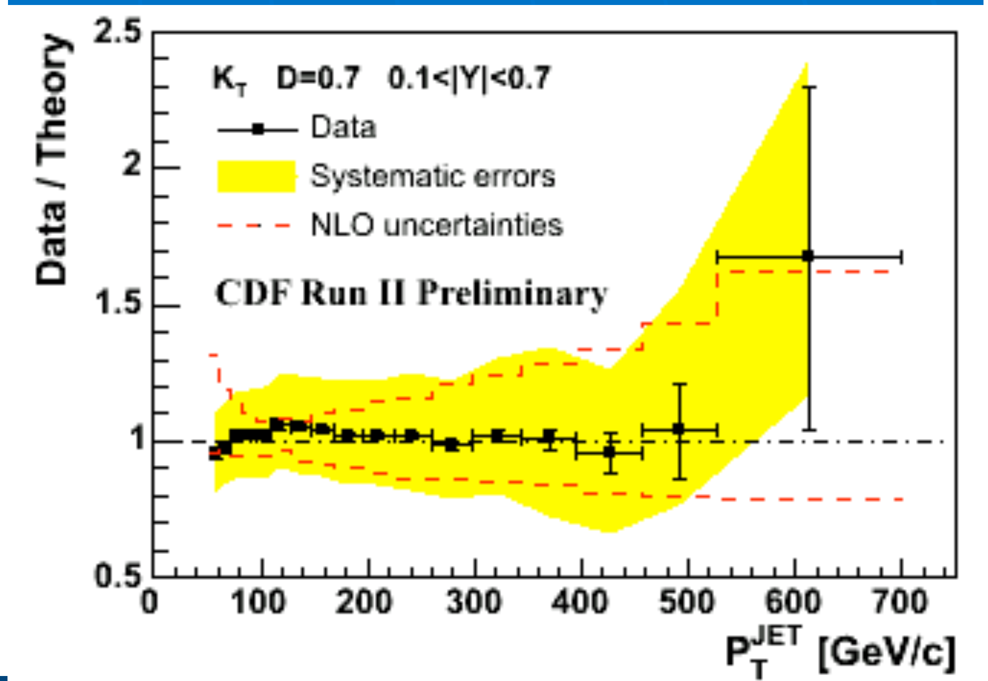

Good agreement over nine orders of magnitude

http://www-cdf.fnal.gov/physics/new/qcd/ktjets/ktjets.html

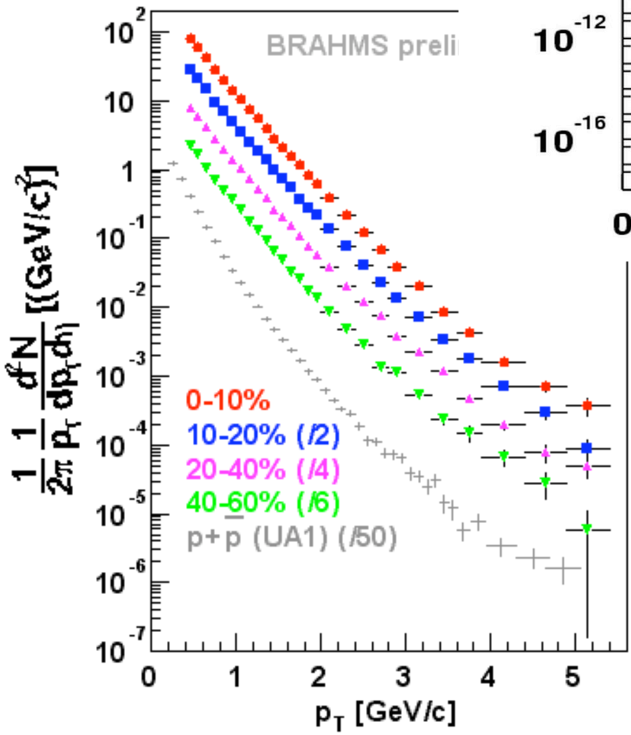
BRAHMS preli
0-10%
10-20% (/2)
20-40% (/4)
40-60% (/6)
p+p (UA1) (/50)
p_T [GeV/c]

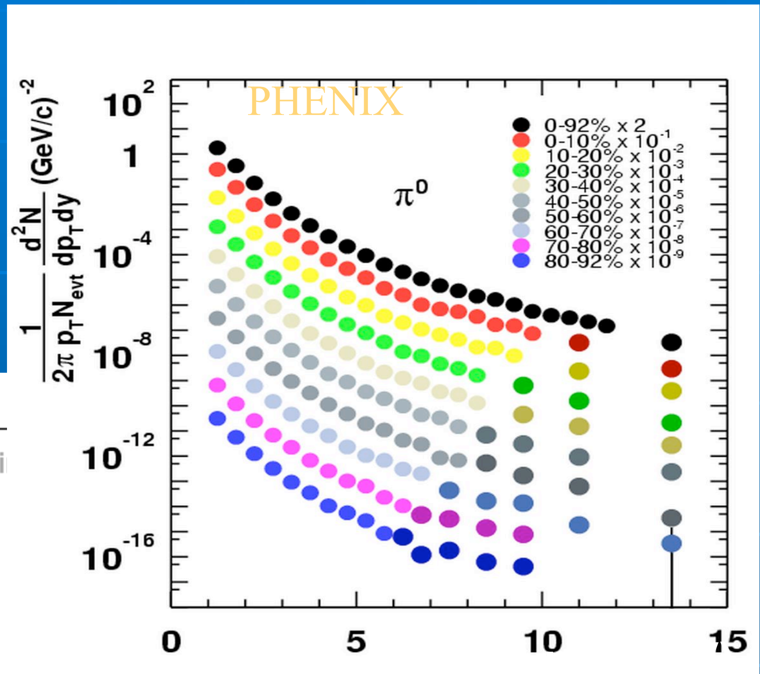
PHENIX
π0
0-92% x 2
0-10% x 10^-1
10-20% x 10^-2
20-30% x 10^-3
30-40% x 10^-4
40-50% x 10^-5
50-60% x 10^-6
60-70% x 10^-7
70-80% x 10^-8
80-92% x 10^-9

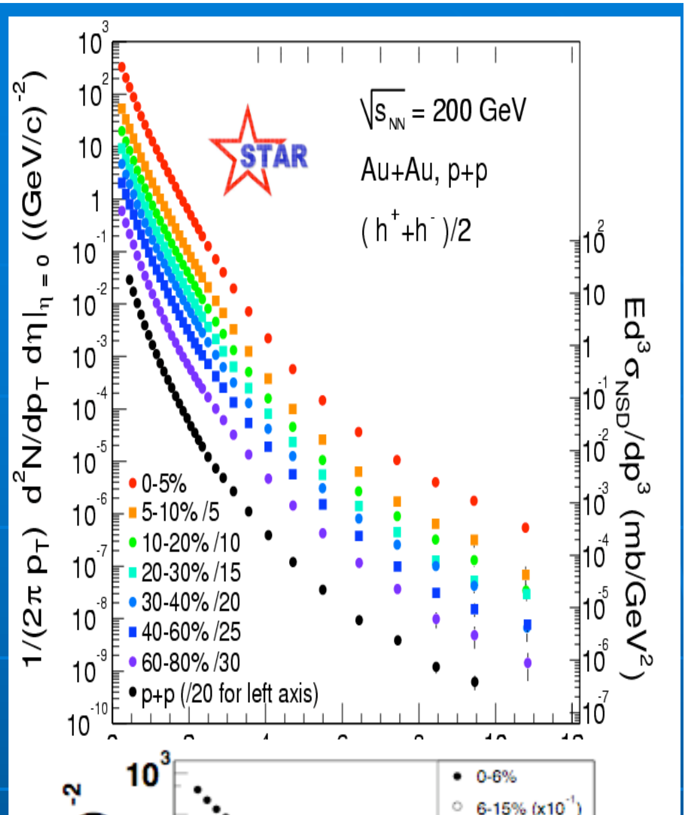
STAR
√s_NN = 200 GeV
Au+Au, p+p
(h+ + h-)/2
0-5%
5-10% /5
10-20% /10
20-30% /15
30-40% /20
40-60% /25
60-80% /30
p+p (/20 for left axis)

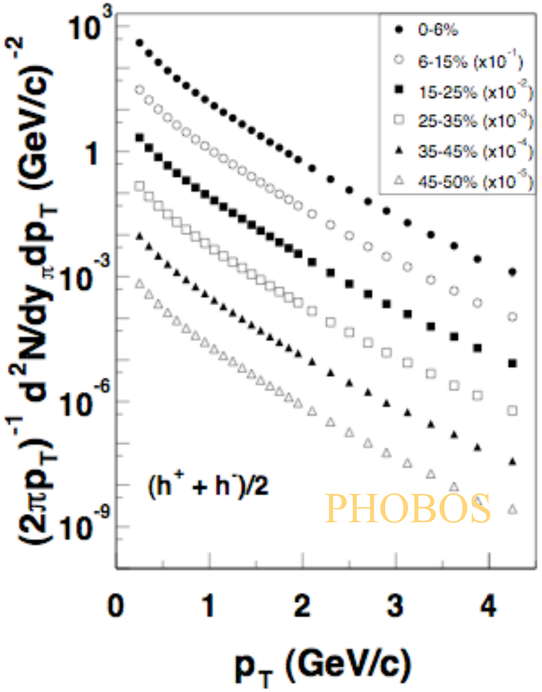
0-6%
6-15% (x10^-1)
15-25% (x10^-2)
25-35% (x10^-3)
35-45% (x10^-4)
45-50% (x10^-5)
(h+ + h-)/2
PHOBOS
p_T (GeV/c)

High p_T suppression

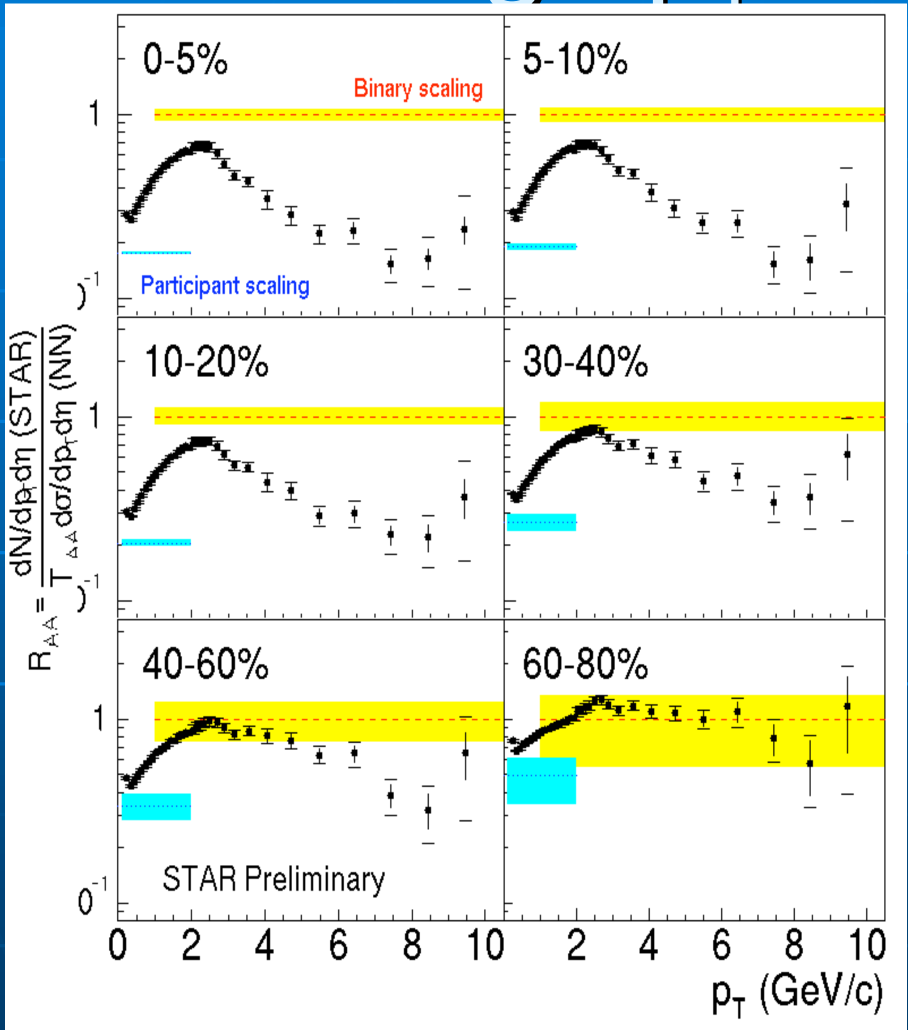

$$R_{AA} = \frac{\text{Yield}_{AA}}{\text{Yield}_{pp}} \cdot \frac{1}{\langle Nbin \rangle_{AA}}$$

- High p_T particle production expected to scale with number of binary NN collisions if no medium effects
- Clearly does not work for more central collisions

Partonic energy loss via leading hadrons

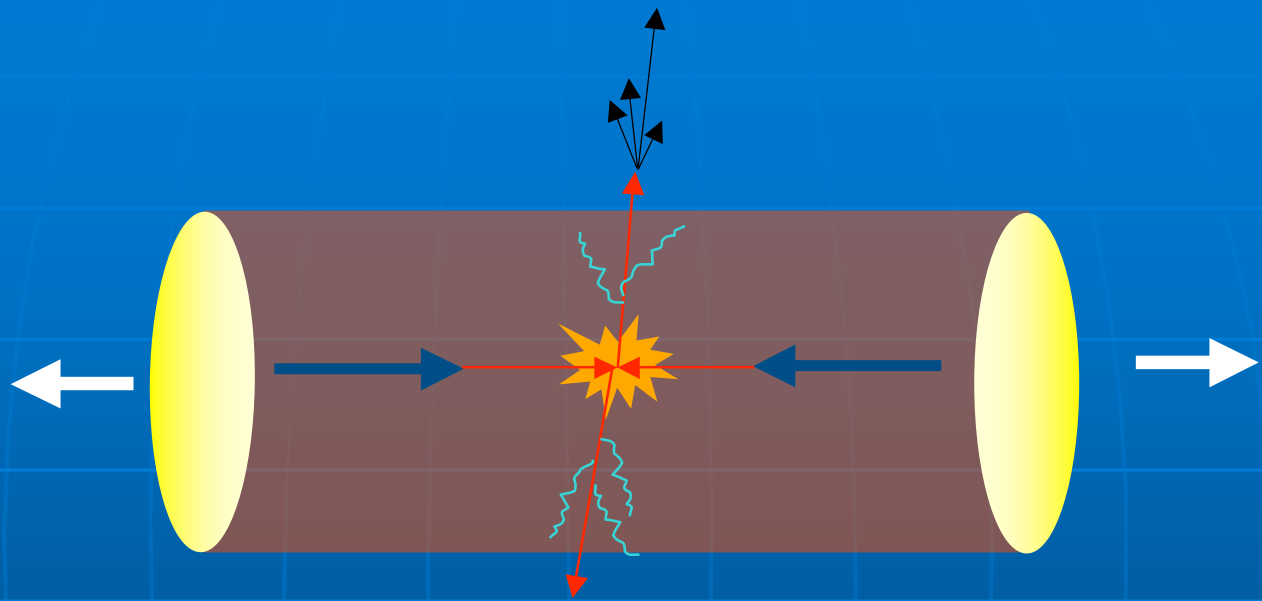

Energy loss $\Rightarrow$ softening of fragmentation $\Rightarrow$ suppression of leading hadron yield

$$R_{AA}(p_T) = \frac{d^2N^{AA}/dp_T d\eta}{T_{AA} d^2\sigma^{NN}/dp_T d\eta}$$

Binary collision scaling

p+p reference

Inclusive hadrons yields in central Au+Au collisions are

$$R_{AA}(p_T) = \frac{d^2N^{AA}/dp_T d\eta}{T_{AA} d^2\sigma^{NN}/dp_T d\eta}$$

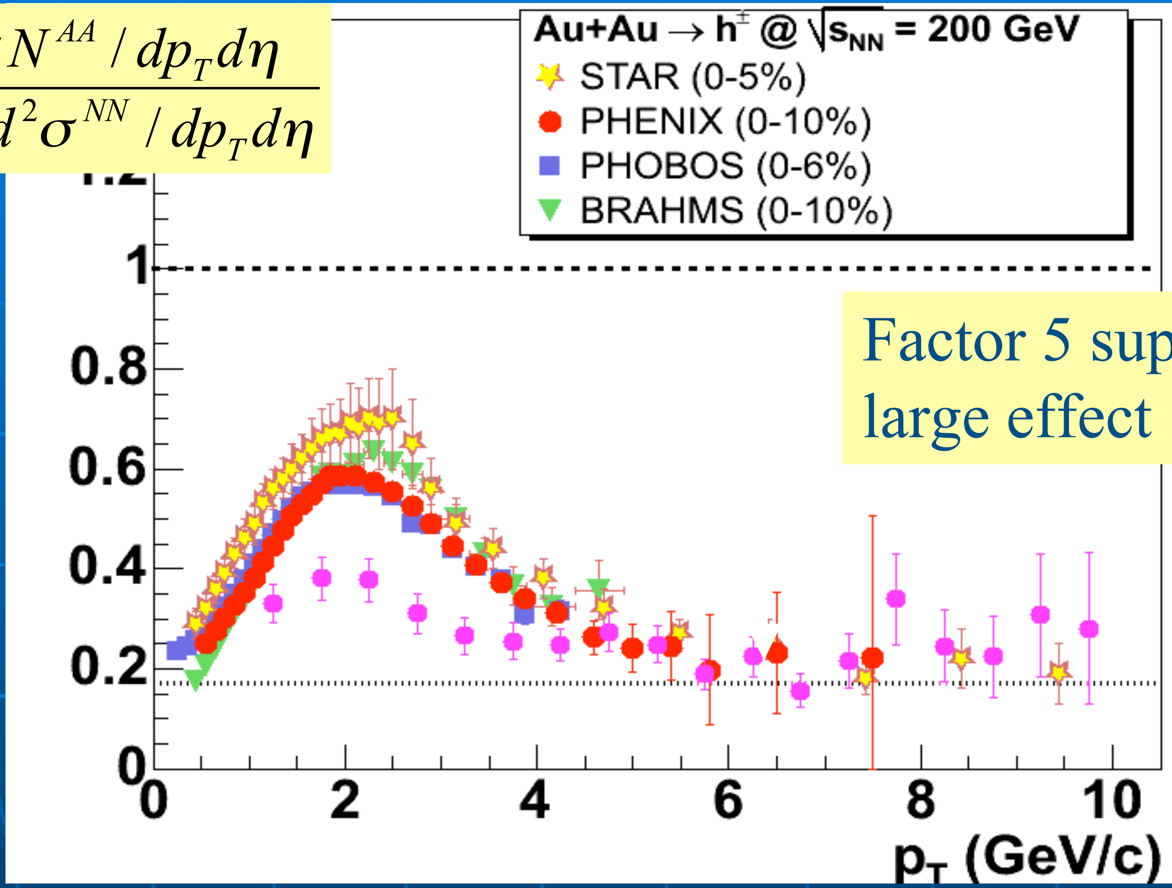

Factor 5 suppression: large effect

Qualitatively inconsistent with conventional nuclear effects:

- initial state multiple scattering ("Cronin enhancement")
- shadowing

Suppression of fast pions

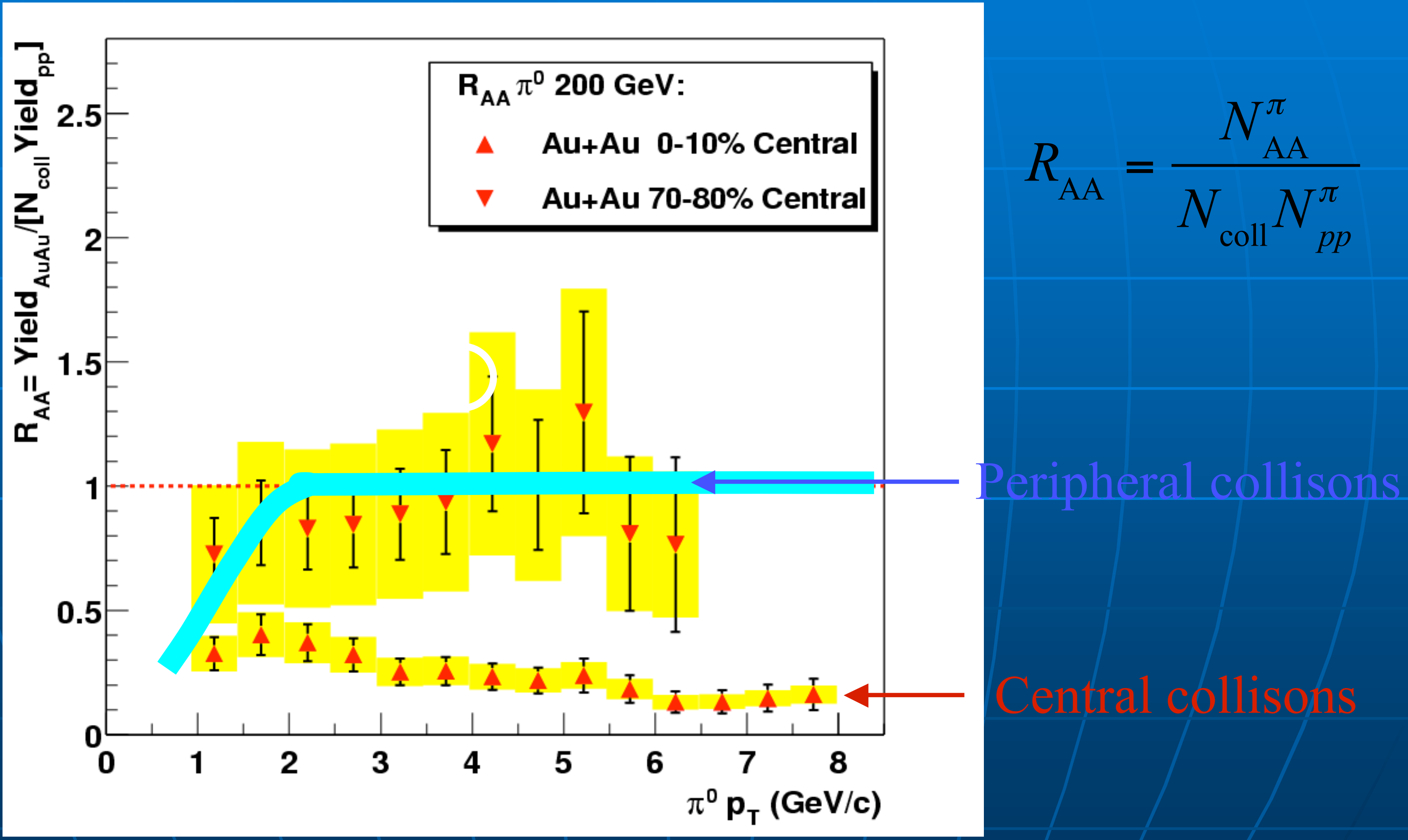

$$R_{AA} = \frac{N_{AA}^{\pi}}{N_{coll} N_{pp}^{\pi}}$$

Initial or final state effect?

Initial state?

e.g. gluon saturation

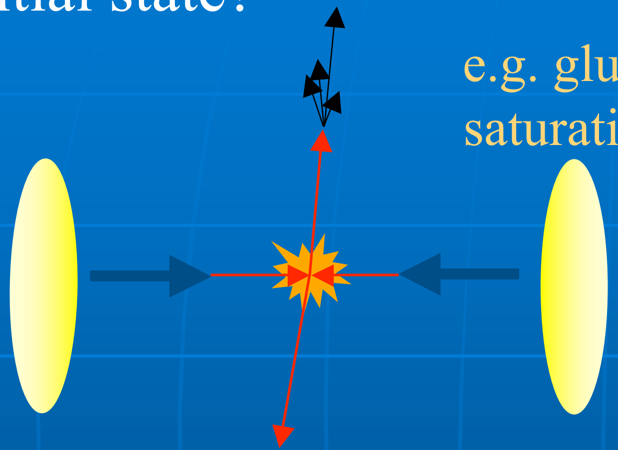

Final state?

partonic energy loss

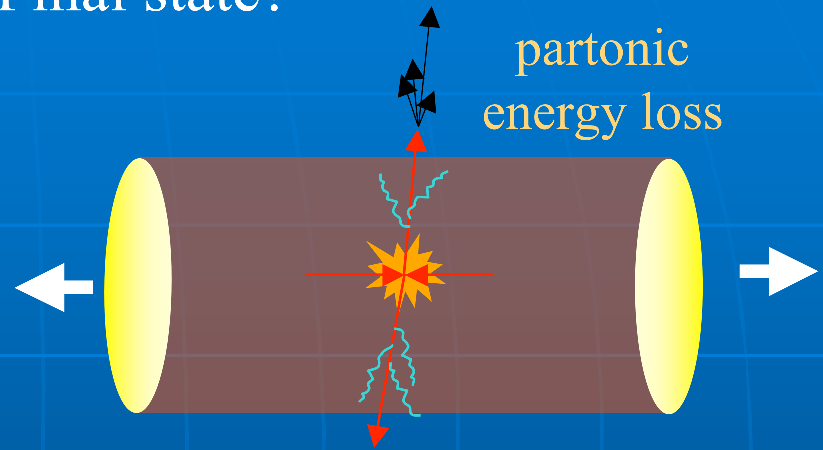

How to discriminate? Turn off final state ⇒ d+Au collisions

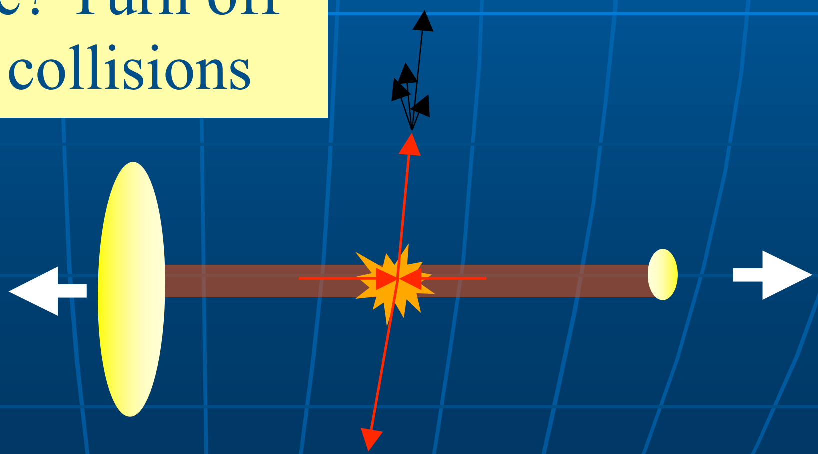

STAR

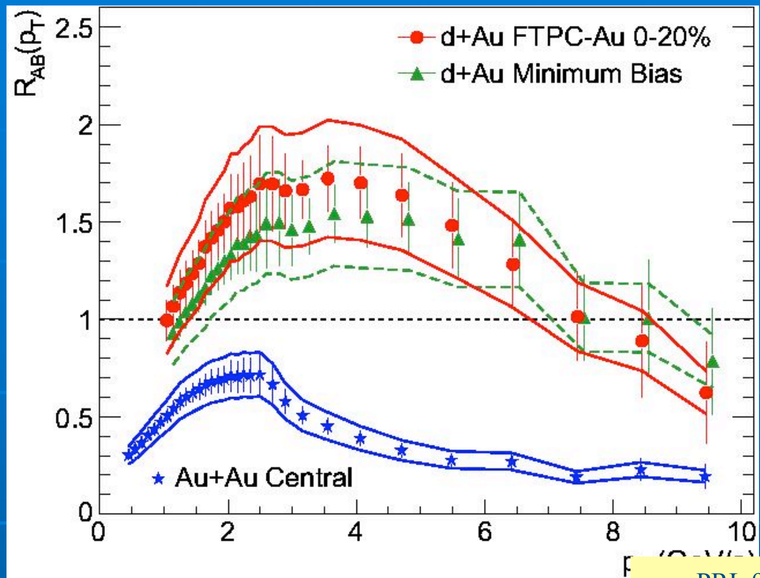

PHOBOS

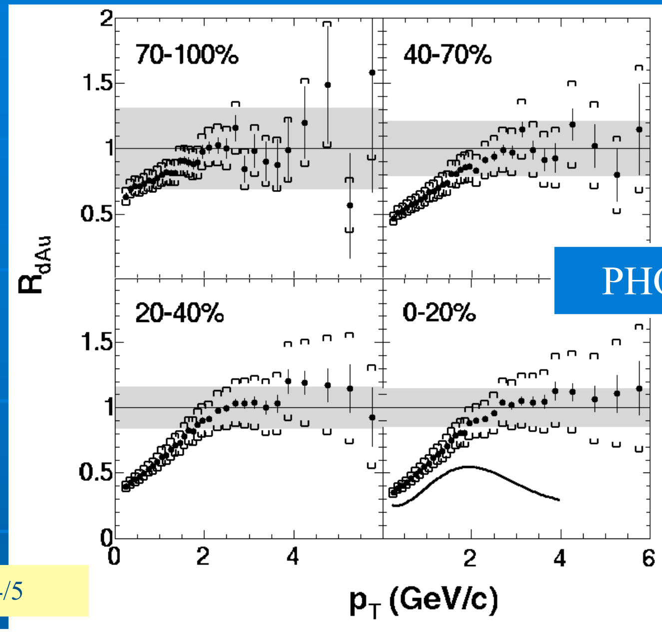

PRL 91, 072302/3/4/5

PHENIX

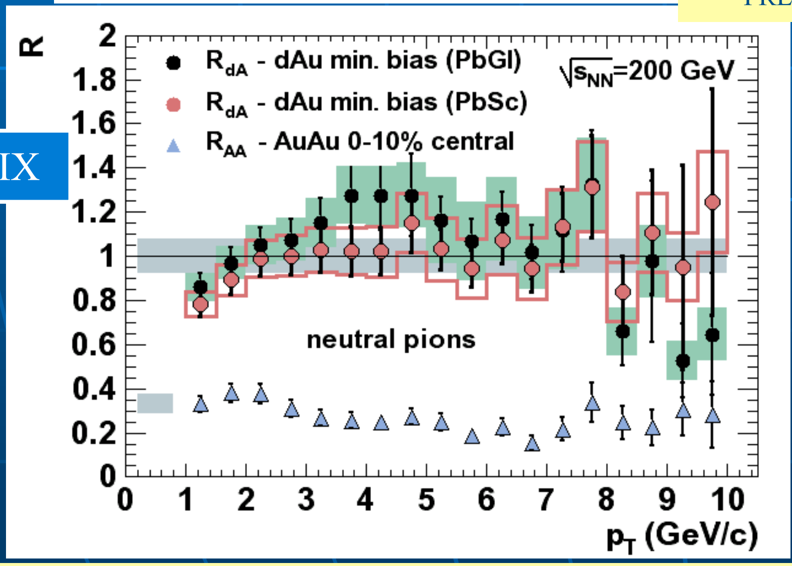

BRAHMS

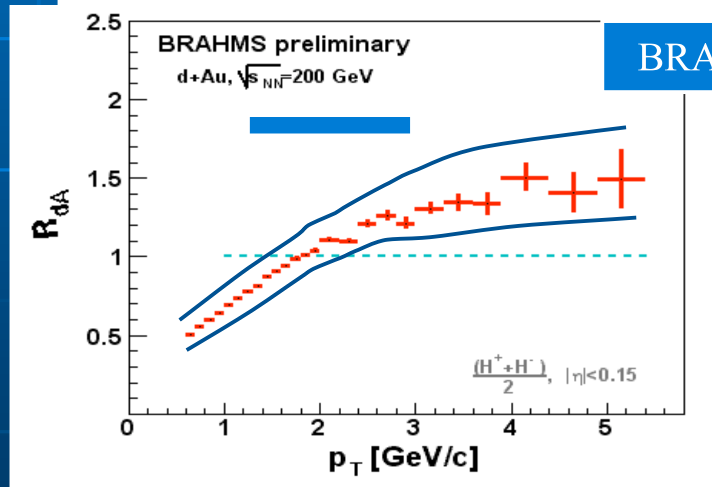

Hadron suppression in central Au+Au is a final state effect

Direct γ: dominant channel for p_T>10 GeV is Compton process

$q+g \rightarrow jet+\gamma$

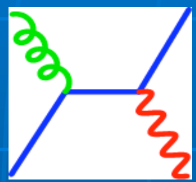

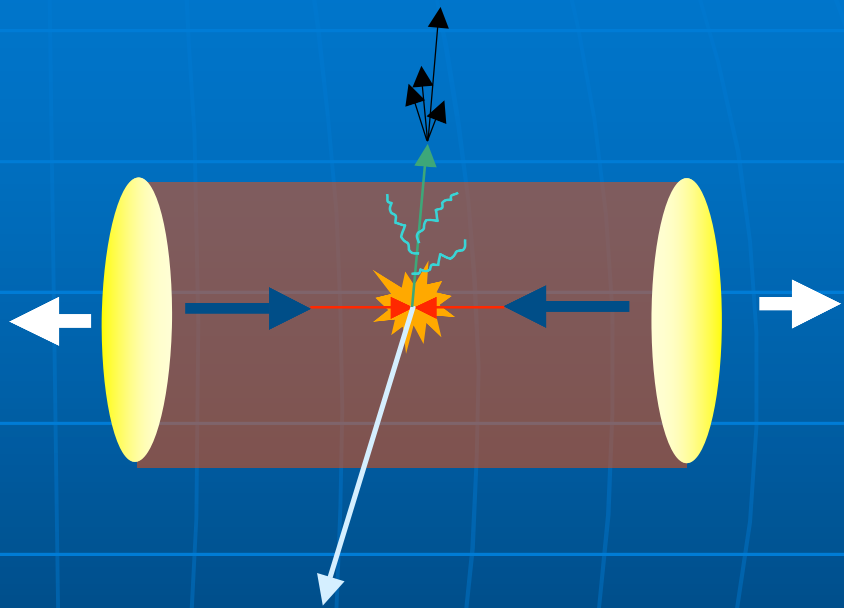

Photon does not carry color charge ⇒ production should not be suppressed by medium-induced radiation

Direct photons are not suppressed

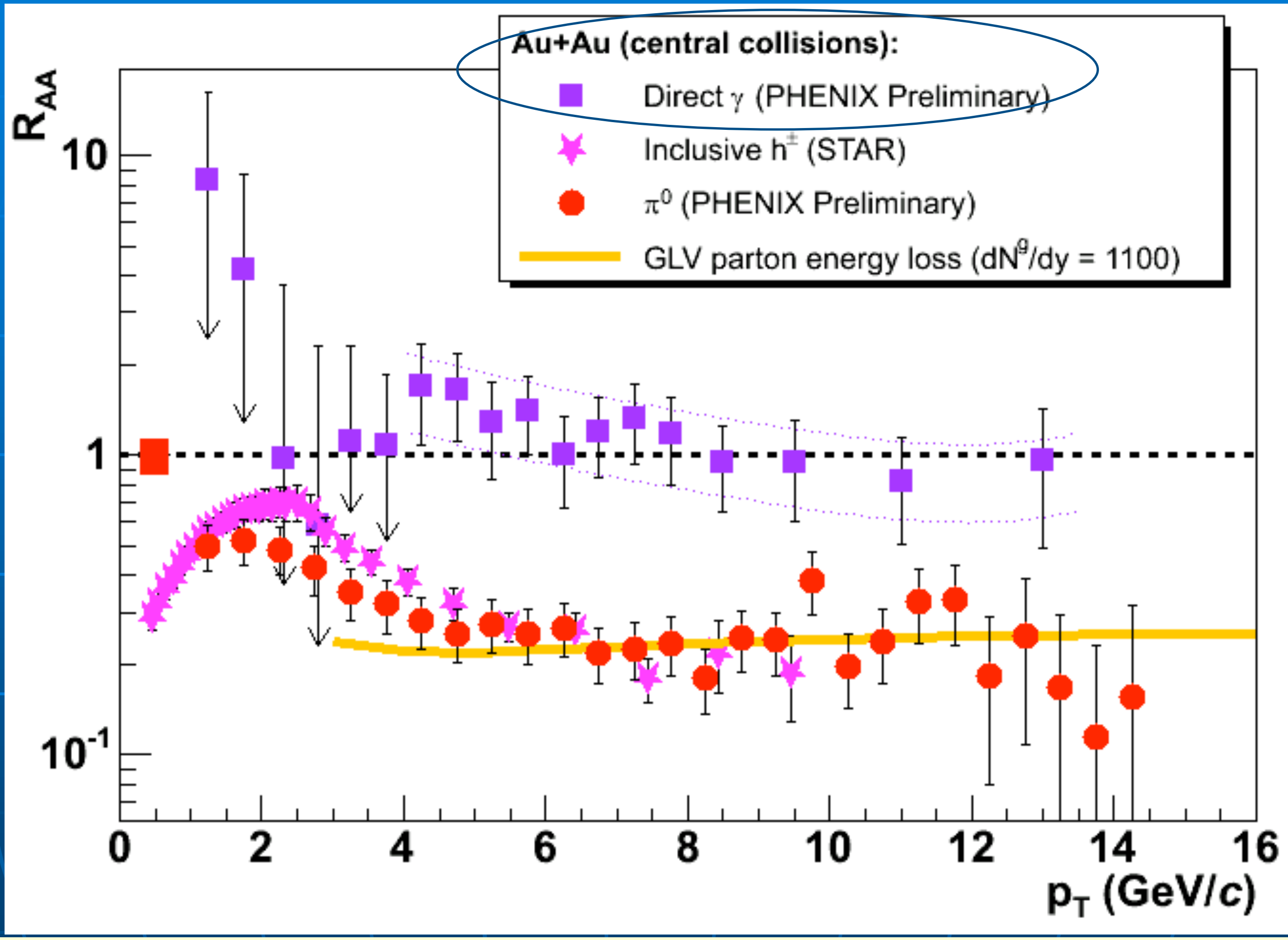

Photons scale as binary collisions while π^0 are suppressed:

⇒ consistent with partonic energy loss

Surface emission (“trigger bias”)

Eskola et al., hep-ph/0406319

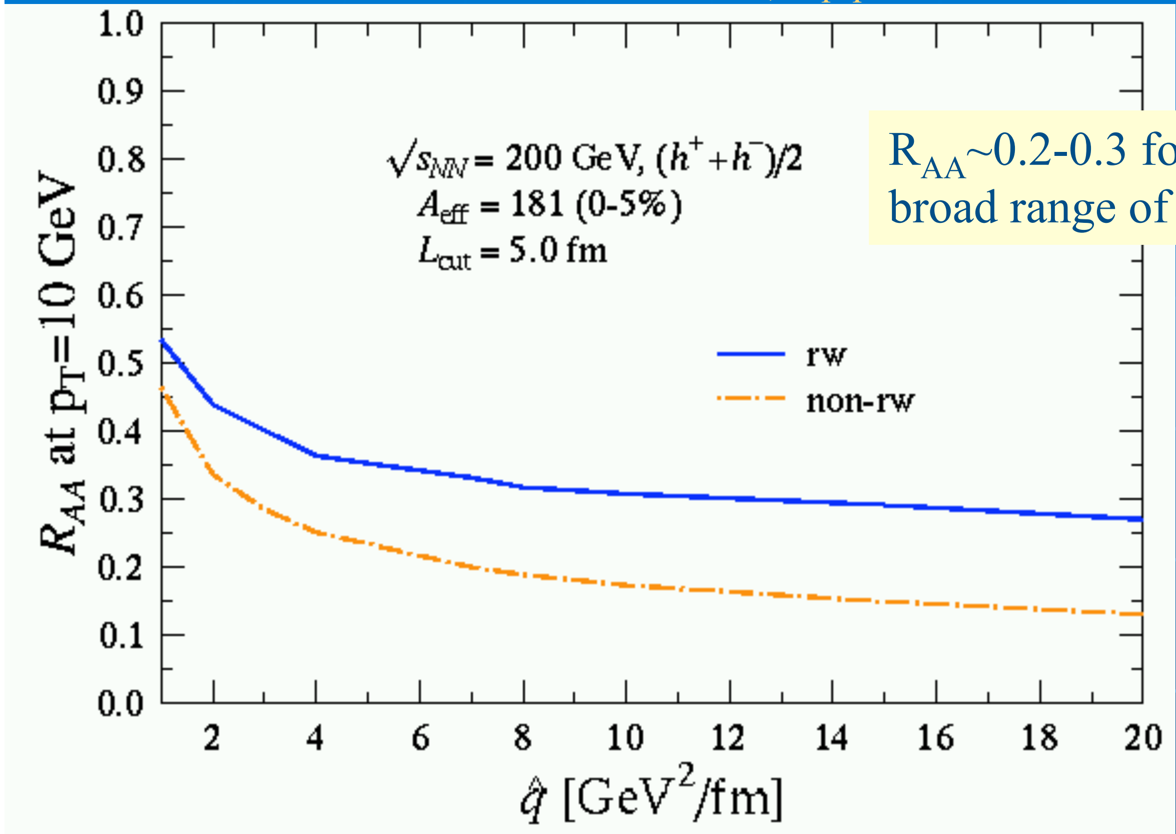

R_{AA}~0.2-0.3 for broad range of $\hat{q}$

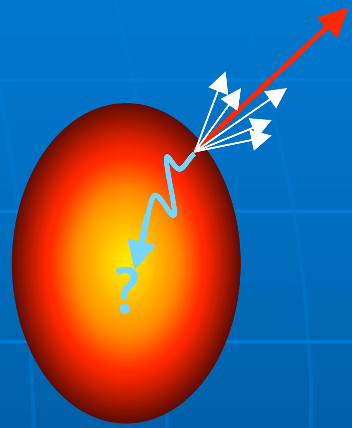

Large energy loss ⇒ opaque core

Inclusive measurements insensitive to opacity of bulk
⇒ need coincidence measurements to probe deeper

"Jets" via dihadron azimuthal distributions

p+p → dijet

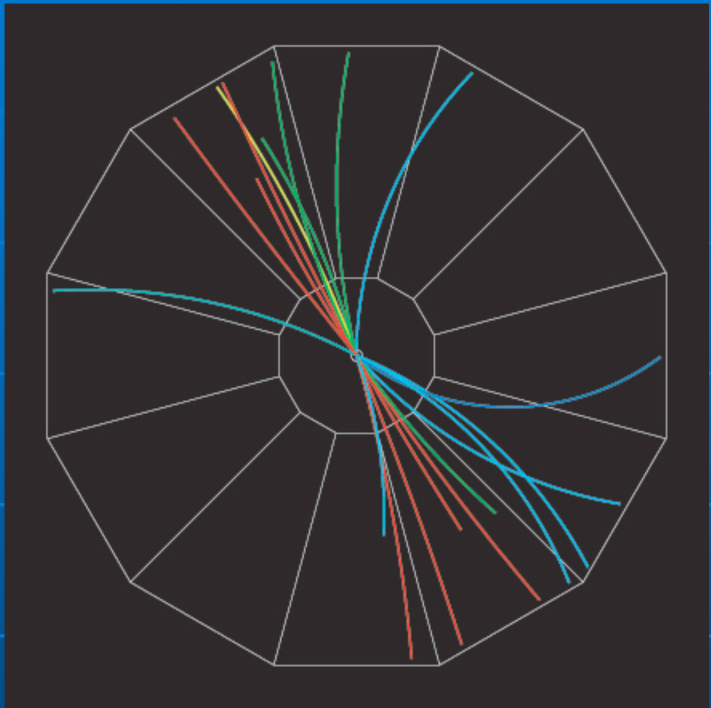

- trigger: highest p_T track, p_T>4 GeV/c
- $\Delta\phi$ distribution: 2 GeV/c<p_T<$p_T^{trigger}$
- normalize to number of triggers

Phys Rev Lett 90, 082302

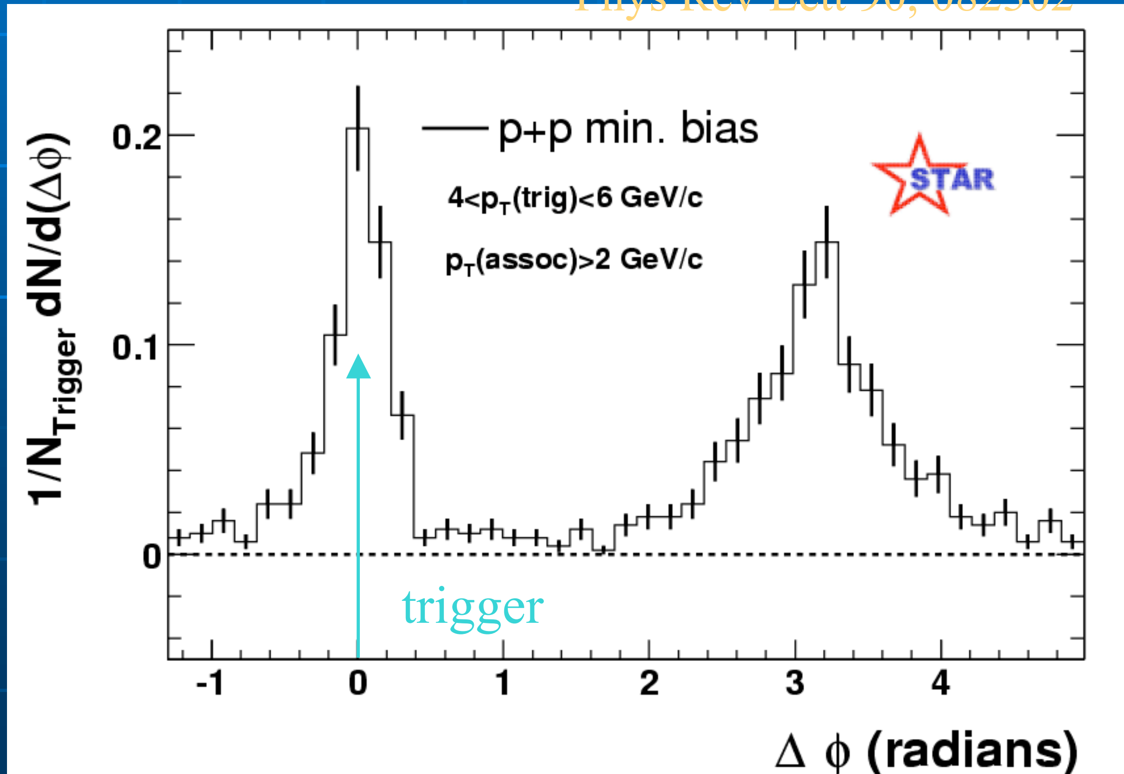

Dihadrons in Au+Au vs p+p

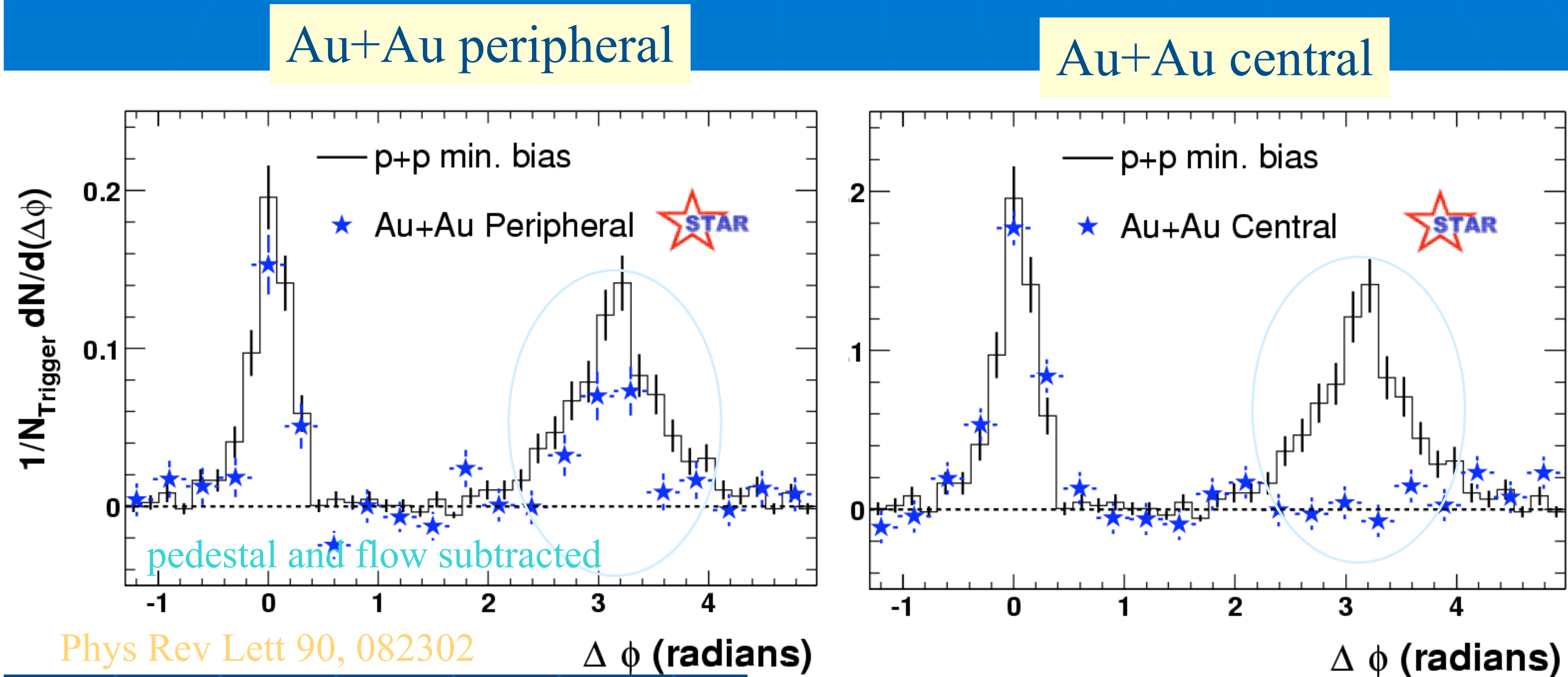

Near-side: peripheral and central Au+Au similar to p+p
⇒ trigger bias: recoil heads towards core

Strong suppression of back-to-back correlations in central Au+Au

Azimuthal Correlations (pp)

- In high energy collisions particles are correlated in azimuth due to jets

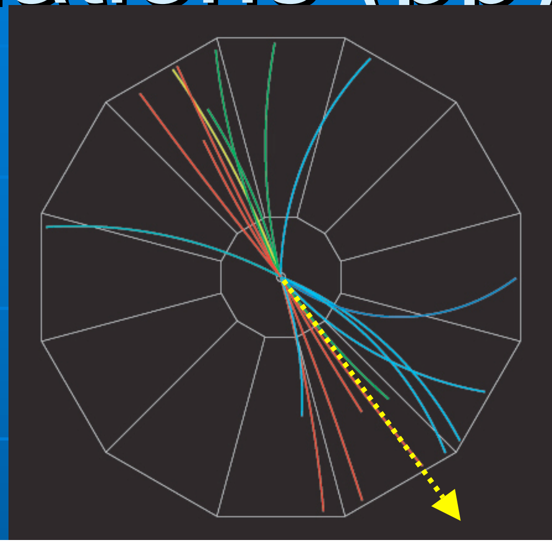

- e.g.: at RHIC in proton-proton collisions from STAR
  - "trigger" particle: $4 < p_T < 6$ GeV/c
  - associated particles: $p_T > 2$ GeV/c

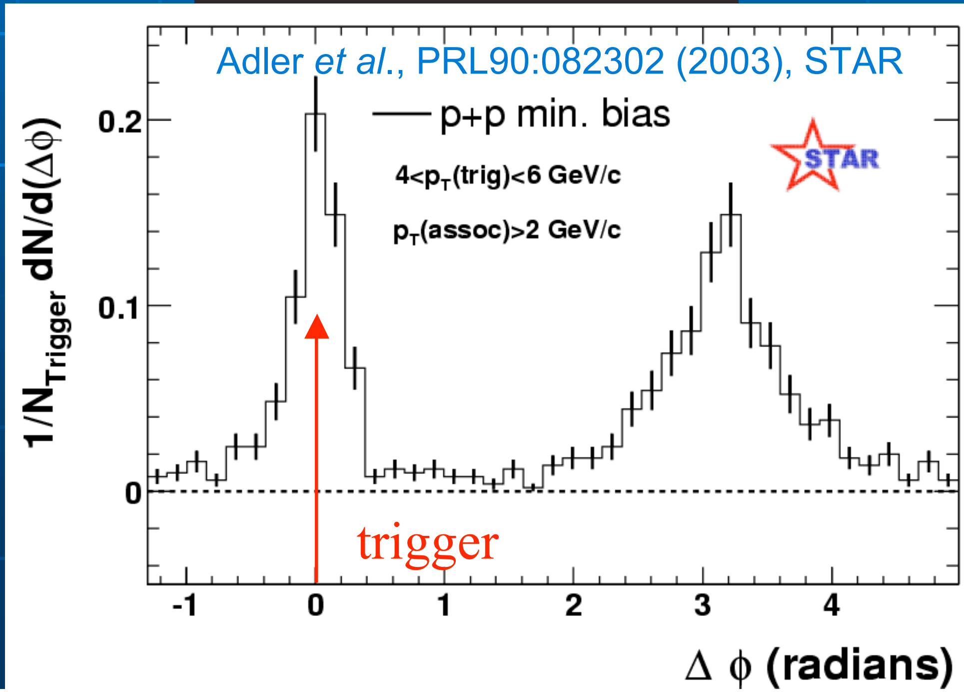

Initial or final state effect?

Initial state?

e.g. gluon saturation

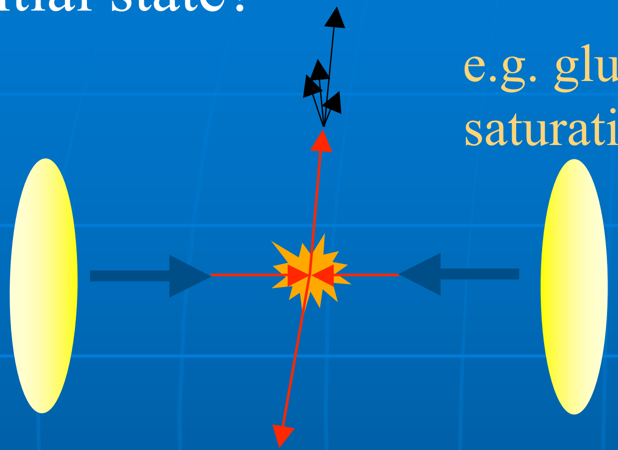

Final state?

partonic energy loss

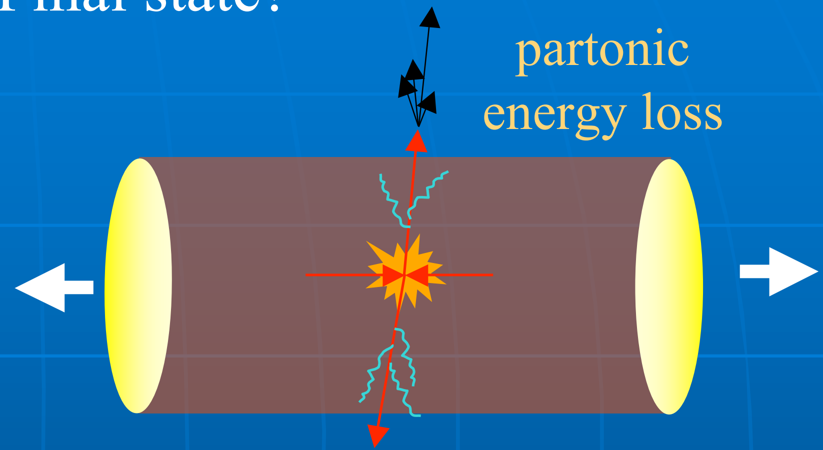

How to discriminate? Turn off final state ⇒ d+Au collisions

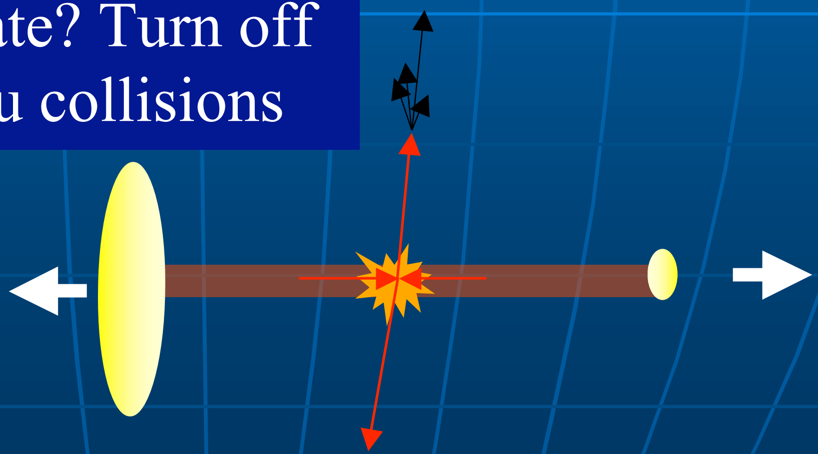

Final state suppression? d+Au dihadrons

Phys Rev Lett 91, 072304

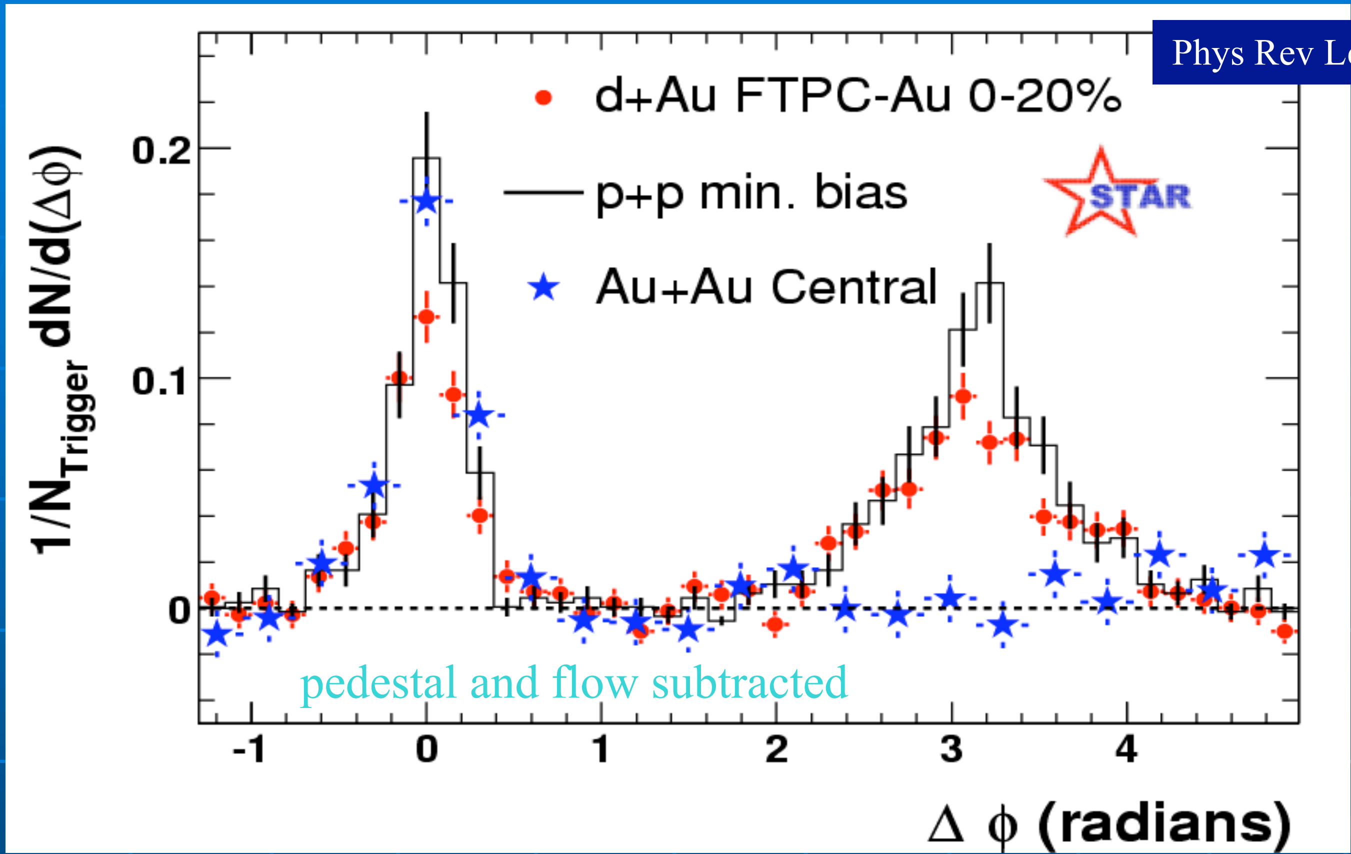

Near-side: p+p, d+Au, Au+Au similar

Back-to-back: Au+Au strongly suppressed relative to p+p and d+Au

Suppression of the back-to-back high p_T correlation in central Au+Au is a final-state effect

Jet quenching at RHIC: Summary

High p_T measurements:

✓inclusive hadrons suppressed
✓direct photons unsuppressed (no color charge)
✓ near-side dihadron correlations ~unchanged
✓ back-to-back dihadron correlations suppressed
✓azimuthal modulation of correlations vis a vis reaction plane

Consistent picture: core of reaction volume is opaque to jets

$\Rightarrow$ surface-biased trigger
observed jets fragment in vacuum

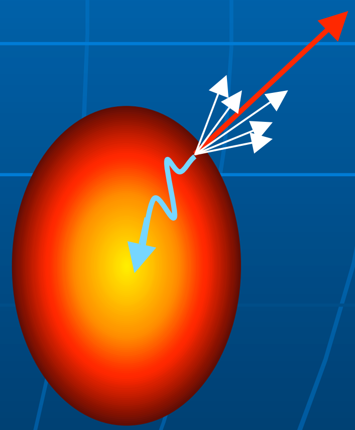

Dihadrons in Au+Au vs p+p

Au+Au peripheral

Au+Au central

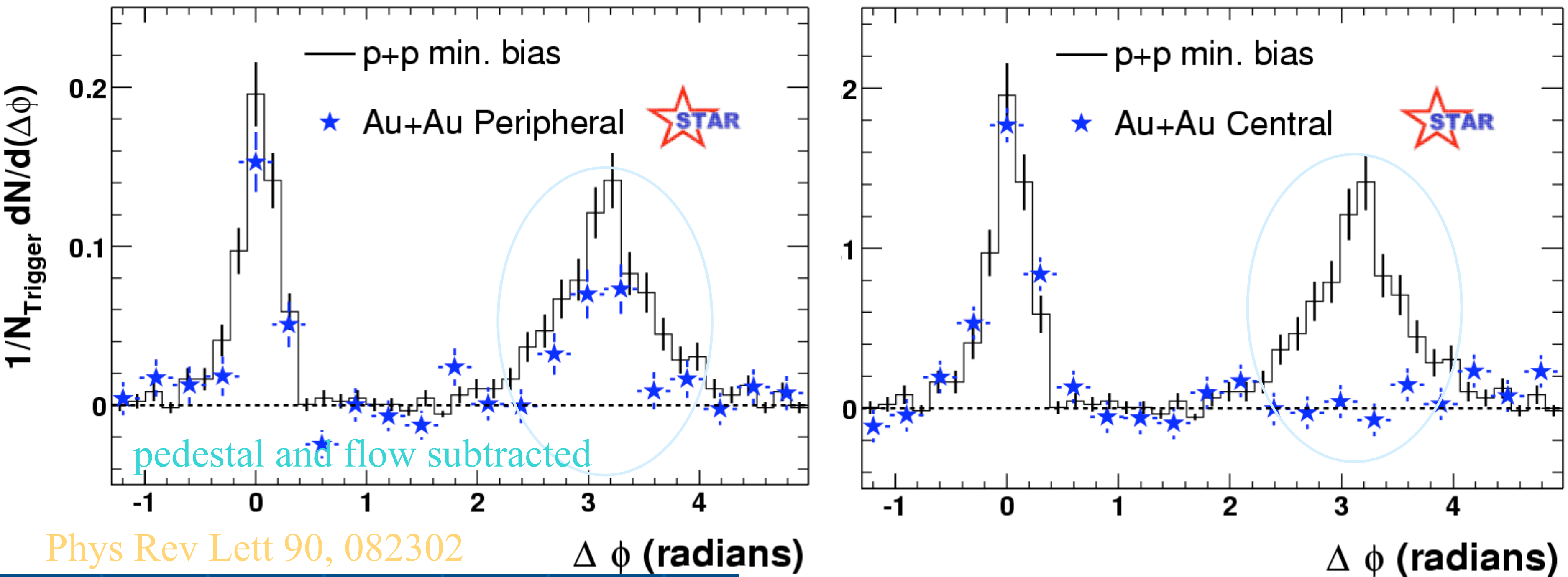

Phys Rev Lett 90, 082302

Near-side: peripheral and central Au+Au similar to p+p
$\Rightarrow$ trigger bias: recoil heads towards core

Strong suppression of back-to-back correlations in central Au+Au

Jet quenching models

Fermi National Accelerator Laboratory

FERMILAB-Pub-82/59-THY
August, 1982

Energy Loss of Energetic Partons in Quark-Gluon Plasma:
Possible Extinction of High p_T Jets in Hadron-Hadron Collisions.

J. D. BJORKEN
Fermi National Accelerator Laboratory
P.O. Box 500, Batavia, Illinois 60510

Abstract

High energy quarks and gluons propagating through quark-gluon plasma suffer differential energy loss via elastic scattering from quanta in the plasma. This mechanism is very similar in structure to ionization loss of charged particles in ordinary matter. The dE/dx is roughly proportional to the square of the plasma temperature. For

FERMILAB-Pub-82/59-THY
August, 1982

Energy Loss of Energetic Partons in Quark-Gluon Plasma: Possible Extinction of High p_T Jets in Hadron-Hadron Collisions.

J. D. BJORKEN
Fermi National Accelerator Laboratory
P.O. Box 500, Batavia, Illinois 60510

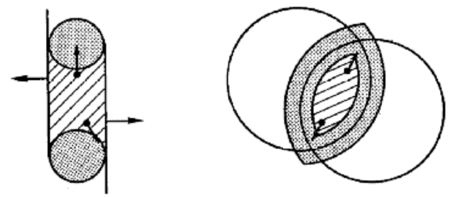
(a)

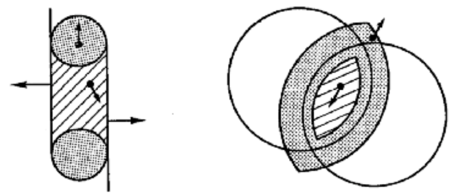
(b)

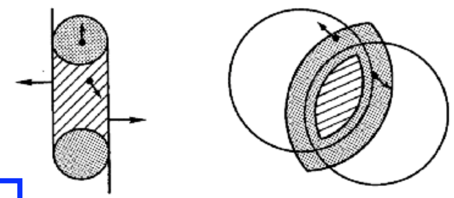
(c)

produced in its local environment. High energy hadron jet experiments should be analysed as function of associated multiplicity to search for this effect. An interesting signature may be events in which the hard collision occurs near the edge of the overlap region, with one jet escaping without absorption and the other fully absorbed.

RICHIAMI DI CINEMATICA

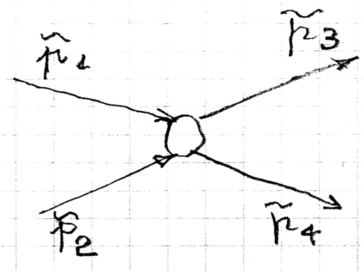

$\tilde{p}\,(E, \vec{p})$

$E^2 - |\vec{p}|^2 = m^2$

$$\begin{cases} s = (\tilde{p}_1 + \tilde{p}_2)^2 = (\tilde{p}_3 + \tilde{p}_4)^2 \\ u = (\tilde{p}_1 - \tilde{p}_4)^2 = (\tilde{p}_2 - \tilde{p}_3)^2 \\ t = (\tilde{p}_1 - \tilde{p}_3)^2 = (\tilde{p}_2 - \tilde{p}_4)^2 \end{cases}$$

$$s + t + u = \sum_{1}^{4}{}_i\, m_i^2$$

- $\underline{\text{cross section}}$ $\equiv$ number of events per second per unit incoming flux per target particle

- (Möller) $\underline{\text{Invariant Flux Factor}}$

$$f = \left[(\tilde{p}_1 \cdot \tilde{p}_2)^2 - m_1^2 m_2^2 \right]^{1/2}$$

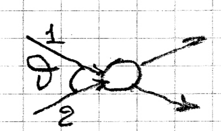

for $m_1 = m_2 = 0$ $\quad E = |\vec{p}| = p$

$$f = p_1 p_2 (1 - \cos\vartheta)$$

for $\underline{\text{collinear}}$ collisions $\vartheta = \pi$

$$f = 2 p_1 p_2$$

B. Rossi High Energy Particles 4ª ed. pag 24-25

distinzione tra "close collisions" (la particella eietta un elettrone dal mezzo con energia $> \eta$) e "distant collisions".

- se $10^4\,eV < \eta < 10^5\,eV$ possiamo trattare gli elettroni come liberi.

$$\left(dE/dx\right)_{(>\eta)} = 2\frac{C\, m_e}{\beta^2}\left[\ln\frac{T_{max}}{\eta} - \beta^2\right]$$

$$C = \pi N_A \frac{Z}{A} r_e^2 = 0.150\frac{Z}{A}\ g^{-1}\,cm^2$$

[N_A = numero di Avogadro; Z e A del mezzo. r_e = raggio classico dell'elettrone; β velocità particella incidente; T_{max} massima energia trasferibile all'elettrone bersaglio]

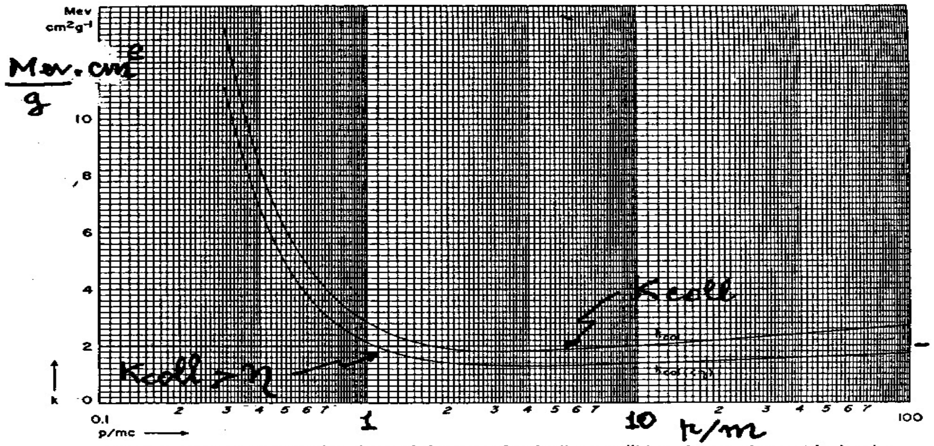

$\eta = 10^4\,eV$

Fig. 2.5.1. The total collision loss, k_{col}, and the energy loss in distant collisions, $k_{col(<\eta)}$, for particles heavier than electrons in air, as functions of p/mc ($\eta = 10^4$ ev). $k_{col(<\eta)}$ was computed from Eq. (2.5.1); k_{col} was obtained from a paper by Smith (SJH47).

PARTON ENERGY LOSS	
COLLISION QCD	1

$$\boxed{\frac{d\sigma}{dt} = \frac{\pi \alpha_s}{s^2}\,\overline{|M|^2}}$$

Scattering partone-partone QCD
(non polarizzati)

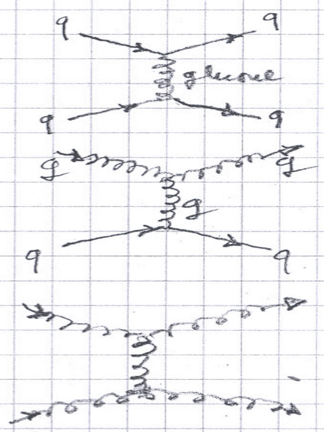

Processo	Diagramma dominante	$\overline{\lvert M\rvert^2}$
$qq \to qq$ $q\bar{q} \to q\bar{q}$		$\frac{4}{9}\left(\frac{s^2+u^2}{t^2}\right)$
$gq \to gq$ $qg \to qg$		$\left(\frac{s^2+u^2}{t^2}\right)$
$gg \to gg$		$\frac{9}{4}\left(\frac{s^2+u^2}{t^2}\right)$

$$s + t + u = \Sigma\, m_i^2 = 0 \qquad u^2 = s^2 + t^2 + 2st$$

$u^2 \sim s^2$ per $|t| \ll s$

$$\left.\frac{d\sigma}{dt}\right|_{|t|\ll s} = \frac{2\pi\alpha_s^2}{t^2}\begin{cases}(2/3)^2 & qq \to qq,\ q\bar{q}\to q\bar{q}\\ 1 & qg \to qg\\ \left(\frac{3}{2}\right)^2 & gg \to gg\end{cases}$$

C
(2 × colour factor)

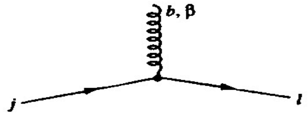

$ig(t^b)_{lj}\gamma^\beta$

quark–gluon
vertex

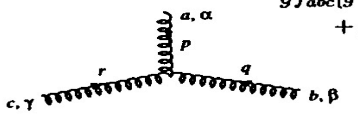

$$g f_{abc}[g^{\alpha\beta}(p-q)^\gamma + g^{\beta\gamma}(q-r)^\alpha + g^{\gamma\alpha}(r-p)^\beta]$$

triple gluon
vertex

$(p+q+r=0)$

The qqG vertex involves a factor of t^a:

$$t^a \equiv \tfrac{1}{2}\lambda^a \tag{A2.5.1}$$

where the $SU(3)$ matrices λ^a are those introduced by Gell-Mann. The commutation relations for the t^a are given by the structure constants of the group,

$$[t^a, t^b] = \mathrm{i} f_{abc} t^c \tag{A2.5.2}$$

$$[t^a, t^b] = \frac{1}{N}\delta_{ab} I_{(N)} + d_{abc} t^c, \tag{A2.5.3}$$

where $I_{(N)}$ is the N-dimensional unit matrix. The f_{abc} are antisymmetric and the d_{abc} symmetric under the interchange of any two indices. In $SU(2)$, the quantities analogous to (t^a, f_{abc}, d_{abc}) are $(\sigma^a/2, \epsilon_{abc}, 0)$. Some useful identities involving the matrices t^a are

$$\left.\begin{aligned}
t^a t^b &= \frac{1}{2}\Big[\frac{1}{N}\delta_{ab} I_{(N)} + (d_{abc} + \mathrm{i} f_{abc}) t^c\Big],\\
t^a_{ij} t^a_{kl} &= \frac{1}{2}\Big[\delta_{il}\delta_{jk} - \frac{1}{N}\delta_{ij}\delta_{kl}\Big],\\
\mathrm{Tr}\, t^a &= 0,\\
\mathrm{Tr}(t^a t^b) &= \frac{1}{2}\delta_{ab},\\
\mathrm{Tr}(t^a t^b t^c) &= \frac{1}{4}(d_{abc} + \mathrm{i} f_{abc}),\\
\mathrm{Tr}(t^a t^b t^a t^c) &= -\frac{1}{4N}\delta_{bc}.
\end{aligned}\right\} \tag{A2.5.4}$$

$$\underline{f_{acd}\cdot f_{bcd} = N\delta_{ab}}$$

E. Leader & E. Predazzi
An Introduction to gauge theories
vol II Appendix 2

abc	f_{abc}	abc	f_{abc}
123	1	345	1/2
147	1/2	367	−1/2
156	−1/2	458	$\sqrt{3}/2$
246	1/2	678	$\sqrt{3}/2$
257	1/2		

Table A2.1. Non-zero f_{abc} for $SU(3)$.

The λ-matrices are familiar[9] from the study of flavor-$SU(3)$ symmetry. They have a number of simple properties, including

$$\operatorname{tr}(\lambda^l) = 0, \tag{8.1.7}$$

$$\operatorname{tr}(\lambda^k \lambda^l) = 2\delta^{kl}, \tag{8.1.8}$$

and

$$[\lambda^j, \lambda^k] = 2if^{jkl}\lambda^l, \tag{8.1.9}$$

which parallel those of the Pauli isospin matrices given in (4.2.18) and (4.2.25). Indeed, in the canonical basis

$$\lambda_1 = \begin{array}{cc} \begin{pmatrix} 0 & 1 & 0 \\ 1 & 0 & 0 \\ 0 & 0 & 0 \end{pmatrix} & \begin{array}{c} \bar{R} \\ \bar{B}, \\ \bar{G} \end{array} \\ \begin{array}{ccc} R & B & G \end{array} & \end{array} \qquad \lambda_2 = \begin{pmatrix} 0 & -i & 0 \\ i & 0 & 0 \\ 0 & 0 & 0 \end{pmatrix},$$

$$\lambda_3 = \begin{pmatrix} 1 & 0 & 0 \\ 0 & -1 & 0 \\ 0 & 0 & 0 \end{pmatrix}, \qquad \lambda_4 = \begin{pmatrix} 0 & 0 & 1 \\ 0 & 0 & 0 \\ 1 & 0 & 0 \end{pmatrix}, \tag{8.1.10}$$

$$\lambda_5 = \begin{pmatrix} 0 & 0 & -i \\ 0 & 0 & 0 \\ i & 0 & 0 \end{pmatrix}, \qquad \lambda_6 = \begin{pmatrix} 0 & 0 & 0 \\ 0 & 0 & 1 \\ 0 & 1 & 0 \end{pmatrix},$$

$$\lambda_7 = \begin{pmatrix} 0 & 0 & 0 \\ 0 & 0 & -i \\ 0 & i & 0 \end{pmatrix} \qquad \lambda_8 = \frac{1}{\sqrt{3}}\begin{pmatrix} 1 & 0 & 0 \\ 0 & 1 & 0 \\ 0 & 0 & -2 \end{pmatrix},$$

Averaging on the initial & summing over final state colours:

- the colour parts of the amplitude separate from the spin and momentum parts, we can ignore them to begin with and reinstate the result of the colour sum at the end.

- Ex. Consider one of the two lowest order diagrams for $q\,q$ scattering

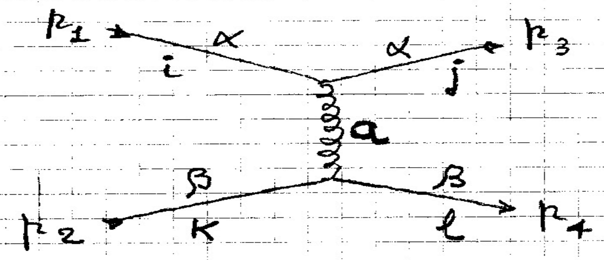

$$M_t(q^i_\alpha\, q^k_\beta \to q^j_\alpha\, q^l_\beta)$$

α, β	flavour labels	
i, j, k	quark colour labels	$(1,2,3)$
a	gluon " label	$(1 \cdots 8)$

$$- \quad M_t = \left[\bar{u}_\beta(p_4)\, i g\, (t^a)_{lk}\, \gamma^\mu\, u_\beta(p_2)\right] \frac{-i g_{\mu\nu}}{q^2} \times$$

$$\times \left[\bar{u}_\alpha(p_3)\, i g\, (t^a)_{ji}\, \gamma^\nu\, u_\alpha(p_1)\right]$$

here $(t^a)_{lk}$ and $(t^a)_{ja}$ are just numbers, and we can perfectly well bring them in front and write:

(2)

$$M_t(q^i_\alpha q^k_\beta \to q^j_\alpha q^l_\beta) = (t^a_{lk}\, t^a_{ji}) \times [\; - - - - - \;]$$

- $|M_t|^2$ for $qq \to qq$ is obtained by summing over final colours (and spins) and averaging over initial colours (and spins).
- The colour and spin parts are separated. Consider the colour factor for $|M_t|^2$.

$$C = \frac{1}{3}\sum_i \frac{1}{3}\sum_k \sum_{jl} (t^a_{lk}\, t^a_{ji})(t^a_{lk}\, t^a_{ji})^*$$

where the colour a is summed over at the end.
Since $t^{a*}_{lk} = t^a_{kl}$, $t^{a*}_{ji} = t^a_{ij}$ (t hermitian)
one has:

$$t^a = \frac{\lambda^a}{2}$$

$$\frac{1}{9}\sum_{ijkl} (t^a_{lk}\, t^a_{kl})(t^a_{ji}\, t^a_{ij})$$

now $\sum_{lk} t^a_{lk} t^b_{kl} = \mathrm{Tr}(t^a t^b) \underset{\text{definition}}{=} \frac{1}{2}\delta_{ab}$

$$C = \frac{1}{9}\cdot\left(\sum_a \mathrm{Tr}(t^a t^a)\,\mathrm{Tr}(t^a t^a)\right) = \frac{1}{9}\left(8\cdot\frac{1}{4}\right) = \frac{2}{9}$$

o.k

$\mathrm{Tr}(t^a t^b) = \frac{1}{2}\delta_{ab}$

PARTON ENERGY LOSS	
COLLISION IQCD	1

$$\boxed{\frac{d\sigma}{dt} = \frac{\pi \alpha_s}{s^2} \overline{|M|^2}}$$

Scattering partone-partone QCD
(non polarizzati)

Processo	Diagramma dominante	$\overline{\vert M\vert^2}$
$qq \to qq$ $q\bar{q} \to q\bar{q}$		$\frac{4}{9}\left(\frac{s^2+u^2}{t^2}\right)$
$gq \to gq$ $qg \to qg$		$\left(\frac{s^2+u^2}{t^2}\right)$
$gg \to gg$		$\frac{9}{4}\left(\frac{s^2+u^2}{t^2}\right)$

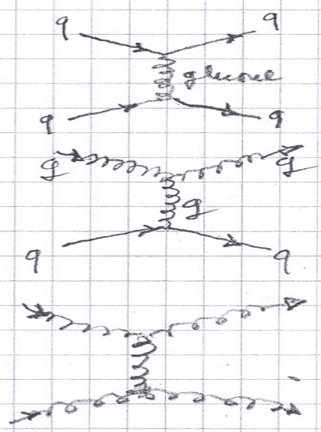

$s + t + u = \sum m_i^2 = 0$ $\quad u^2 = s^2 + t^2 + 2st$

$u^2 \sim s^2$ per $|t| \ll s$

$$\left.\frac{d\sigma}{dt}\right|_{|t|\ll s} = \frac{2\pi\alpha_s^2}{t^2}\begin{cases} (2/3)^2 & qq \to qq,\ q\bar{q} \to q\bar{q} \\ 1 & qg \to qg \\ \left(\frac{3}{2}\right)^2 & gg \to gg \end{cases}$$

$\downarrow$
C
(2 × colour factor)

PARTON ENERGY LOSS BY COLLISION QCD	2

(Bjorken Fermilab-Pub-82/59-THY + erratum unpubl.)

Partone ad alta energia (> 1 GeV) che attraversa un plasma ideale ed uniforme di quark e gluoni in equilibrio ad una temperatura $T \equiv \beta^{-1}$ e potenziale chimico = 0

$$\begin{cases} \rho_g(K) = \dfrac{dn_g}{d^3K} = \dfrac{16}{(2\pi)^3}\left(e^{\beta K} - 1\right)^{-1} \\[2ex] \rho_{q+\bar q}(K) = \dfrac{12\,N_f}{(2\pi)^3}\left(e^{\beta K} + 1\right)^{-1} \end{cases}$$

- masse g e q = 0 ; $N_f = N$ flavours attivi nel QGP
- $\vec{K} \equiv$ momento del partone del plasma

consideriamo lo scattering elastico:

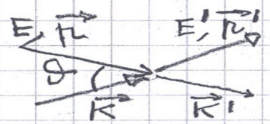

$$-\Delta E \equiv \nu = E' - E$$

$\vec{p} \equiv$ momento del partone incidente $|\vec{p}| \gg |\vec{K}|$

$$\frac{dE}{dx} = \int d^3K \cdot \rho(K) \cdot (1 - \cos\vartheta) \int dt \cdot \frac{d\sigma}{dt} \cdot \nu$$

- il fattore $(1 - \cos\vartheta)$ tiene conto del fatto che il fattore di flusso F usato in $d\sigma/dt = 2\pi\alpha_s$ è calcolato per eventi collineari ($\vartheta = 180°$) e che in realtà il numero di eventi sarà minore. (vedi Møller invariant flux)

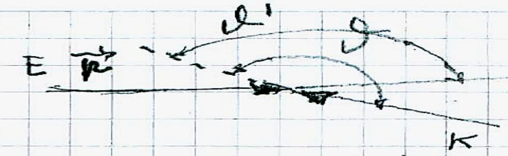

$$\begin{cases} \cos\vartheta = \dfrac{\vec{p}\cdot\vec{k}}{|\vec{p}|\cdot|\vec{k}|} \\ \cos\vartheta' = \dfrac{\vec{p}'\cdot\vec{k}}{|\vec{p}'|\cdot|\vec{k}|} \end{cases}$$

$$\begin{cases} s = 2Ek(1-\cos\vartheta) \\ u = -2E'k(1-\cos\vartheta') \end{cases}$$

per $E, E' \gg k \qquad \cos\vartheta \sim \cos\vartheta'$

$$t = -(s+u) = -2Ek(1-\cos\vartheta)\left(\frac{E-E'}{E}\right) = \frac{s\cdot\nu}{E}$$

$$\int \nu \frac{d\sigma}{dt}\, dt = 2\pi\alpha_s^2 C \int \frac{dt}{t^2}\,\nu = 2\pi\alpha_s C \int \frac{dt}{t^2}\cdot\frac{t\cdot E}{2Ek(1-\cos\vartheta)}$$

$$= 2\pi\alpha_s^2 C \frac{1}{2k(1-\cos\vartheta)} \int \frac{dt}{t}$$

$$\left(\frac{dE}{dx}\right)_{qq} = \frac{4}{9}\pi\alpha_s^2 \int \frac{d^3k}{k}\,\rho(k) \int \frac{dt}{t}$$

$$= \frac{8}{3\pi}\alpha_s^2 N_f T^2 \underbrace{\int_0^\infty \frac{x\,dx}{e^x+1}}_{\pi^2/12} \int_{|t|_{min}}^{|t|_{max}} \frac{dt}{t}$$

$$\boxed{\begin{array}{l} d^3k = 4\pi k^2 dk \\ x = \beta k \\ \beta \equiv T^{-1} \end{array}}$$

$|t| = q^2$

$$-\left(\frac{dE}{dx}\right)_{qq} = \frac{4}{9}\pi\alpha_s^2 N_f T^2 \log\left(\frac{q_{max}}{q_{min}}\right)$$

$$= \frac{8}{3}\pi\alpha_s^2 \frac{N_f}{6} T^2 \log\left(\frac{q_{max}}{q_{min}}\right)$$

PARTON ENERGY LOSS BY COLLISION QCD 4

Analogamente:

$$-\left(\frac{dE}{dx}\right)_{qg} = \frac{16}{\pi}\alpha_s^2 \cdot \log\frac{q_{max}}{q_{min}} \, T^2 \underbrace{\int_0^\infty x\,(e^x-1)^{-1}\,dx}_{\pi^2/6}$$

$$= \frac{8}{3}\cdot\alpha_s^2\,\pi\,\ln\frac{q_{max}}{q_{min}} .$$

$$\begin{cases} -\left(\frac{dE}{dx}\right)_{qq,q\bar{q}+qg} = \frac{8}{3}\pi\alpha_s^2 T^2\left(1+\frac{N_f}{6}\right)\log\frac{q_{max}}{q_{min}} \\ \left(\frac{dE}{dx}\right)_{gq,g\bar{q}+gg} = \frac{9}{4}\left(\frac{dE}{dx}\right)_{qq,q\bar{q}+qg} \end{cases}$$

→ vedi Thoma Phys. Lett. B 273 (1991) 128

Queste formule hanno però l'inconveniente di avere dei cutoff q_{max} e q_{min} un po' ambigui

e.g. $q_{max} = \sqrt{4ET}$ $E \gg T$ (?)

$q_{min} = \frac{1}{r_{Debye}} = \sqrt{1+\frac{N_f}{6}}\cdot g\,T$

$$\boxed{\alpha_s = \frac{g^2}{4\pi}}$$

Ex: $\alpha_s \simeq 0.2$ $g = 1.59$ $T = 0,25$ GeV

$E = 20$ GeV

$$\left(\frac{dE}{dx}\right)_q \simeq 0.06 \text{ GeV}^2 \simeq 0.3 \text{ GeV/fm}$$

Debye length

DEBYE LENGTH
Analogia con il plasma e.m

Plasma e.m. (Jackson Clas. El.)

$$r_D = \left(\frac{4\pi\alpha n_0}{K_B T}\right)^{-1/2} \qquad \left(\alpha = \frac{e^2}{\hbar c} \quad n_0 = n° \text{ elettroni/vol}\right)$$

Ex. $T = 10^6\ °K \longrightarrow K_B T \simeq 85\ eV$

$$n_0 = 10^{15}\ cm^{-3} = 10^{-24}\ fm^{-3}$$

$$\Longrightarrow \quad r_D = 2.2 \times 10^{-4}\ cm = 2.2 \times 10^{9}\ fm$$

QGP usiamo la stessa espressione

$$\alpha \rightarrow \alpha_S = 0.2$$

$$n_0 = \underbrace{\frac{37 \cdot \pi^2}{30} \cdot T^4}_{\text{Stefan-Boltzmann}} \Big/ \underbrace{3T}_{\text{energia media}} \simeq 4T^3$$

$$\boxed{\begin{array}{l} 1\ GeV = 5\ fm^{-1} \\ 1\ fm = 5\ GeV^{-1} \end{array}}$$

$$r_D = \left(\frac{16 \cdot \pi \cdot \alpha_s T^3}{T}\right)^{-1/2} \simeq \frac{1}{T} \cdot \frac{1}{\sqrt{50 \cdot \alpha_s}}$$

Ex. $T = 250\ MeV \qquad n_0 \simeq 0.062\ GeV^3 \simeq 7\ fm^{-3}$

$$r_D \simeq 1.3\ GeV^{-1} \simeq 0.25\ fm$$

CONFRONTO CON L'ESPRESSIONE IN USO

$$r_D \simeq \frac{1}{T} \frac{1}{4\pi\alpha_s} \qquad (\text{Ex } r_D \simeq 2.5\ GeV^{-1})$$

o, più esattamente $r_D^{-1} = g T \sqrt{1 + N_f/6}$

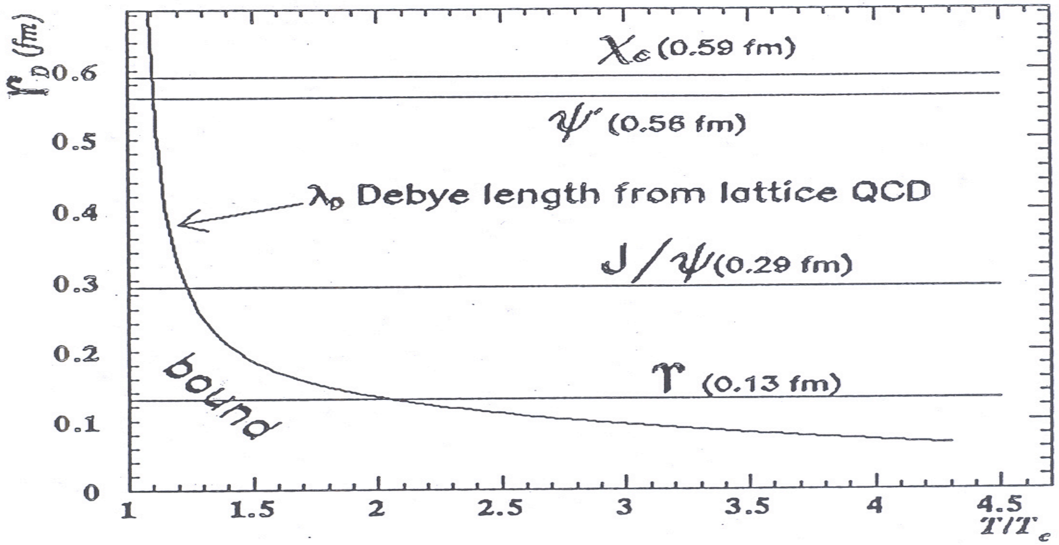

r_D (fm)
0.6
0.5
0.4
0.3
0.2
0.1
0
1
1.5
2
2.5
3
3.5
4
4.5
T/T_c
χ_c (0.59 fm)
ψ' (0.56 fm)
λ_D Debye length from lattice QCD
J/ψ (0.29 fm)
Υ (0.13 fm)
bound

Bremsstrahlung elettromagnetica: richiami

$$-\left(\frac{dE}{dx}\right)_{\substack{rad.\\ elettrone}} = X_0^{-1}\cdot E_i$$

E_i = energia elettrone
X_0 = radiation length

$$X_0^{-1} = 4\alpha Z_{12}^2 r_e^2 N \ln\left(183\cdot Z_{12}^{-\frac{1}{3}}\right)$$

N = numero di nuclei / cm^3

Z_2 = numero atomico nucleo considerato fisso.

$$-\left(\frac{dE}{dx}\right)_{\substack{rad\\ z=1 \;\; massa = M}} \simeq \left(\frac{m_e}{M}\right)^2$$

$$-\quad \omega\frac{d\sigma}{d\omega} \simeq \text{costante sino ad } \omega_{max} = E_i - m$$

ω = energia del fotone irradiato

– angolo medio di emissione

$$\vartheta_\gamma \simeq \gamma^{-1} \quad (\gamma \gg 1) \qquad \gamma = \frac{E}{m}$$

	SOFT PHOTON BREMSSTRAHLUNG $\omega_\gamma \to 0$	2

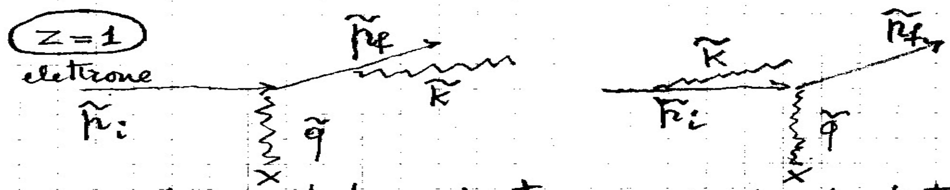

final state radiation   initial state radiation

$$\left(\frac{d\sigma}{d\Omega_f}\right)_{rad} = \left(\frac{d\sigma}{d\Omega_f}\right)_0 \frac{\alpha}{(2\pi)^2}\left[\frac{\tilde{\varepsilon}\cdot\tilde{p}_f}{\tilde{k}\cdot\tilde{p}_f} - \frac{\tilde{\varepsilon}\cdot\tilde{p}_i}{\tilde{k}\cdot\tilde{p}_i}\right]^2 \frac{d^3k}{\omega}$$

inv. PH.SP

$\left(\frac{d\sigma}{d\Omega_f}\right)_0$ è la sezione d'urto per scattering elastico

$\tilde{k} \equiv (\omega, \omega\vec{n})$ 4-momento del fotone emesso
$\tilde{p}_f$ " dell'elettrone uscente
$\tilde{p}_i$ " " entrante
$\tilde{\varepsilon} \equiv (0, \vec{\varepsilon})$ " polarizzazione fotone (Coulomb gauge)

Risultato generale: ottenuto sia con un trattamento quantistico che classico

e.g. Q.M. C. Itzykson, J.B. Zuber
Quantum Field Theory McGraw-Hill 1980
equation 8-103 pag. 167

classico J.D. Jackson
Classical Electrodynamics (3rd edition)
equation 15-6 pag. 710

L'intensità della radiazione emessa (Jackson) è

$$\frac{d^2 I}{d\omega\, d\Omega} = \frac{\alpha}{(2\pi)^2}\left|\frac{\vec{\varepsilon}\cdot\vec{\beta}_f}{1-\vec{n}\cdot\vec{\beta}_f} - \frac{\vec{\varepsilon}\cdot\vec{\beta}_i}{1-\vec{n}\cdot\vec{\beta}_i}\right|^2$$

$\vec{\beta} = \frac{\vec{p}}{E}$ $\qquad \vec{\varepsilon} = \vec{\varepsilon}_\perp + \vec{\varepsilon}_\parallel$

Coulomb gauge
$\tilde{\varepsilon}(0, \vec{\varepsilon})$ $\qquad \vec{\varepsilon}\cdot\vec{k} = 0$

Somma sulle polarizzazioni (Jackson)

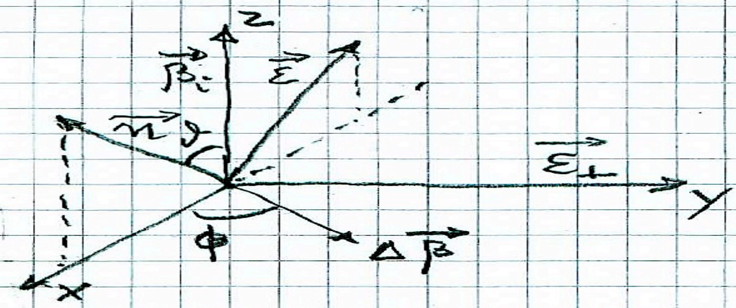

$1/\sqrt{1-\beta^2} \gg 1$

$\Delta\vec{\beta}$ piccolo e $\perp \vec{\beta}_i$

$$\begin{cases} \vec{\varepsilon}_\perp\,(0,\ 1,\ 0) \\ \vec{\varepsilon}_\parallel\,(-\cos\vartheta,\ 0,\ \operatorname{sen}\vartheta) \\ \Delta\vec{\beta}\,(|\Delta\vec{\beta}|\cos\phi,\ |\Delta\vec{\beta}|\operatorname{sen}\phi,\ 0) \end{cases}$$

$$\frac{d^2 I_\perp}{d\omega\, d\Omega} = \frac{\alpha}{8\pi^2}\,\frac{1}{(1-\beta\cos\vartheta)^2}\cdot|\Delta\vec{\beta}|^2$$

verifica:

$$\vec{\varepsilon}_\perp\cdot\left(\frac{\vec{\beta}_f}{1-\vec{n}\cdot\vec{\beta}_f} - \frac{\vec{\beta}_i}{1-\vec{n}\cdot\vec{\beta}_i}\right) = \vec{\varepsilon}_\perp\cdot\Big[(\vec{\beta}_i+\Delta\vec{\beta})(1-\vec{n}\cdot\vec{\beta}_i) -$$
$$- \vec{\beta}_i\cdot[1-\vec{n}\cdot(\vec{\beta}_i+\Delta\vec{\beta})\Big]\cdot\frac{1}{(1-\vec{n}\cdot\vec{\beta}_i)^2}$$

$\vec{\varepsilon}_\perp\cdot\vec{\beta}_i = 0$ $\qquad \vec{\varepsilon}_\perp\cdot\Delta\vec{\beta} = \Delta\beta\operatorname{sen}\phi$

$\vec{\varepsilon}_\perp\cdot\vec{\beta}_f = \vec{\varepsilon}_\perp\cdot\Delta\vec{\beta} = \Delta\beta\operatorname{sen}\phi$

$$\frac{dI^2_\perp}{d\omega\, d\Omega} = \frac{\alpha}{(2\pi)^2}\left(\frac{|\Delta\vec{\beta}|\cdot\operatorname{sen}\phi}{1-\beta\cos\vartheta}\right)^2 \xrightarrow[\text{over }\phi]{\text{averaged}} \frac{\alpha}{8\pi^2}\,\frac{|\Delta\vec{\beta}|^2}{(1-\beta\cos\vartheta)^2}$$

SOFT PHOTON BREMSSTRAHLUNG

$$\begin{cases} \dfrac{d^2 I_\perp}{d\omega\, d\Omega} = \dfrac{\alpha}{8\pi^2} \dfrac{1}{(1-\beta\cos\vartheta)^2} \cdot |\vec{\Delta\beta}|^2 \\[2ex] \dfrac{d^2 I_\parallel}{d\omega\, d\Omega} = \dfrac{\alpha}{8\pi^2} \dfrac{(\beta-\cos\vartheta)^2}{(1-\beta\cos\vartheta)^4} \cdot |\vec{\Delta\beta}|^2 \end{cases}$$

$\gamma \gg 1$

– $$\frac{d^2 I}{d\omega\, d\Omega} = \frac{\alpha\gamma^4 \cdot |\vec{\Delta\beta}|^2}{\pi^2} \frac{(1+\gamma^4\vartheta^4)}{(1+\gamma^2\vartheta^2)^4}$$

$$\langle\vartheta\rangle \sim \frac{1}{\gamma}$$

– $$\frac{dI}{d\omega} = \frac{2}{3\pi} \alpha \gamma^2 |\vec{\Delta\beta}|^2 = \boxed{\frac{2}{3\pi} \alpha \frac{Q^2}{m^2}} \quad \frac{1}{m^2}$$

$$\vec{p} = \gamma m \vec{\beta} \qquad Q = |\vec{p}_f - \vec{p}_i|$$

– se $\vec{\beta}_i$ e $\vec{\beta}_f$ hanno un angolo tra loro $\vartheta_s > 2/\gamma$

$$\boxed{\frac{dI}{d\omega} \simeq \frac{4\alpha}{\pi} \ln(Q/m)}$$

il termine $\frac{1}{m^2}$ sparisce.
Appare il "dead cone" !

Bremsstrahlung in Coulomb collisions (summary)

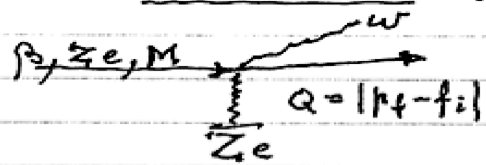

differential radiation cross-section

$$\frac{d^2\chi}{d\omega\, d\Omega} = \frac{dI(\omega,Q)}{d\omega} \cdot \frac{d\sigma_{scatt}(Q)}{dQ}$$

$$\cong \frac{16}{3} Z^2 e^2 \left(\frac{z^2 e^2}{M}\right)^2 \frac{1}{\beta^2} \cdot \frac{1}{Q}$$

$$\frac{d\chi}{d\omega} \cong \frac{16}{3} Z^2 e^2 \left(\frac{z^2 e^2}{M}\right)^2 \frac{1}{\beta^2} \ln\left(\frac{Q_{max}}{Q_{min}}\right)$$

$$\boxed{\begin{array}{l}\text{Jackson} \\ \hbar = c = 1 \\ e^2 = \alpha_{em}\end{array}}$$

noi usiamo

$$\alpha_{em} = \frac{e^2}{4\pi}$$

Origine del « dead cone »

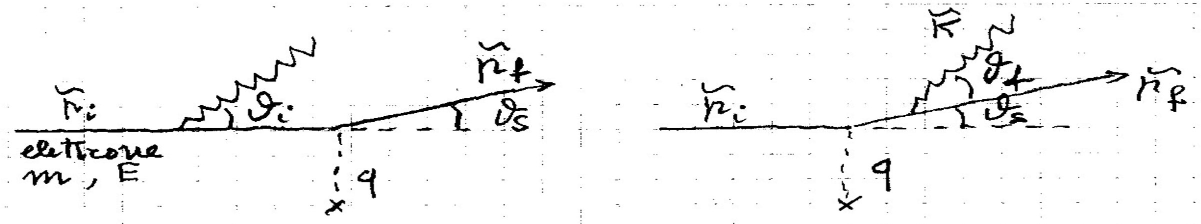

– angolo medio di emissione $\approx \frac{1}{\gamma} = \frac{m}{E}$ (see later)
(elettrone relativistico)

– se $\vartheta_s \gg \vartheta_i, \vartheta_f$ i due termini nell'ampiezza non interferiscono $\longrightarrow$ la distribuzione angolare del fotone emesso sarà di due fasci separati: uno centrato intorno a $\vec{p}_i$, l'altro a $\vec{p}_f$.

– $\frac{|\Delta \vec{p}|}{|\vec{p}|} = \frac{|\Delta \vec{\beta}|}{|\vec{\beta}|} > \frac{2}{\gamma} \longrightarrow$ due fasci

$$\left| \frac{\tilde{\varepsilon}\cdot\tilde{p}_f}{\tilde{k}\cdot\tilde{p}_f} - \frac{\tilde{\varepsilon}\cdot\tilde{p}_i}{\tilde{k}\cdot\tilde{p}_i} \right|^2 \Longrightarrow \left| \frac{\tilde{\varepsilon}\cdot\tilde{p}_f}{\tilde{k}\cdot\tilde{p}_f} \right|^2 + \left| \frac{\tilde{\varepsilon}\cdot\tilde{p}_i}{\tilde{k}\cdot\tilde{p}_i} \right|^2$$

– Appare il "dead cone"!

considériamo ad ex. il primo termine

$$\left(\frac{d\sigma}{d\Omega_f}\right) \Big/ \left(\frac{d\sigma}{d\Omega_f}\right)_{elastic} \equiv dP = \frac{\alpha \cdot d^3k}{\omega_i \cdot (2\pi)^2} \cdot \sum_{\lambda=1,2} \left[\frac{\tilde{\varepsilon}_\lambda \cdot \tilde{p}_f}{\tilde{k}\cdot\tilde{p}_f} \right]$$

- Per la somma sulle polarizzazione del fotone uscente, assumo che questo sia emesso lungo l'asse x.

$$\begin{cases} K \equiv (\omega, \omega, 0, 0) \\ \varepsilon_1 \equiv (0, 0, 1, 0) \\ \varepsilon_2 \equiv (0, 0, 0, 1) \\ p_f \equiv (E, p\cos\vartheta, p\,\mathrm{sen}\,\vartheta, 0) \end{cases}$$

(Coulomb gauge) $\vec{\varepsilon}\cdot\vec{K}=0$

$\vartheta \equiv \vartheta_f$

Quindi:

$$\sum_{\lambda=1,2}\left[\frac{\varepsilon_\lambda\cdot p_f}{K\cdot p_f}\right]^2 = \frac{p^2\,\mathrm{sen}^2\vartheta}{\omega^2(E-p\cos\vartheta)^2}$$

(per ϑ piccolo)
$$\simeq \frac{p^2\vartheta^2}{p^2\omega^2\left(E/p-1+\frac{\vartheta^2}{2}\right)^2}$$

$\left(\frac{\beta-1}{\beta}\simeq\frac{1}{2\gamma^2}=\frac{1}{2}\left(\frac{M}{E}\right)^2\right)$
$$\simeq \frac{4\omega^2\vartheta^2}{\left[\omega^2\left(\frac{M}{E}\right)^2+\omega^2\vartheta^2\right]^2}$$

$K_\perp \simeq \omega\vartheta$

$\vartheta_0 \equiv \frac{M}{E}$
$$= \frac{4K_\perp^2}{\left[\omega^2\vartheta_0^2+K_\perp^2\right]^2}$$

– Infine:

$$dP = \frac{\alpha}{(2\pi)^2}\,\frac{4k_\perp^2}{(\omega^2\vartheta_0^2+k_\perp^2)^2}\,\frac{d^3k}{k}$$

$$= \frac{\alpha}{\pi}\,\frac{d\omega}{\omega}\,\frac{k_\perp^2\,dk_\perp^2}{(k_\perp^2+\omega^2\vartheta_0^2)^2} \qquad \left(\vartheta_0 = \frac{M}{E}\right)$$

– passando ai "soft gluons"

$$\alpha \longrightarrow \alpha_s C_F$$

ritrovo la formula 13 del paper di Dokshitzer & Kharzeev – Phys. Lett. B 519 (2001) 199

Altro modo:

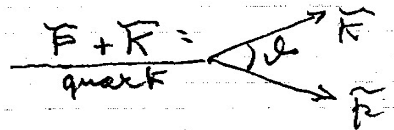

la probabilità di radiazione è proporzionale al quadrato del propagatore del quark virtuale:

$$\text{Prop} = \frac{1}{(\tilde{p}+\tilde{k})^2 - M^2} = \frac{1}{2\,\tilde{p}\cdot\tilde{k}} = \frac{1}{2\omega(E - p\cos\vartheta)} \simeq \frac{1}{2\omega p\left(\frac{E}{p} - 1 + \frac{\vartheta^2}{2}\right)}$$

$$= \frac{1}{2\omega p\left(\frac{1-\beta}{\beta} + \frac{\vartheta^2}{2}\right)} = \frac{1}{\omega p\left[\left(\frac{M}{E}\right)^2 + \vartheta^2\right]}$$

$$\frac{1-\beta}{\beta} \simeq \frac{1}{2\gamma^2} = \frac{1}{2}\left(\frac{M}{E}\right)^2$$

(causalità)

– Infine:

$$dP = \frac{\alpha}{(2\pi)^2} \frac{4 k_\perp^2}{(\omega^2 \vartheta_0^2 + k_\perp^2)^2} \frac{d^3 k}{k}$$

$$= \frac{\alpha}{\pi} \frac{d\omega}{\omega} \frac{k_\perp^2 \, dk_\perp^2}{(k_\perp^2 + \omega^2 \vartheta_0^2)^2}$$

$\left(\vartheta_0 = \frac{M}{E} \right)$

angolo di apertura del "dead cone"

- – passando ai "soft gluons"

$$\alpha \longrightarrow \alpha_s C_F$$

ritrovo la formula 13 del paper di Dokshitzer & Kharzeev $\Rightarrow$ Phys. Lett. B519 (2001) pag. 199

- $\vartheta < \vartheta_0$ soppressione della radiazione

Importante solo per la radiazione di gluoni da parte di quark pesanti: charm e beauty

Photon/gluon Formation time

$\hbar = c = 1$

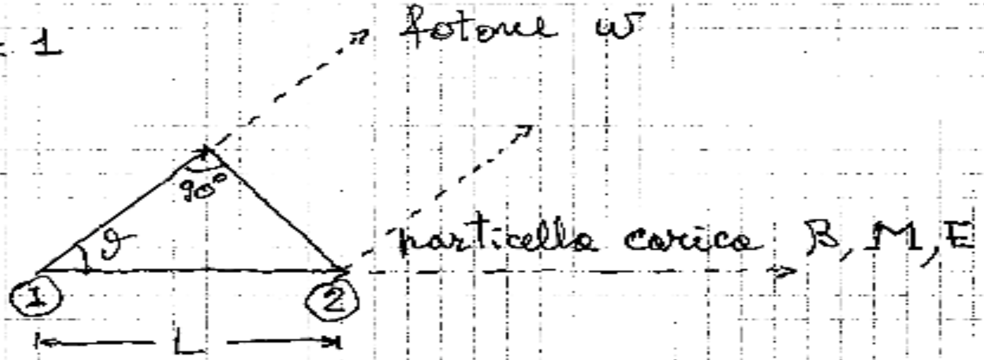

Condizione di coerenza ① vs ②

$\Delta\varphi$ = fase part. − fase fotone ≤ 1

vedi: relazione di incertezza numero fotoni − fase $\Delta n \cdot \Delta\varphi \leq \frac{1}{2}$

$\Delta\varphi = \omega L/\beta - \omega L \cos\vartheta$

$\Delta\varphi = 1 \Rightarrow$

$$L_{form} = 1/\omega(1-\beta\cos\vartheta)$$

$$\stackrel{!}{=} 1/\omega\left(\frac{1}{2\gamma^2}+\frac{\vartheta^2}{2}\right) \quad \begin{cases}\vartheta \text{ piccolo} \\ \beta \approx 1\end{cases}$$

$$\stackrel{!}{=} 2\,\omega/(\omega^2\vartheta_0^2 + K_t^2) \qquad \begin{matrix}\vartheta_0 = M/E \\ K_t = \omega\vartheta\end{matrix}$$

per $M = 0$ $\quad L_{form} = t_{form} = 2\omega/K_t^2$

{qualcuno usa anche $t_{form} = \omega/K_t^2$) $(\Delta\varphi = 1/2)$

Altra interpretazione:

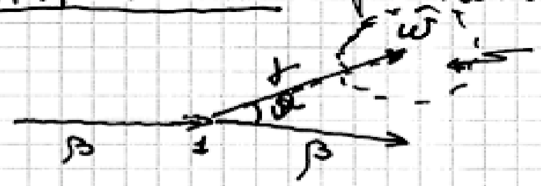

larghezza del fotone

$R_\gamma \sim \frac{1}{\omega}$

Velocità relativa γ-particella

$$v^{relat} = 1-\beta\cos\vartheta$$

$$t_{separazione} \sim \frac{R_\gamma}{v^{relat}} \sim \frac{1}{\omega(1-\beta\cos\vartheta)}$$

Durante il tempo di separazione il fotone "sente" ancora la particella carica.

Oppure (Dokshitzer) come tempo di vita dello stato virtuale:

particella carica + fotone

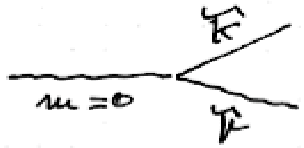

$k \equiv (\omega, \vec{k})$

$$t_{form} \cdot M = 1$$

nel laboratorio $t_{form} \Rightarrow \gamma\, t_{form} = \frac{E}{M} t_{form}$

$$t_{form} \simeq \frac{E}{M^2} = \frac{E}{(p+k)^2} \simeq \frac{E}{\omega E \vartheta^2} \approx \frac{\omega}{k_\perp^2}$$

Esempio:

$$L_{form} = \frac{1}{\omega(1-\beta\cos\vartheta)} \simeq \frac{1}{\omega\left(\frac{1}{2\gamma^2}+\frac{\vartheta^2}{2}\right)} \qquad \vartheta \text{ piccoli} \qquad \gamma = \frac{1}{\sqrt{1-\beta^2}}$$

– ad ω fissato L_{form} è massima per $\vartheta = 0$

$$L_{form\ max} = \frac{2\gamma^2}{\omega}$$

$m = 0.5$ MeV
$E = 5$ GeV
$\gamma = \frac{E}{m} \simeq 10^4$

– per $\omega = 1$ GeV

$$L_{form\ max} = 2\times 10^4 \text{ GeV}^{-1}$$

$$\simeq 10^5 \text{ fermi} = 10^{-8} \text{ cm} \quad !$$

$\simeq$ diametro atomo H

Nel plasma QCD invece, il libero cammino medio di un gluone $\simeq O(1 \text{ fermi})$

- $t_{form} = 1/(\omega(1 - \beta \cos(\theta))$

  small $\theta \rightarrow t_{form} \approx 2\omega/(\omega^2 \theta_0^2 + k_t^2)$,
  where $\theta_0 = M/E = 1/\gamma$ and $k_t = \omega \theta$

- For $M = 0$: $t_{form} = 2\omega/k_t^2$

- $L_{form} = \beta\, t_{form}$ and λ determine the radiation regime in multiple scattering:

  - $L_{form} < \lambda$(mean free path) → Bethe – Heitler
  - $L_{form} > \lambda$ → LPM
  - $L_{form} > L$(medium length) → factorization

$$t_{form} \cong \frac{2 \cdot \omega}{\omega^2 \left(\frac{M^2}{E^2} + \theta^2\right)}$$

For a given ω and θ,, t_{form} is smaller for heavy than for light quarks thus extending the Bethe-Heitler regime for heavier quarks and reducing the domain of the LPM suppression

EXAMPLE: for θ=1/γ , t_{form}(heavy) = ½ t_{form}(M=0)

Landau-Pomeranchuk Migdal (LPM) regime

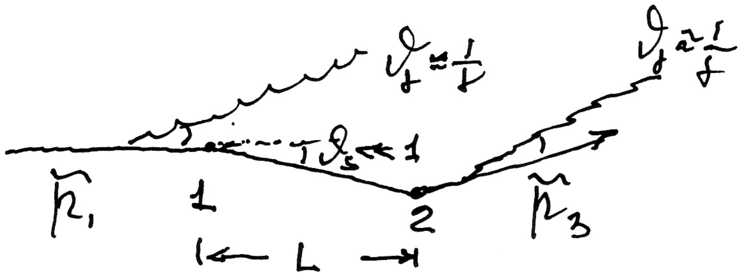

QED

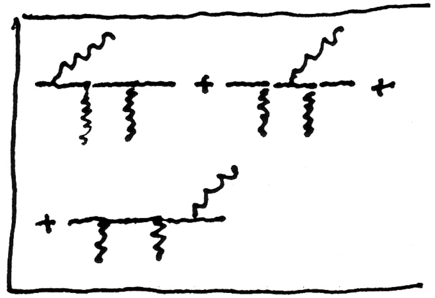

$$\text{Ampiezza radiazione} \doteq \left[\frac{\tilde{\varepsilon}\cdot\tilde{p}_2}{\tilde{p}_2\cdot\tilde{k}} - \frac{\tilde{\varepsilon}\cdot\tilde{p}_1}{\tilde{p}_1\cdot\tilde{k}}\right] e^{i\tilde{k}\cdot\tilde{x}_1} + \left[\frac{\tilde{\varepsilon}\cdot\tilde{p}_3}{\tilde{p}_3\cdot\tilde{k}} - \frac{\tilde{\varepsilon}\cdot\tilde{p}_2}{\tilde{p}_2\cdot\tilde{k}}\right] e^{i\tilde{k}\cdot\tilde{x}_2}$$

$$\tilde{k} \equiv (\omega, \omega\cos\vartheta, \omega \,\mathrm{sen}\,\vartheta, 0)$$

$$\tilde{p} \equiv (E, p, 0, 0) \qquad \frac{p}{E} = \beta$$

$$\tilde{x}_1 \equiv (0, x_1, 0, 0)$$

$$\tilde{x}_2 \equiv (t_2, x_2, 0, 0) \quad \text{dove } t_2 = \frac{(x_2 - x_1)}{\beta} = \frac{L\cdot E}{p}$$

$$\mathrm{Amp} = \left\{ (A_2 - A_1)\, e^{i\tilde{k}\cdot\tilde{x}_1} + (A_3 - A_2)\, e^{i\tilde{k}\cdot\tilde{x}_2} \right\}$$

$$|Amp|^2 = (A_2 - A_1)^2 + (A_3 - A_2)^2 + (A_2 - A_1)\cdot(A_3 - A_2)\cdot\left[e^{i\tilde{k}\cdot(\tilde{x}_1 - \tilde{x}_2)} + e^{-i\tilde{k}\cdot(\tilde{x}_1 - \tilde{x}_2)}\right]$$

$$\tilde{k}\cdot(\tilde{x}_1 - \tilde{x}_2) = \omega(t_2 - t_1) - \omega L \cos\vartheta \stackrel{\downarrow}{=} \omega\left(\frac{1}{\beta} - \cos\vartheta\right) L$$

ma $$\tau_{form} = \left[\omega\left(\frac{1}{\beta} - \cos\vartheta\right)\right]^{-1}$$

$$\tilde{k}\cdot(\tilde{x}_1 - \tilde{x}_2) = \frac{L}{\tau} = 2\omega / k_\perp^2$$

se $$\tilde{k}\cdot(\tilde{x}_1 - \tilde{x}_2) \Longrightarrow 0 \qquad \begin{cases} L \Rightarrow 0 \\ \tau \Rightarrow \infty \end{cases}$$

$$|Amp|^2 = (A_2 - A_1)^2 + (A_3 - A_2)^2 + 2(A_2 - A_1)(A_3 - A_2)$$

$$\stackrel{!}{=} A_1^2 + A_3^2 - 2 A_1 A_3$$

$$\stackrel{!}{=} |A_3 - A_1|^2$$

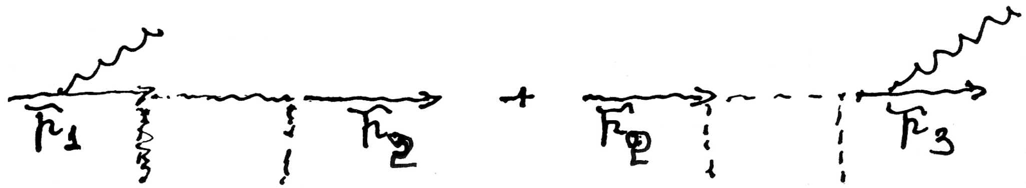

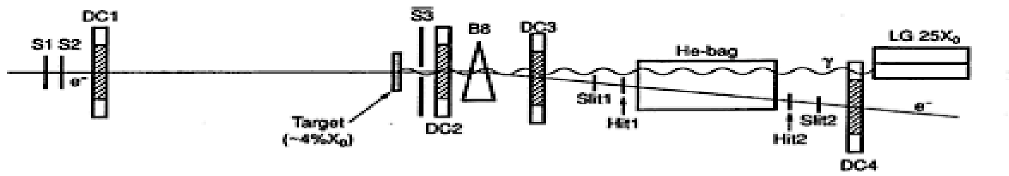

FIG. 2. A schematical drawing of the setup used in the CERN LPM experiment. Not to scale.

for $v=(1-1/\gamma^2)c\approx c$

$$l_f=\frac{2\gamma^2 c}{\omega}$$

where v is the speed of the electron, c the speed of light and $\gamma=E/mc^2$ the Lorentz factor related to the energy of the electron, E, and its rest mass, m.

The length over which a particle statistically scatters an angle $1/\gamma$ in an amorphous material due to multiple Coulomb scattering is given by

$$l_\gamma=\frac{\alpha}{4\pi}X_0 \qquad (5)$$

where α is the fine-structure constant and X_0 the radiation length.

combined with Eq. (5) leads to the threshold of the LPM effect at energies,

$$\hbar\omega^q_{\mathrm{LPM}}=\frac{E^2}{E+E_{\mathrm{LPM}}} \quad \left(\hbar\omega^c_{\mathrm{LPM}}=\frac{E^2}{E_{\mathrm{LPM}}}\right) \qquad (6)$$

where

$$E_{\mathrm{LPM}}=mc^2X_0/4\pi a_0=7.684\times X_0 \quad \mathrm{TeV/cm} \qquad (7)$$

and a_0 is the Bohr radius. The value in parentheses denotes the classical (recoil-less) limit. As an example for Ir the value of E_{LPM} is 2247 GeV which means that $E=287$ GeV electrons yield threshold values of $\hbar\omega^q_{\mathrm{LPM}}=32.4$ GeV and $\hbar\omega^c_{\mathrm{LPM}}=36.7$ GeV in the quantum and classical cases, i.e., a quantum correction of 13%.

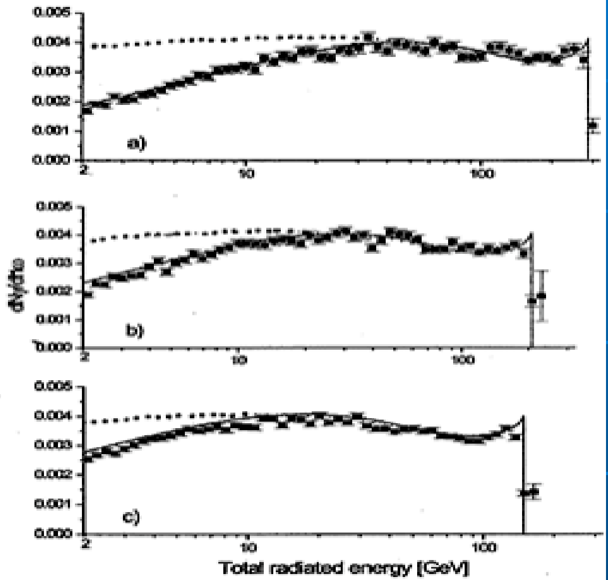

FIG. 9. Bremsstrahlung spectrum, $dN_\gamma/d\hbar\omega$, for (a) 287 GeV, (b) 207 GeV and (c) 149 GeV electrons on 0.128 mm Ir (4.36% X_0). The total radiated energy, $\hbar\omega$, is presented in logarithmic bins (25 per decade) and plotted on a logarithmic scale. The vertical scale is normalized to the number of incoming electrons. The dotted line is the result of a simulation based on a pure Bethe-Heitler spectrum while the full line includes the LPM suppression.

QCD L.P.M. $L/\tau \ll 1$

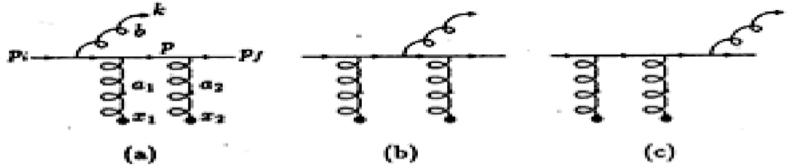

FIG. 2. Diagrams for gluon radiation from the quark line induced by double scatterings.

X. N. Wang et al. Phys. Rev. D 51(1995)3436

Ciascun diagramma ha i suoi "color factors".
Il segno negativo che porta all'interferenza distruttiva nasce dalla "color algebra".

In QED invece l'interferenza aveva origine nel segno opposto delle "momentum space amplitudes" che contribuivano all'ampiezza (totale) di radiazione.

QCD bremsstrahlung

Sparisce la dipendenza da 1/M**2

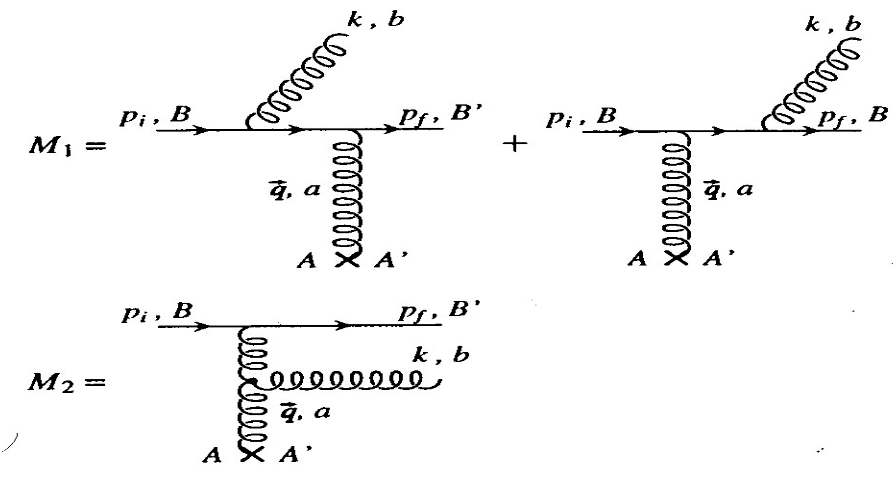

Fig. 2. Gluon emission amplitude induced by one scattering.

$$M_{\rm el} = T^a_{B'B}\ M^a_{A'A}\,, \qquad M^a_{A'A} = g_{\mu\nu}\ M^{a,\mu\nu}_{A'A}\,. \tag{2.5a}$$

Here

$$M^{a,\mu\nu}_{A'A} = ig^2(p_i + p_f)^\mu \frac{1}{\vec{q}^{\,2}}\ \delta^\nu_0 T^a_{A'A}\,, \tag{2.5b}$$

where we neglected spin effects in the high-energy limit. The static source can be viewed as if it were a heavy quark.

In Feynman gauge, the amplitude M_1 (Fig. 2) for soft gluon emission may be expressed as the elastic scattering amplitude times a radiation factor as

$$M_1 \simeq -g\left\{\frac{\varepsilon\cdot p_f}{k\cdot p_f}(T^bT^a)_{B'B} - \frac{\varepsilon\cdot p_i}{k\cdot p_i}(T^aT^b)_{B'B}\right\} M^a_{A'A}\,, \tag{2.6}$$

where ε denotes the gluon polarization state. The generators of the fundamental representation of $SU(N_c)$ are $T^a (a = 1,\dots,N_c^2 - 1)$, satisfying $[T^a, T^b] = if^{abc}\,T^c$. In the same way we get

$$M_2 \simeq -g\frac{2}{(p_f - p_i)^2}\{g_{\mu\nu}\varepsilon\cdot(p_f - p_i) - k_\mu\varepsilon_\nu + k_\nu\varepsilon_\mu\}\cdot M^{a,\mu\nu}_{A'A}\ [T^b, T^a]_{B'B}\,. \tag{2.7}$$

In addition to M_1 and M_2, there is a term M_3 coming from gluon radiation off the static source. The sum of the three terms is gauge invariant.

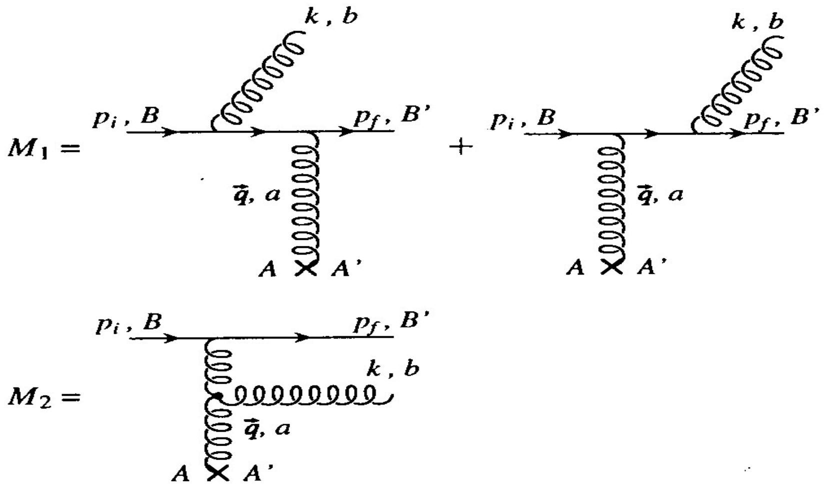

Fig. 2. Gluon emission amplitude induced by one scattering.

In light-cone gauge

$$\varepsilon = (\varepsilon_0, -\varepsilon_0, \boldsymbol{\varepsilon}_\perp) , \qquad \varepsilon \cdot k = 0 \Rightarrow \varepsilon_0 = \frac{\boldsymbol{\varepsilon}_\perp \cdot \boldsymbol{k}_\perp}{\omega + k_\parallel} \simeq \frac{\boldsymbol{\varepsilon}_\perp \cdot \boldsymbol{k}_\perp}{2\omega} . \tag{2.8}$$

In the high-energy limit

$$\frac{\varepsilon \cdot p_i}{k \cdot p_i} \simeq \frac{\varepsilon \cdot p_f}{k \cdot p_f} \simeq 2\boldsymbol{\varepsilon}_\perp \cdot \frac{\boldsymbol{k}_\perp}{\boldsymbol{k}_\perp^2} , \tag{2.9}$$

where $\boldsymbol{k}_\perp$ is the transverse momentum of the gluon with respect to the direction of the incident particle. Thus,

$$M_1 \simeq -2g\, \boldsymbol{\varepsilon}_\perp \cdot \frac{\boldsymbol{k}_\perp}{\boldsymbol{k}_\perp^2} \, [T^b, T^a]_{B'B} \, M^a_{A'A} . \tag{2.10}$$

In QED [9], the photon radiation amplitude vanishes in the limit $E \to \infty$. In QCD, in the high-energy limit only the purely non-abelian contribution to the gluon radiation spectrum survives. This is underlined by the presence of the commutator in (2.10). As a result, we can use the eikonal approximation where the trajectory of the projectile is taken to be a straight line. Also,

$$M_2 \simeq 2g\, \boldsymbol{\varepsilon}_\perp \cdot \frac{\boldsymbol{k}_\perp - \boldsymbol{q}_\perp}{(\boldsymbol{k}_\perp - \boldsymbol{q}_\perp)^2} \, [T^b, T^a]_{B'B} \, M^a_{A'A} . \tag{2.11}$$

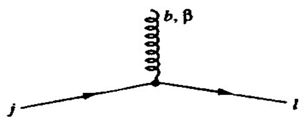

$ig(t^b)_{lj}\gamma^\beta$

quark–gluon
vertex

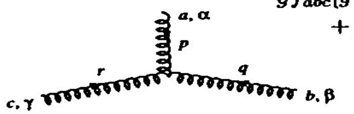

$$g f_{abc}[g^{\alpha\beta}(p-q)^\gamma + g^{\beta\gamma}(q-r)^\alpha + g^{\gamma\alpha}(r-p)^\beta]$$

triple gluon
vertex

$(p+q+r=0)$

The qqG vertex involves a factor of t^a:

$$t^a \equiv \tfrac{1}{2}\lambda^a \qquad \text{(A2.5.1)}$$

where the $SU(3)$ matrices λ^a are those introduced by Gell-Mann. The commutation relations for the t^a are given by the structure constants of the group,

$$[t^a, t^b] = \mathrm{i} f_{abc} t^c \qquad \text{(A2.5.2)}$$

$$\{t^a, t^b\} = \frac{1}{N}\delta_{ab} I_{(N)} + d_{abc} t^c, \qquad \text{(A2.5.3)}$$

where $I_{(N)}$ is the N-dimensional unit matrix. The f_{abc} are antisymmetric and the d_{abc} symmetric under the interchange of any two indices. In $SU(2)$, the quantities analogous to (t^a, f_{abc}, d_{abc}) are $(\sigma^a/2, \epsilon_{abc}, 0)$. Some useful identities involving the matrices t^a are

$$\left.\begin{aligned}
t^a t^b &= \frac{1}{2}\left[\frac{1}{N}\delta_{ab} I_{(N)} + (d_{abc} + \mathrm{i} f_{abc}) t^c\right], \\
t^a_{ij} t^a_{kl} &= \frac{1}{2}\left[\delta_{il}\delta_{jk} - \frac{1}{N}\delta_{ij}\delta_{kl}\right], \\
\mathrm{Tr}\, t^a &= 0, \\
\mathrm{Tr}(t^a t^b) &= \frac{1}{2}\delta_{ab}, \\
\mathrm{Tr}(t^a t^b t^c) &= \frac{1}{4}(d_{abc} + \mathrm{i} f_{abc}), \\
\mathrm{Tr}(t^a t^b t^a t^c) &= -\frac{1}{4N}\delta_{bc}.
\end{aligned}\right\} \qquad \text{(A2.5.4)}$$

$$f_{acd} \cdot f_{bcd} = N \delta_{ab}$$

E. Leader & E. Predazzi
An Introduction to gauge theories
vol II Appendix 2

abc	f_{abc}	abc	f_{abc}
123	1	345	1/2
147	1/2	367	−1/2
156	−1/2	458	$\sqrt{3}/2$
246	1/2	678	$\sqrt{3}/2$
257	1/2		

Table A2.1. Non-zero f_{abc} for $SU(3)$.

The λ-matrices are familiar[9] from the study of flavor-$SU(3)$ symmetry. They have a number of simple properties, including

$$\mathrm{tr}(\lambda^l) = 0, \tag{8.1.7}$$

$$\mathrm{tr}(\lambda^k \lambda^l) = 2\delta^{kl}, \tag{8.1.8}$$

and

$$[\lambda^j, \lambda^k] = 2if^{jkl}\lambda^l, \tag{8.1.9}$$

which parallel those of the Pauli isospin matrices given in (4.2.18) and (4.2.25). Indeed, in the canonical basis

$$\lambda_1 = \begin{array}{cc} \begin{pmatrix} 0 & 1 & 0 \\ 1 & 0 & 0 \\ 0 & 0 & 0 \end{pmatrix} & \begin{array}{c} \bar{R} \\ \bar{B}, \\ \bar{G} \end{array} \\ \begin{array}{ccc} R & B & G \end{array} & \end{array} \qquad \lambda_2 = \begin{pmatrix} 0 & -i & 0 \\ i & 0 & 0 \\ 0 & 0 & 0 \end{pmatrix},$$

$$\lambda_3 = \begin{pmatrix} 1 & 0 & 0 \\ 0 & -1 & 0 \\ 0 & 0 & 0 \end{pmatrix}, \qquad \lambda_4 = \begin{pmatrix} 0 & 0 & 1 \\ 0 & 0 & 0 \\ 1 & 0 & 0 \end{pmatrix},$$

$$\lambda_5 = \begin{pmatrix} 0 & 0 & -i \\ 0 & 0 & 0 \\ i & 0 & 0 \end{pmatrix}, \qquad \lambda_6 = \begin{pmatrix} 0 & 0 & 0 \\ 0 & 0 & 1 \\ 0 & 1 & 0 \end{pmatrix}, \tag{8.1.10}$$

$$\lambda_7 = \begin{pmatrix} 0 & 0 & 0 \\ 0 & 0 & -i \\ 0 & i & 0 \end{pmatrix}, \qquad \lambda_8 = \frac{1}{\sqrt{3}} \begin{pmatrix} 1 & 0 & 0 \\ 0 & 1 & 0 \\ 0 & 0 & -2 \end{pmatrix},$$

$$[t^a, t^b] = i f_{abc}\, t^c \qquad t^a \equiv \frac{1}{2}\lambda^a$$

$$[t^a, t^b]^2 = \sum_{abij} \left(f_{cba}\, t^c_{ji}\right)\left(f_{dba}\, t^d_{ji}\right)^*$$

$$= \sum_{abij} f_{cba} \cdot f_{dba} \cdot t^c_{ji}\, t^d_{ij}$$

$$= \sum_{a,b} f_{cba} \cdot f_{dba}\, \mathrm{Tr}\left(t^c \cdot t^d\right)$$

$$= \left(N\, \delta_{cd}\right)\left(\frac{1}{2}\, \delta_{cd}\right) = 12 \qquad (N=3)$$

Partonic energy loss in a coloured medium

Matter affects evolution.

- A quark or gluon (traveling in vacuum) with virtuality Q^2 will radiate gluons to become on-shell: DGLAP-like evolution.
- Gluon radiation modified when the particle traverses a medium: medium-induced gluon radiation.

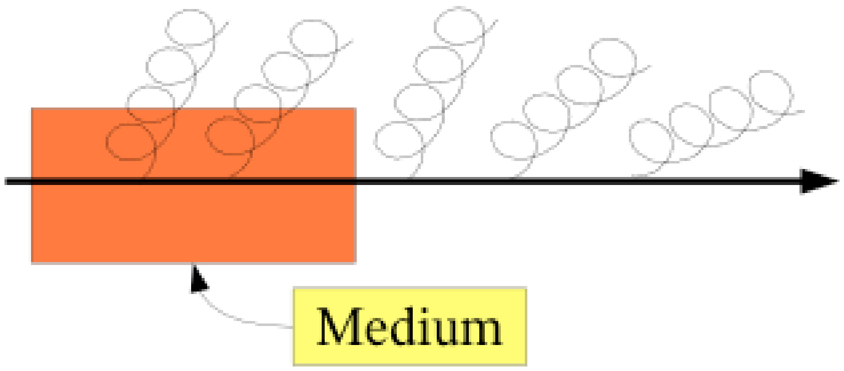

- Where to look?
  - Inclusive particle (suppression).
  - Heavy quarks
  - Jets: Jetshapes, particle correlations...

Bjorken, Gyulassy, Pluemer, Wang, Baier, Dokshitzer, Mueller, Pegne, Schiff, Levai, Vitev, Zhakarov, Wang, Salgado, Wiedemann, Armesto…

- Bjorken’s collisional energy loss generates only small effects
- Is medium-induced bremsstrahlung is more effective?

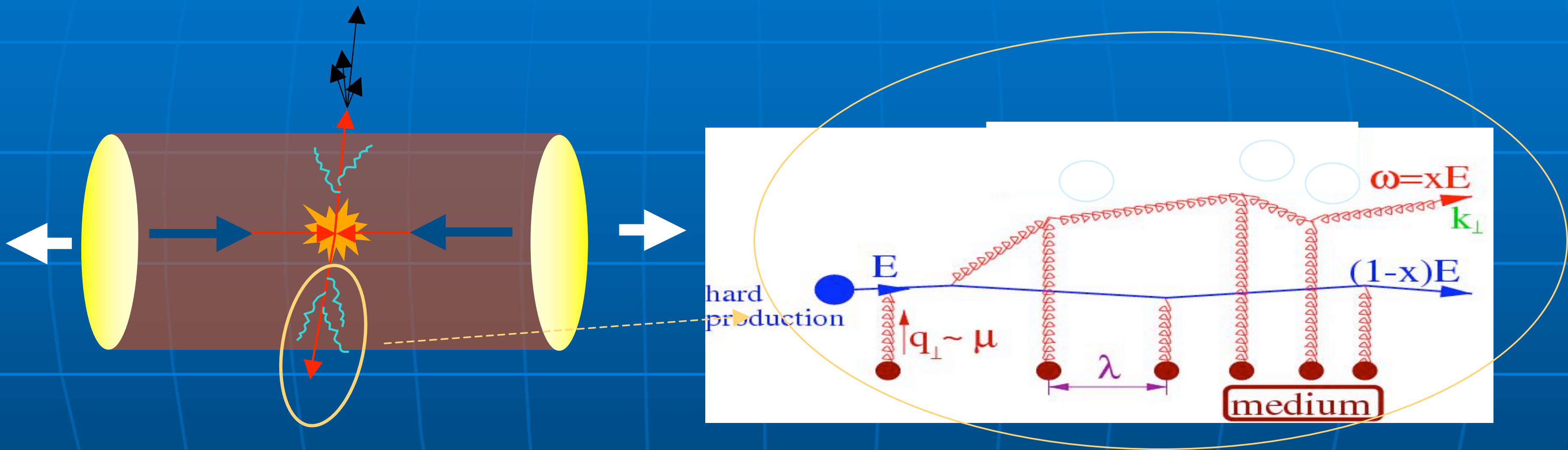

- Essential physics: radiated gluon decoheres due to multiple interactions with medium

Baier et al. Nucl. Phys. B 433 (1997) 291

— main feature: scattering centers are static.

Each center creates a screened Coulomb potential:

$$V(x) = \frac{g}{4\pi}\,\frac{e^{-\mu|\vec{x}-\vec{x}_i|}}{|\vec{x}-\vec{x}_i|}$$

scatterer

$r_D = \mu^{-1} \equiv$ Debye screening length

$\mu \equiv$ Debye " mass

$\mu^{-1} \ll \lambda$ mean free path of incident parton

$\omega \ll E_{inc.}$ soft gluon approximation

$\mu \simeq \langle k_\perp \rangle$ acquired by the gluon in each scattering

$$l_{coh} \simeq \frac{\omega}{\langle k_\perp^2 \rangle_{l_{coh}}} \qquad \text{ma} \quad \langle k_\perp^2 \rangle_{l_{coh}} \simeq \frac{l_{coh}}{\lambda}\mu^2$$

random walk

$$\Rightarrow \quad l_{coh} = \sqrt{\frac{\lambda}{\mu^2}\,\omega}$$

$$N_{coh} \simeq \sqrt{\frac{\omega}{\lambda\mu^2}} \equiv \sqrt{\frac{\omega}{\omega_c}}$$

Scattering power of the QCD medium

Scattering centers = color charges

Density of scattering centers

$$\hat{q} = \rho \int q^2 dq^2 \frac{d\sigma}{dq^2} \equiv \rho\sigma \left\langle k_{\mathrm{T}}^2 \right\rangle = \frac{\mu^2}{\lambda_f}$$

Range of color force

— $\omega_{BH} \stackrel{\wedge}{=} \lambda\mu^2 = \hat{q}\lambda^2$ B.H valida $\omega \lesssim \omega_{BH}$

— $\omega_{fact} \stackrel{\wedge}{=} \frac{\mu^2 L^2}{\lambda} = \hat{q} L^2$ $\quad \hat{q} \simeq \frac{\mu^2}{\lambda}$

se la lunghezza di coerenza è maggiore della lunghezza L del mezzo.

$$N_{coh} = \frac{L}{\lambda}$$

$$L/\lambda = \sqrt{\frac{\omega_{fact}}{\lambda\mu^2}} \Rightarrow \omega_{fact} = \frac{\mu^2 L^2}{\lambda}$$

For the following qualitative derivations we neglect logarithmic factors. Thus we ignore numerical factors of order 1, and do not distinguish between propagating quarks and gluons. However, we explicitly keep the parameters representing the medium.

In terms of the gluon energy the condition (3.1) is

$$\omega_{BH} \sim \lambda\mu^2 \ll \omega \ll \omega_{fact} \sim \frac{\mu^2 L^2}{\lambda} \leqslant E\,. \tag{3.2}$$

Obviously, $\omega_{fact} \leqslant E$ only holds when L is less than the critical length,

$$L \leqslant L_{cr} = \sqrt{\frac{\lambda E}{\mu^2}}\,. \tag{3.3}$$

We note that the case $\omega_{fact} \ll E$ is consistent with the soft gluon approximation for the induced spectrum.

The radiation spectrum per unit length behaves in the $E \to \infty$ limit as

$$\omega \frac{dI}{d\omega dz} \simeq \begin{cases} \dfrac{\alpha_s}{\lambda} & \omega < \omega_{BH} \\ \dfrac{\alpha_s}{\lambda}\sqrt{\dfrac{\lambda\mu^2}{\omega}} & \omega_{BH} < \omega < \omega_{fact} \\ \dfrac{\alpha_s}{L} & \omega_{fact} < \omega < E \end{cases} \tag{3.4}$$

for a finite length $L \leqslant L_{cr}$. These main features are illustrated schematically in Fig. 8. In the BH regime the radiation is due to $N = L/\lambda$ incoherent scatterings, whereas in the factorization regime the medium behaves as one single scattering centre. In the LPM regime N_{coh} elementary centres act as a single scattering centre.

Integrando il contributo LPM

$$\Delta E \simeq \int_0^L dz \int_{\omega_{BH}}^{\omega_{fact}} \frac{\alpha_s}{\lambda} \omega_{BH}^{\frac{1}{2}} \omega^{-\frac{1}{2}} d\omega$$

$$= \frac{2\alpha_s}{\lambda} \omega_{BH}^{1/2} \left[\omega_{fact}^{-\frac{1}{2}} - \omega_{BH}^{-\frac{1}{2}} \right] \cdot L$$

$$= \frac{2\alpha_s}{\lambda} \left(\omega_{BH}^{1/2} \cdot \omega_{fact}^{-1/2} - 1 \right) \cdot L$$

$$\simeq \frac{2\alpha_s}{\lambda} \sqrt{\lambda \mu^2} \cdot \sqrt{\frac{\mu^2}{\lambda}} \cdot L^2$$

$$= 2\alpha_s \frac{\mu^2}{\lambda} L^2 = 2\alpha_s \hat{q} L^2$$

$$\boxed{\Delta E \sim \alpha_s \hat{q} L^2}$$

dipendenza dello spettro di radiazione da:

$\hat{q}$ ed L^2

energy loss

$$\langle \Delta E \rangle \propto \alpha_s \, C_R \, \hat{q} \, L^2$$

average energy loss

Casimir coupling factor

transport coefficient of the medium

distance travelled in the medium

→ R.Baier et al., Nucl. Phys. **B483** (1997) 291 ("BDMPS")

Ex Consider the following diagram

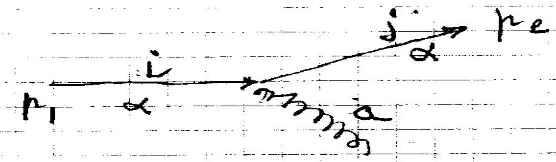

the colour factor will be

$$\frac{1}{3}\sum_a\left(\sum_{ij} t^a_{ij}\right)^2 = \frac{1}{3}\sum_{a}^{8}\sum_{ij} t^a_{ij}\, t^a_{ji} = \frac{1}{3}\sum_a \mathrm{Tr}\left(t^a t^a\right) =$$

$$= \frac{1}{3}\sum_a^{8} \frac{1}{2} = \frac{1}{3}\,\frac{8}{2} = \frac{4}{3} \quad C_F$$

Ex | consider its gluon counterpart

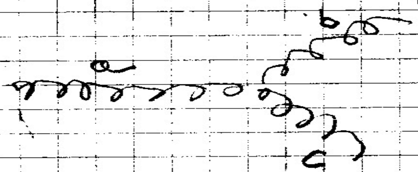

the colour factor will be

$$\frac{1}{8}\sum_{a,bc}\left(f_{abc}\cdot f_{abc}\right) = \frac{1}{8}\,\underset{\text{abc permutations}}{6}\cdot\overbrace{\sum_a\left(f_{abc}\, f_{abc}\right)}^{4} = \frac{24}{8} = 3 \quad C_A$$

---

f_{abc} structure constants antisymmetric under the interchange of any two indices

$f_{abb} = 0$ $\quad f_{acd}\, f_{bcd} = 3\,\delta_{ab}$

$\sum_a f_{acd}\, f_{acd} = 24 \quad (3\times 8$

Riassumendo

Three bremsstrahlung regions

(BDMPS and N.Armesto lecture, Torino 2005)

Set $\omega_{BH} = \mu^2\lambda = E_{LPM}$ and $\omega_c = E_{LPM}/(\lambda/L)^2 = \mu^2 L^2/\lambda$ and ignore logs and constants. We have three regimes in the spectrum:

A) $\omega < E_{LPM}$ or $t_{coh} < \lambda$: Bethe-Heitler, incoherent regime, 1 scattering.

$$\omega \left.\frac{dI}{d\omega dz}\right|_{BH} \sim \frac{1}{\lambda}\,\omega \left.\frac{dI}{d\omega dz}\right|_{1\ scattering} \sim \frac{\alpha_s C_F}{\lambda}$$

B) $E_{LPM} < \omega < \omega_c$ or $\lambda < t_{coh} < L$: LPM regime, $N_{coh} > 1$, suppression from Bethe-Heitler.

$$\omega \left.\frac{dI}{d\omega dz}\right|_{LPM} \sim \frac{1}{t_{coh}}\,\omega \left.\frac{dI}{d\omega dz}\right|_{1\ scattering} \sim \alpha_s C_F \sqrt{\frac{\hat{q}}{\omega}} = \frac{\alpha_s C_F}{\lambda}\sqrt{\frac{E_{LPM}}{\omega}}$$

C) $\omega > \omega_c$ or $t_{coh} > L$: factorization regime, enhancement from LPM.

$$\omega \left.\frac{dI}{d\omega dz}\right|_{facto} \sim \frac{1}{L}\,\omega \left.\frac{dI}{d\omega dz}\right|_{1\ scattering} \sim \alpha_s C_F \sqrt{\frac{\hat{q}}{\omega}}\sqrt{\frac{\omega}{\omega_c}}$$

Bjorken, Gyulassy, Pluemer, Wang, Baier, Dokshitzer, Mueller, Pegne, Schiff, Levai, Vitev, Zhakarov, Wang, Salgado, Wiedemann, Armesto…

- Bjorken's collisional energy loss generates only small effects
- But medium-induced bremsstrahlung is more effective:

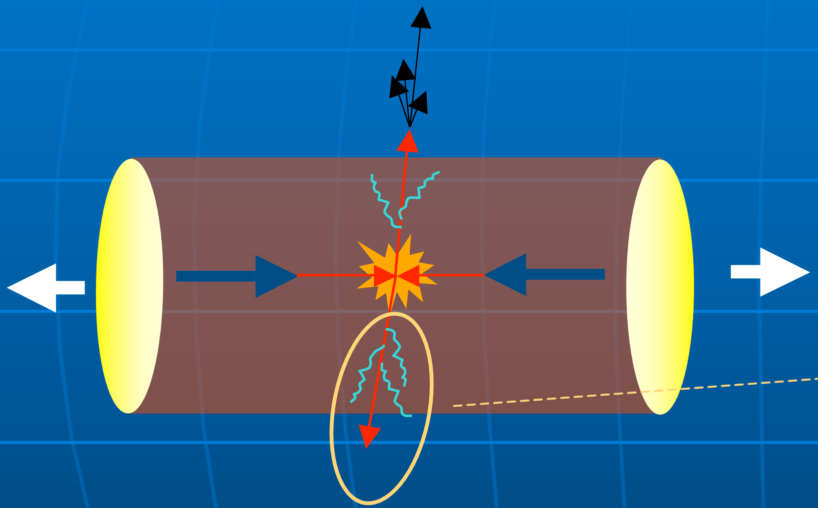

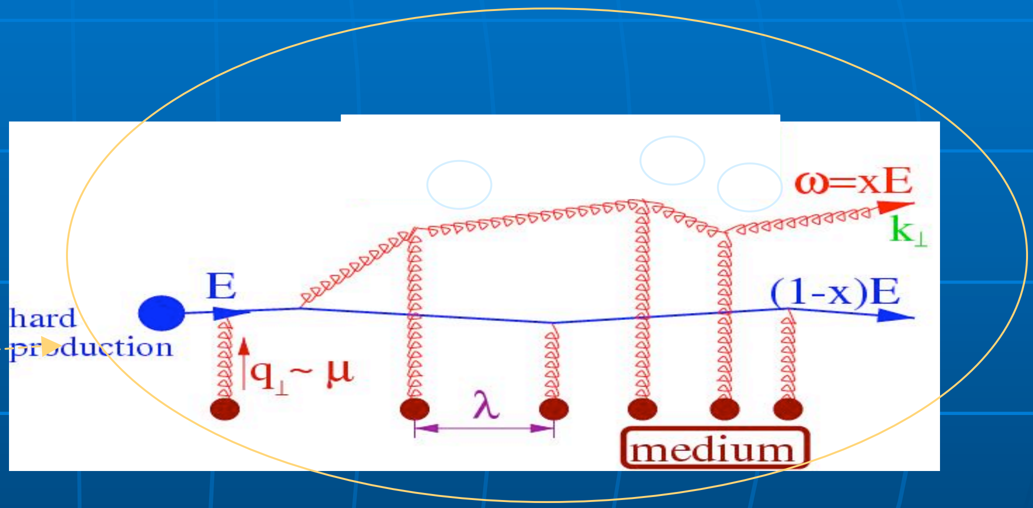

- Essential physics: radiated gluon decoheres due to multiple interactions with medium
- ΔE sensitive to color-charge density of the medium
- Unique non-abelian feature: system size dependence $\Delta E \sim L^2$

What do we learn from inclusive hadron suppression?

see lectures by Nestor Armesto

Partonic energy loss calculations: observed suppression requires initial density >~30 times cold nuclear matter density

$$\hat{q} \sim \rho_{glue} \sim \varepsilon^{3/4}$$

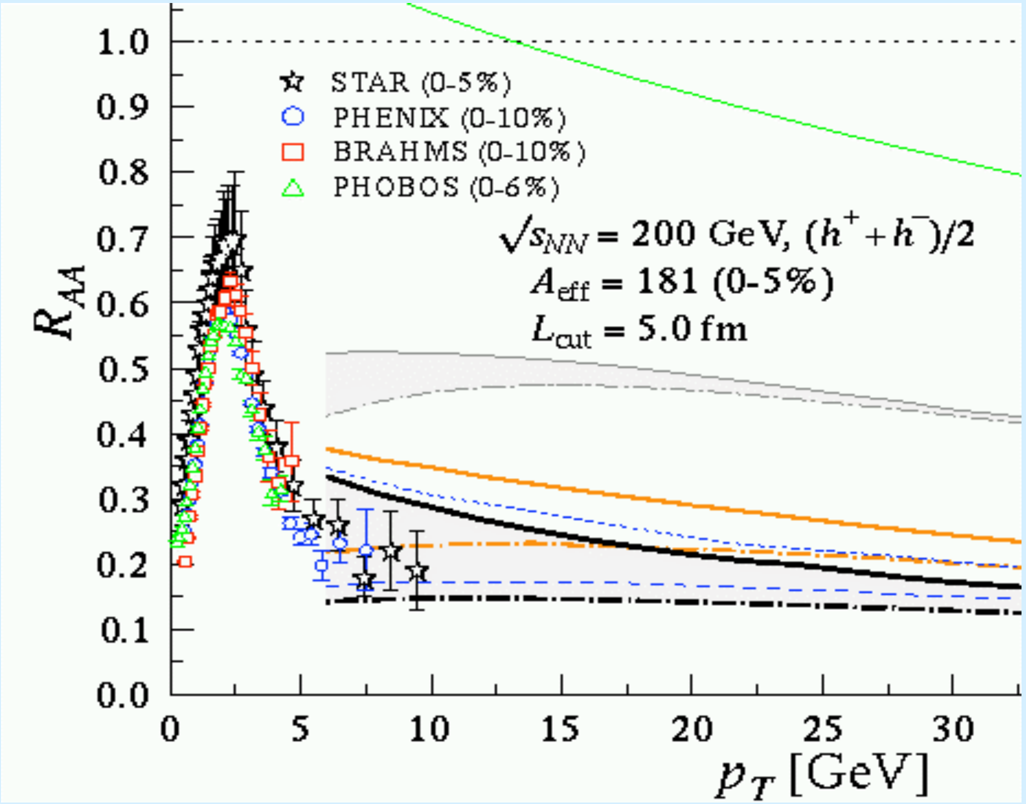

$\hat{q} = 0\ GeV^2/fm$

$\hat{q} = 1\ GeV^2/fm$

$\hat{q} = 5-15\ GeV^2/fm$

Suppression only supplies lower bound on $\hat{q}$ ~ density

How large is q-hat?

- Data are described by a large loss parameter for central collisions:

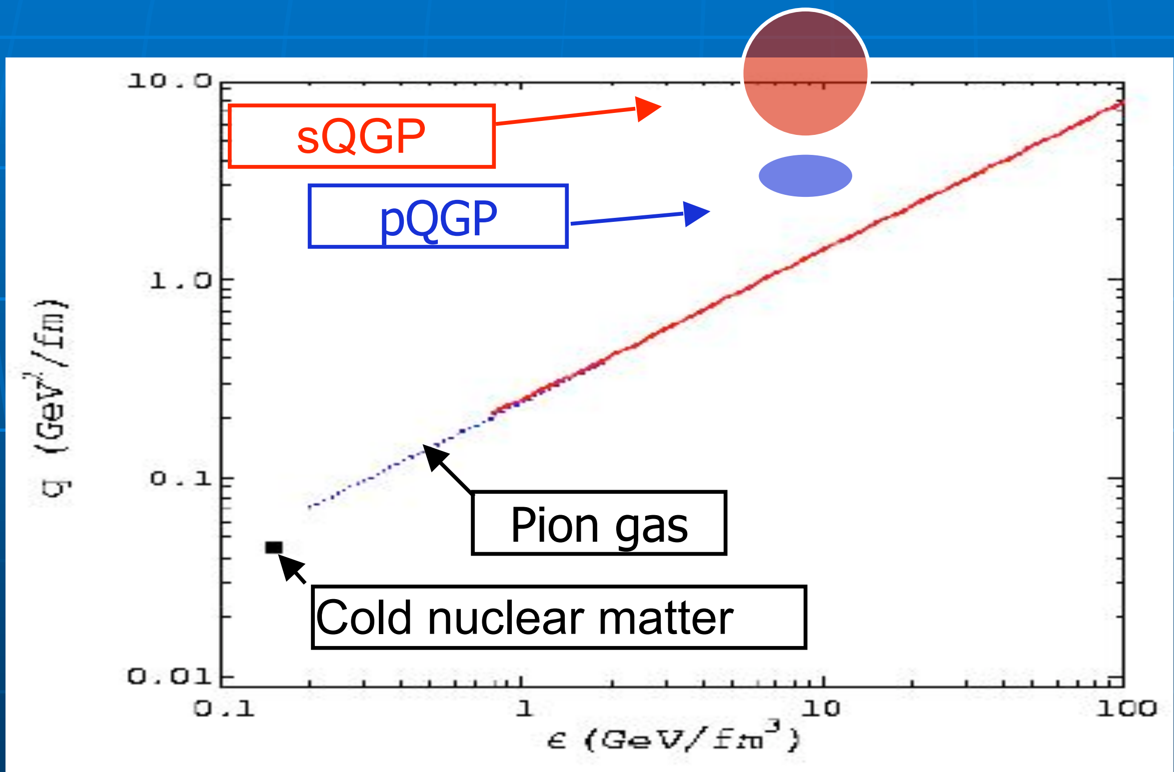

RHIC data

R. Baier

Larger than expected from perturbation theory ?

Heavy flavour energy loss

Heavy flavour energy loss?

Energy loss for heavy flavours is expected to be reduced:

i) Casimir factor

- light hadrons originate predominantly from gluon jets, heavy flavoured hadrons originate from heavy quark jets
- C_R is 4/3 for quarks, 3 for gluons

ii) dead-cone effect

- gluon radiation expected to be suppressed for $\theta < M_Q/E_Q$

[Dokshitzer & Karzeev, Phys. Lett. **B519** (2001) 199]

Weak decays of charm

- typically:

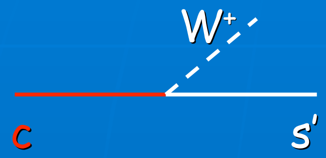

$$|s'\rangle = \cos\vartheta_C |s\rangle - \sin\vartheta_C |d\rangle \approx 0.97|s\rangle - 0.22|d\rangle$$

ϑ_C = "Cabibbo angle"

→ large branching ratio to kaons:
- D^+:
  - $D^+ \to K^- + X$ BR ~ 28 %
  - "golden" channel: $D^+ \to K^-\pi^+\pi^+$ BR ~ 9%
- D^0:
  - $D^0 \to K^- + X$ BR ~ 50%
  - "golden" channels: $D^0 \to K^-\pi^+$ BR ~ 4% ; $D^0 \to K^-\pi^+\pi^+\pi^-$ BR ~ 7%

- $W^\pm$ branchings:

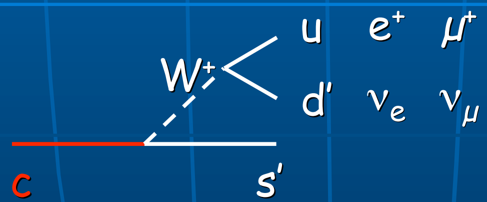

(similarly:

)

→ large semileptonic branching ratio, typical ~ 10%

~ 10% heavy flavour hadrons give in final state an $e^\pm$ (and ~ 10% a $\mu^\pm$) (and with a respectable p_T...)

[Armesto et al., Phys. Rev. D69 (2004) 114003]

Heavy-quark energy loss at RHIC

A. Dainese et al, hep-ph/0601107 13 Jan 2006

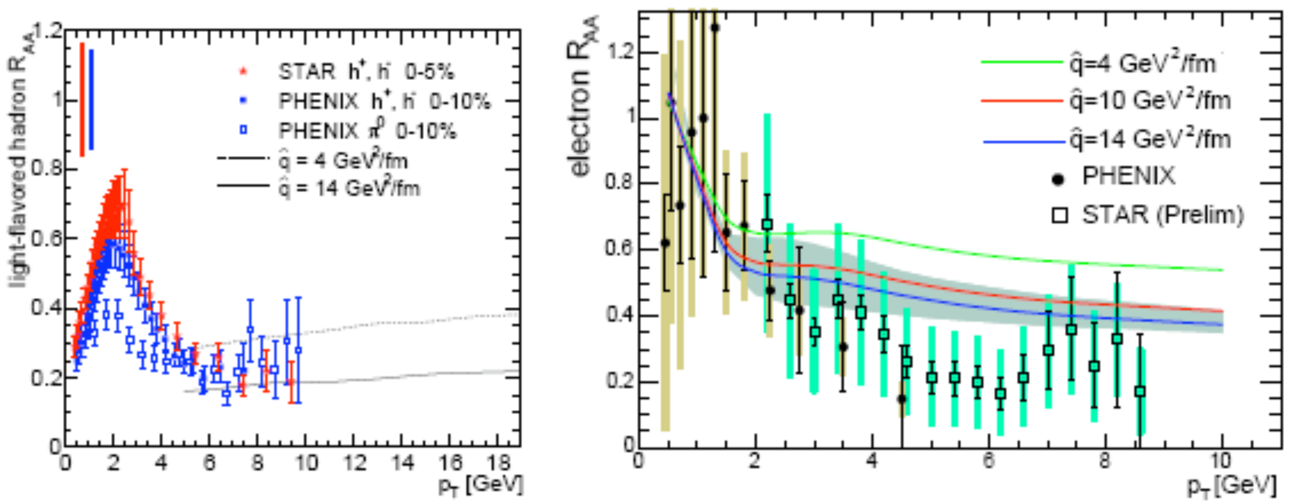

FIGURE 1. Central Au–Au collisions at $\sqrt{s_{NN}} = 200$ GeV: R_{AA} for light-flavored hadrons (left, adapted from [9]) and for heavy-flavor decay electrons (right, from [12])

Heavy quark suppression (QM2005 data) via non-photonic electrons

STAR talk by J. Bielcik

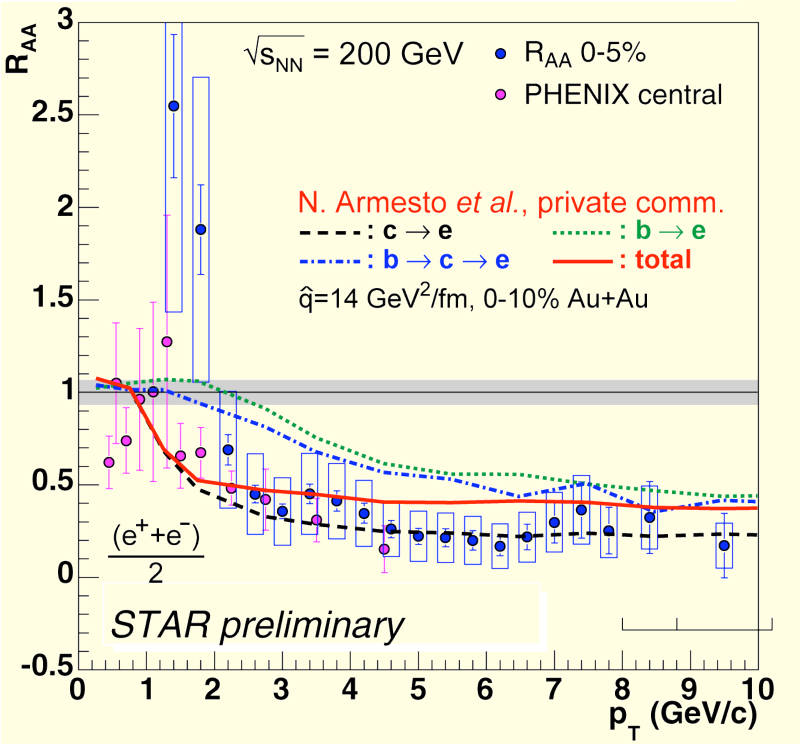

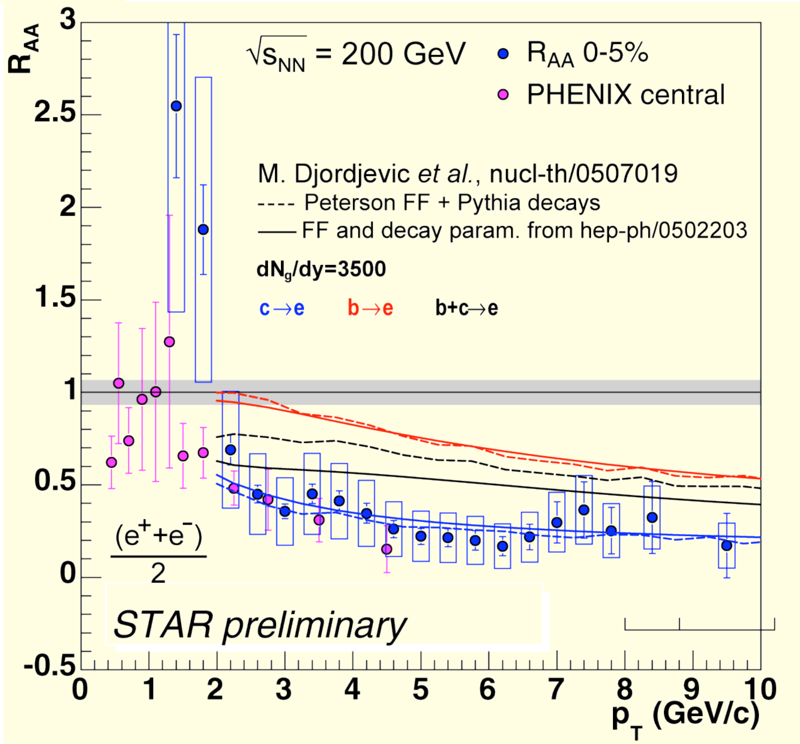

Data indicate:

Large suppression of beauty

…or charm dominance up to electron $p_T \approx 10$ GeV

Medium density inferred from heavy quark energy loss larger than from light quark R_{AA} and I_{AA}

Large Collisional energy loss?

Institute of Physics Publishing Journal of Physics G: Nuclear and Particle Physics

J. Phys. G: Nucl. Part. Phys. **32** (2006) S333–S341 doi:10.1088/0954-3899/32/12/S41

An overview of heavy quark energy loss puzzle at RHIC

Magdalena Djordjevic

Department of Physics, Ohio State University, 191 West Woodruff Avenue, Columbus, OH 43210, USA

Received 1 June 2006
Published 17 November 2006
Online at stacks.iop.org/JPhysG/32/S333

Abstract
We give a theoretical overview of the heavy quark tomography puzzle posed by recent non-photonic single electron data from central Au+Au collisions at $\sqrt{s} = 200$ A GeV. We show that radiative energy loss mechanisms alone are not able to explain large single electron suppression data, as long as realistic parameter values are assumed. We argue that a combined collisional and radiative pQCD approach can solve a substantial part of the non-photonic single electron puzzle.

(Some figures in this article are in colour only in the electronic version)

1. Introduction

Quark gluon plasma (QGP) is a new form of matter, consisting of interacting quarks, antiquarks and gluons. If the QGP can be created in ultrarelativistic heavy ion collisions (URHIC), then a wide variety of probes and observables could be used to diagnose and map out its physical properties.

Measured quenching patterns of pions and η mesons [1] already provided a direct evidence for the creation of a strongly interacting quark gluon plasma (sQGP) in central Au+Au collisions at $\sqrt{s} = 200$ A GeV [2–5]. Further, rare heavy quark jets are considered to be excellent independent probes of the sQGP [6] because their high mass ($m_c \approx 1.2$ GeV, $m_b \approx 4.75$ GeV) changes the sensitivity of the energy loss mechanisms in a well-defined way [7–12] relative to those of light quark and gluon jets [2–4]. Another advantage of heavy quarks jet quenching is that gluon jet fragmentation into heavy mesons can be safely neglected. However, one disadvantage of heavy meson tomography is that direct measurements of identified high $p_\perp$ D and B mesons are very difficult with current detectors and RHIC luminosities [13]. Therefore, the first experimental studies of heavy quark attenuation at RHIC have focused on the attenuation of their single (non-photonic) electron decay products [14, 15].

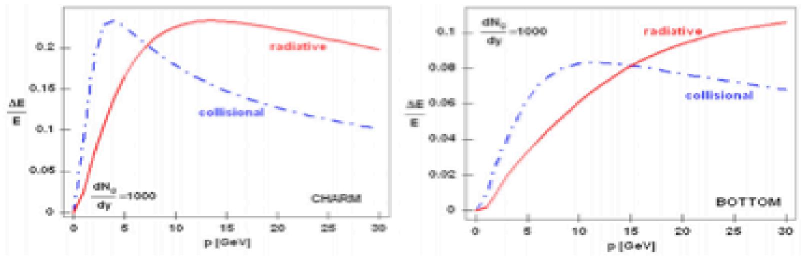

Figure 6. Comparison between collisional and medium-induced radiative fractional energy loss is shown as a function of momentum for charm and bottom quark jets (left and right panels, respectively). Full curves show the collisional energy loss, while dot-dashed curves show the net radiative energy loss. The assumed thickness of the medium is $L = 5$ fm and $\lambda = 1$ fm.

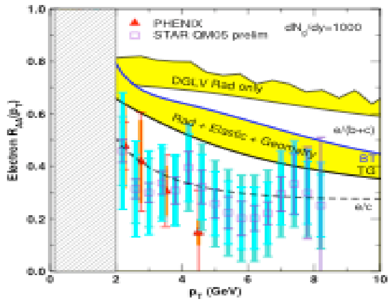

Figure 7. The suppression factor, $R_{AA}(p_\perp)$, of non-photonic electrons from decay of quenched heavy quark (c+b) jets is compared to PHENIX [14] and preliminary STAR data [15] data in central Au+Au reactions at 200 AGeV. The assumed initial gluon rapidity density is $dN_g/dy = 1000$. The upper yellow band from [16] takes into account radiative energy loss only, using a fixed $L =$ 6 fm; the lower yellow band includes both collisional and radiative energy losses as well as jet path length fluctuations [17]. The dashed curve shows the electron suppression using radiative and TG [29] collisional energy loss with bottom quark jets neglected. The figure is adapted from [17].

consistent with the data within present experimental and theoretical errors. Therefore, we may conclude that a combined collisional and radiative pQCD approach may be able to solve a substantial part of the non-photonic single electron puzzle.

We note that collisional energy loss in a finite size QCD medium falls between the two different computations [29, 30] used in [17] (for more details, see [33]). Therefore, we expect that the single electron suppression results—computed with finite size collisional energy loss [33]—should be inside the middle yellow region presented in figure 7.

Jets at RHIC summaey

- jet structure is strongly modified in dense matter
- consistent with partonic energy loss via induced gluon radiation
  medium is very dense: >~ 30 times cold nuclear matter
  heavy quark energy loss not understood

- intermediate p_T: complex phenomena, interplay between bulk medium and hard processes

Open issues:

- differential measurement of ΔE
- shock waves in recoil direction?
- coupling of induced radiation to collective flow?
- direct observation of induced radiation
- accurate accounting of full jet energy
- dependence on color charge (q/g) and quark mass of probe
- …

LHC

collisions at the LHC

CMS

ALICE

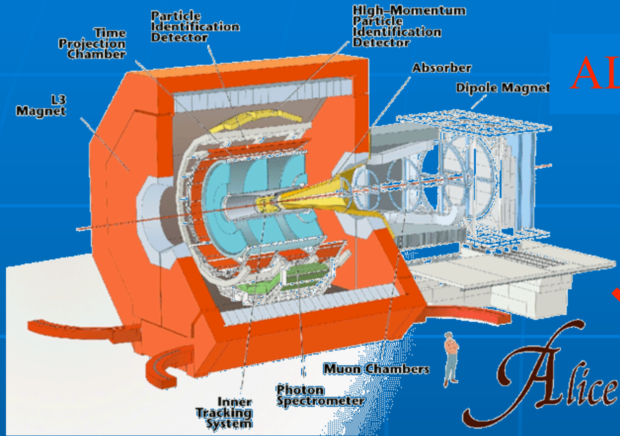

ATLAS

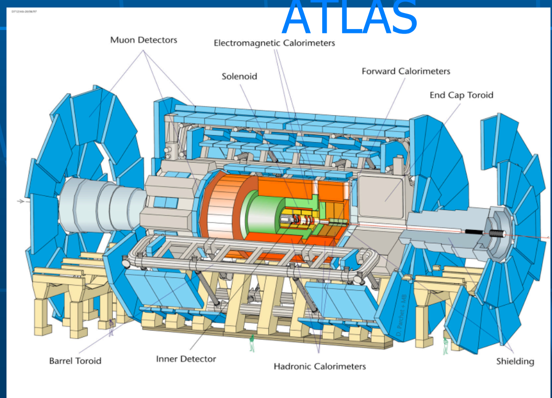

2007: p+p collisions @ 14 TeV
2008: Pb+Pb collisions @ 5.5 TeV

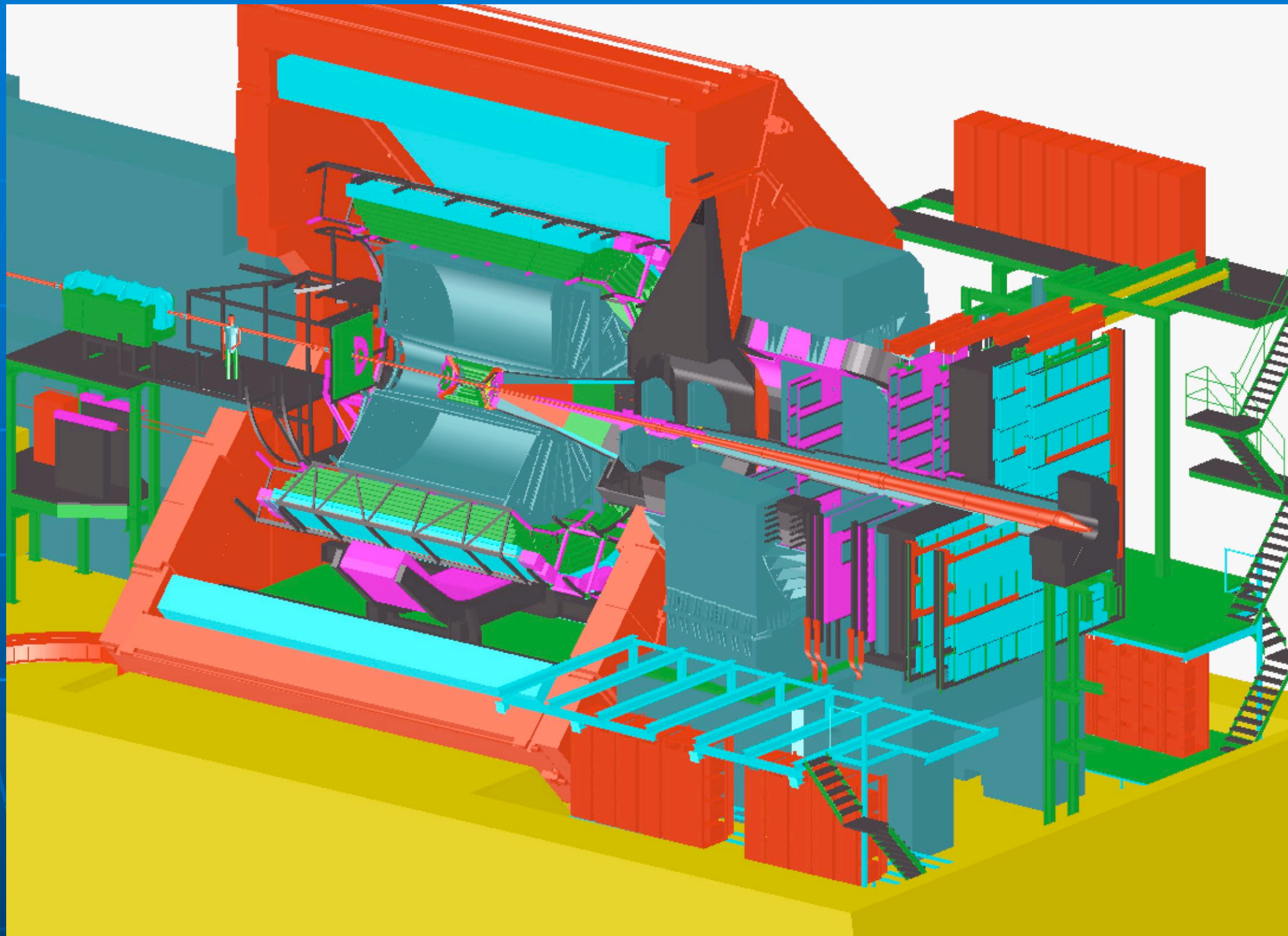

- some prediction …

$$R_{AA}^{D,B}(p_T) = \frac{1}{N_{coll}} \times \frac{dN_{AA}^{D,B} / dp_T}{dN_{pp}^{D,B} / dp_T}$$

charm

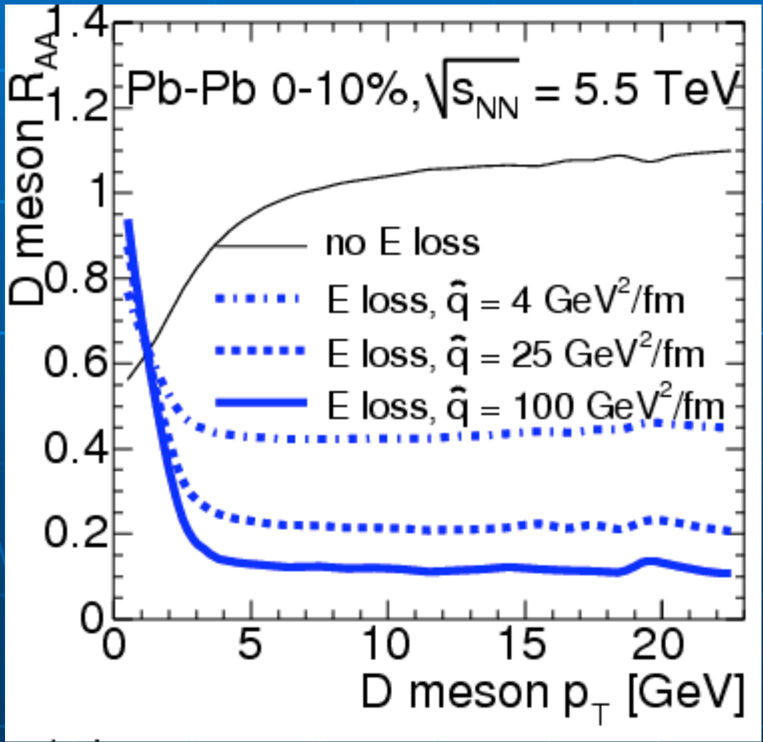

beauty

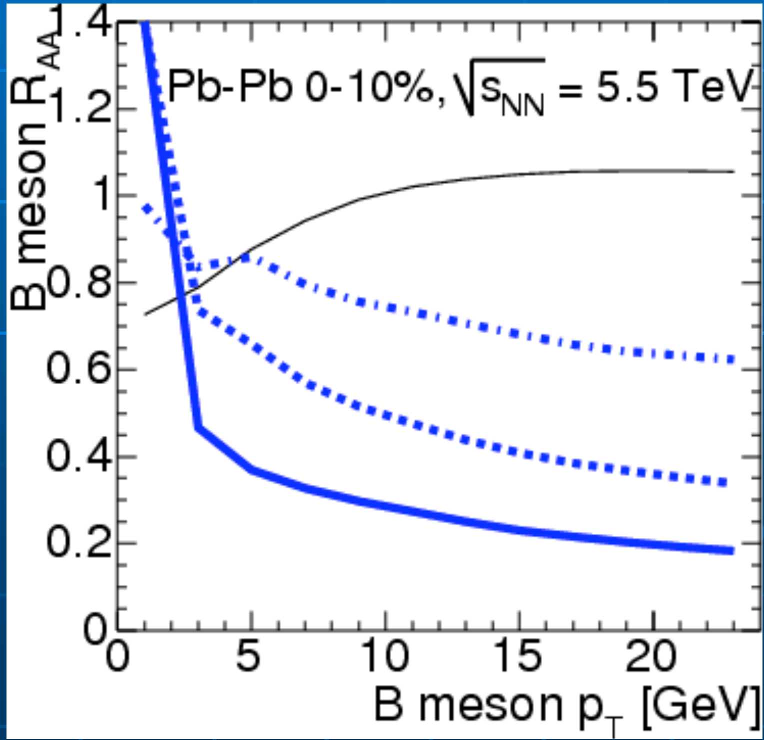

[Armesto et al.: Phys.Rev. D71 (2005) 054027]

Ratio of heavy/light meson yields

Armesto, Dainese, Salgado, Wiedemann, PRD 71 (2005) 054027.

More detailed considerations: multiple scattering fills dead cone; fragmentation; q vs g color charge

charm/light

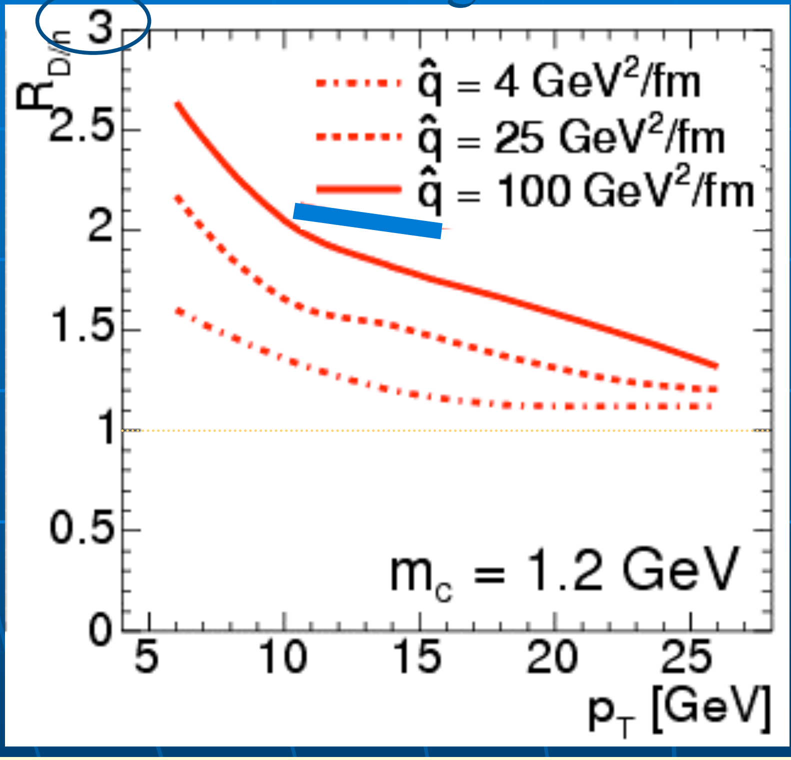

beauty/light

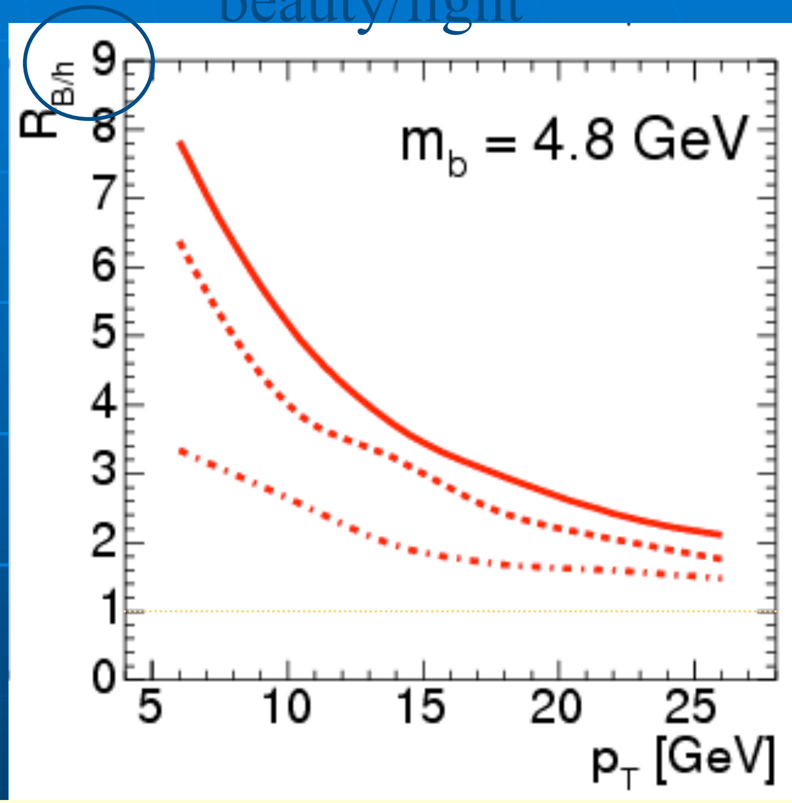

p_T~10-20 GeV/c: light mesons from glue, charm effectively massless
⇒ well-controlled discrimination of color-charge and mass effects

Hard Probe Physics at LHC

- Copious jet production;
- RHIC measurements at much higher pT :
  - single spectra, hadron-hadron correlations ...
- Exclusive jet reconstruction in HIC;
- Photon – jet correlations
- Electroweak-bosons – jet correlations;
- Copious charm production;
- Heavy quark thermalisation in QGP;
- Beauty at LHC like Charm at RHIC;
- Heavy quark energy loss;
- Elliptic flow of J/ψ: $v_{2;}$;
- HQ potential screening:
  - 1st bottomonia measurement in HIC!

Fine!

Some Numbers:

- Transport coefficient: $q = \frac{(1\,GeV)^2}{fm}$, in-medium pathlength: $L = 5\,fm$

  Average momentum broadening: $\langle k_t^2 \rangle \simeq q\,L = (1\,GeV)^2$

  Characteristic gluon energy: $\omega_c = \frac{1}{2} q\,L^2 = 62.5\,GeV \Rightarrow \Delta E_{loss} > 10\,GeV$

- Time scales: Hadronization time scale: $\tau_{hadr} > \frac{1}{Q_0}\frac{E}{Q_0}, Q_0 = 1\,GeV$

  Thermalization time scale: $\tau_{therm} = L_{max} = \sqrt{\frac{4\,E}{\alpha_s C_R q}}$
  $(\Delta E \sim E_q)$

$E_q = 10\,GeV$	(RHIC)	$\tau_{hadr} > 2\,fm$	$\tau_{therm} \sim 4.5\,fm$	Stuck in medium
$E_q = 100\,GeV$	(LHC)	$\tau_{hadr} > 20\,fm$	$\tau_{therm} \sim 13.5\,fm$	Medium-modified
$E_q = 10^{10}\,GeV$		$\tau_{hadr} > 2\,\mu m$	$\tau_{therm} \sim 10^5\,fm$	